MEASURING AIRCRAFT ALTIMETRY SYSTEM ERROR USING AUTOMATIC DEPENDENT SURVEILLANCE-BROADCAST DATA

KALYANI BAHSKARAN

FACULTY OF COMPUTER SCIENCE AND INFORMATION TECHNOLOGY
UNIVERSITY MALAYA
KUALA LUMPUR

2021

MEASURING AIRCRAFT ALTIMETRY SYSTEM ERROR USING AUTOMATIC DEPENDENT SURVEILLANCE-BROADCAST DATA

KALYANI BAHSKARAN

DISSERTATION SUBMITTED IN PARTIAL FULFILMENT OF THE REQUIREMENTS FOR THE DEGREE OF MASTER OF SOFTWARE ENGINEERING

FACULTY OF COMPUTER SCIENCE AND INFORMATION TECHNOLOGY UNIVERSITY MALAYA KUALA LUMPUR

2021

UNIVERSITY MALAYA

ORIGINAL LITERARY WORK DECLARATION

Name of Candidate: Kalyani Bahskaran

Matric No: 17005797/1

Name of Degree: Master of Software Engineering

Title of Project Paper/Research Report/Dissertation/Thesis ("this Work"):

Measuring Aircraft Altimetry System Error Using Automatic Dependent Surveillance-Broadcast Data

Field of Study: Software Engineering

I do solemnly and sincerely declare that:

1) I am the sole author/writer of this Work;
2) This Work is original;
3) Any use of any work in which copyright exists was done by way of fair dealing and for permitted purposes and any excerpt or extract from, or reference to or reproduction of any copyright work has been disclosed expressly and sufficiently and the title of the Work and its authorship have been acknowledged in this Work;
4) I do not have any actual knowledge, nor do I ought reasonably to know that the making of this work constitutes an infringement of any copyright work;
5) I hereby assign all and every right in the copyright to this Work to the University of Malaya ("UM"), who henceforth shall be the owner of the copyright in this Work and that any reproduction or use in any form or by any means whatsoever is prohibited without the written consent of UM having been first had and obtained;
6) I am fully aware that if in the course of making this Work I have infringed any copyright whether intentionally or otherwise, I may be subject to legal action or any other action as may be determined by UM.

Candidate's Signature Date:

Subscribed and solemnly declared before,

Witness's Signature Date:

Name:

Designation:

MEASURING AIRCRAFT ALTIMETRY SYSTEM ERROR USING AUTOMATIC DEPENDENT SURVEILLANCE-BROADCAST DATA

ABSTRACT

The International Civil Aviation Organization (ICAO) introduced Reduced Vertical Separation Minima (RVSM) globally to support increasing traffic volumes on congested airspace. RVSM focused on reducing vertical separation minimum from 2000 feet to 1000 feet between flight level FL290 and FL410. Implementation of RVSM stresses the accuracy of aircraft avionics that report altitude and requires the Regional Monitoring Agency (RMA) to monitor the aircraft's Height Keeping Performance (HKP) to ensure the aviation safety of their airspace. Presently, air traffic and navigation are controlled by an air traffic controller on the ground based on the pressure altitude value, also known as a flight level (FL) measured with barometric altimeter. The pressure altitude was subjected to errors due to various factors including instrument defect, obstructed airflow, presence of foreign materials into the system, variations of temperature and humidity. Altimetry System Error (ASE) is the difference between the actual altitude based on SI units and the pressure altitude displayed. ASE possesses risk to the aviation industry as it is an invisible to the pilots during the flight. According to ICAO, ASE value must be less than 245 feet to ensure the safety of the aircraft. Currently, some of the airspace operators that implement RVSM in their airspace installs Height Monitoring Unit (HMU) on the ground to monitor the aircraft HKP in their airspace. However, HMU methods are disposed to drawbacks. It requires high implementation and maintenance costs, low scalability, and the requirement to have professionals on board to operate the equipment. Alternatively, this research aims to measure the ASE using geometric height data derived from Automatic Dependent Surveillance-Broadcast (ADS-B) message, which is transmitted to the Air Traffic Control (ATC) in the ground. Aircrafts in different regions has been instructed to be equipped with transponders by their authorities. Hence, the ready availability of ADS-B data can be utilized to study the HKP of the aircrafts. This research identifies a process to measure the ASE values using ADS-B data. Subsequently, a computer algorithm and interfacing tool is developed. The tool enables any personal with basic computer literacy and access to the tool and data file to process the data and asses the HKP of the flight at ease. The algorithm reads inputs of the ADS-B data file, stores all the required fields for processing either all or a single flight, and finally the ASE will be calculated. ASE value is calculated by subtracting Flight Level from the Orthometric Height of the aircraft. Orthometric height is calculated using the Geoid Height derived using the EGM96 Geopotential Model. A scatter graph is outputted displaying the FL, Datetime, and ASE values to visualize the ASE pattern and compliance throughout the flight duration. The algorithms' accuracy is evaluated against the method adopted by China RMA comparing the Mean ASE values returned 98.84% accuracy using the same dataset. Further studies require incorporating the algorithm into the real-time Air Traffic Controller System and can be further improved with the Big Data Analytics approach in the future when it comes to processing more volume and variety of data.

Keywords: Altitudes, ASE, ADS-B, Geoid Undulation, Computer Algorithm

MENGUKUR KERALATAN SISTEM ALTIMETRIK UDARA DENGAN MENGGUNAKAN DATA PENGENDALIAN AUTOMATIK-DATA BROADCAST

ABSTRAK

Organisasi Penerbangan Awam Antarabangsa (ICAO) memperkenalkan *Reduced Vertical Separation Minima (RVSM)* secara global untuk menyokong peningkatan jumlah lalu lintas di ruang udara. Focus RVSM ialah pengurangan pemisahan menegak minimum dari 2000 kaki kepada 1000 kaki di antara tahap penerbangan FL290 dan FL410. Implementasi RVSM menekankan ketepatan avionik pesawat yang melaporkan ketinggian dan memerlukan Agensi Pemantauan Wilayah (RMA) memantau prestasi ketinggian pesawat (HKP) untuk memastikan keselamatan penerbangan ruang udara mereka. Pada masa ini, navigasi dan lalu lintas pesawat di udara dikendalikan oleh pengawal lalu lintas udara di darat berdasarkan nilai ketinggian tekanan tang dikenali sebagai tahap penerbangan *(FL) yang* diukur dengan altimeter barometrik. Ketinggian tekanan tertakluk kepada ralat disebabkan oleh pelbagai faktor termasuk kecacatan instrumen, aliran udara terhalang, kehadiran bahan asing ke dalam sistem, variasi suhu dan kelembapan. Ralat Sistem Altimetri (ASE) adalah perbezaan antara ketinggian sebenar berdasarkan unit SI dan ketinggian tekanan yang dipaparkan. ASE memberi risiko kepada industry penerbangan kerana ia tidak dapat dilihat oleh juruterbang semasa penerbangan. Menurut ICAO, nilai ASE mestilah kurang dari 245 kaki untuk memastikan keselamatan pesawat. Pada masa ini, beberapa RMA yang menerapkan RVSM di ruang udara mereka, memasang Unit Pemantauan Tinggi (HMU) di darat untuk memantau HKP pesawat di ruang udara. Walau bagaimanapun, kaedah ini memerlukan kos pelaksanaan dan penyelenggaraan yang tinggi, skalabilitas yang rendah dan memerlukan profesional pada

masa penerbangan di atas kapal untuk mengendalikan peralatan tersebut. Sebagai alternatif, penyelidikan ini bertujuan untuk mengukur ASE menggunakan data ketinggian geometri dari maklumat Siaran Pengawasan Tanggungan Automatik (ADS-B) yang dihantar ke Kawalan Trafik Udara (ATC) yang terletak di darat. Pesawat di wilaya-wilayah berbeza telah diarahkan untuk dilengkapi dengan transponder oleh pihak berkuasa masing-masing. Oleh itu, data ADS-B yang sedia ada boleh digunakan untuk mengkaji HKP pesawat. Penyelidikan ini mengenal pasti proses untuk mengukur nilai ASE menggunakan data ADS-B. Selepas itu, algoritma komputer dan alat perantara dibangunkan. Alat ini membolehkan mana-mana orang peribadi dengan celik komputer asas dan mempunyai akses kepada alat dan fail data untuk memproses data dan menilai HKP penerbangan dengan mudah. Algoritma ini membaca input fail data ADS-B dan menyimpan semua medan-medan penting untuk diproses untuk satu atau kesumua penerbangan dan akhrnya ASE dikira. Nilai ASE dikira dengan menolak Tahap Penerbangan daripada Ketinggian Ortometrik pesawat. Ketinggian ortometrik dikira menggunakan Ketinggian Geoid yang diperoleh menggunakan Model Geopotential EGM96. Output graf serakan akan memaparkan FL, Masa dan nilai ASE untuk menggambarkan corak ASE dan pematuhan sepanjang tempoh penerbangan. Ketepatan algoritma ini dinilai berdasarkan kaedah yang diguna pakai oleh RMA China yang membandingkan nilai purata ASE menunjukkan ketepatan 98.84% menggunakan set data yang sama. Kajian lanjutan memerlukan algoritma ini digabungkan ke dalam Sistem Pengawal Lalulintas Udara masa nyata dan boleh dipertingkatkan lagi dengan pendekatan Analitis Data Besar pada masa hadapan apabila ia melibatkan pemprosesan data yang lebih banyak dan pelbagai.

Kata-kata kunci: Ketinggian, ASE, ADS-B, Lendar Geoid, Algoritma Komputer

ACKNOWLEDGEMENTS

Firstly, I would like to express my heartfelt gratitude to God for his blessings throughout my research journey.

I would like to also thank my former and current research supervisors Dr. Busyairah Syed Ali, Associate Professor Dr. Zarinah Binti Mohd Kasirun and Associate Professor Dr. Mumtaz Begum Binti Peer Mustafa of the University of Malaya's Faculty of Computer Science and Information Technology. My heartfelt appreciation and gratitude for their trust and guidance throughout my research work. I consider myself extremely fortunate to have worked with these three supervisors and guided me along the way for the completion of the research.

Last, but certainly not least, I would like to express my gratitude to my family, friends and colleagues for their unwavering support and encouragement. I believe my late parents would be proud of this achievement and would be blessing me. It would have been an impossible task to complete my research without the assistance and care of each of them.

Many thanks.

TABLE OF CONTENTS

LIST OF FIGURES

LIST OF TABLES

LIST OF SYMBOLS AND ABBREVIATIONS

AAD	:	Assigned Altitude Deviation
ADS-B	:	Automatic Dependent Surveillance-Broadcast (ADS-B)
AGHME	:	Aircraft Geometric Height Measurement Element
AHMS	:	ADS-B Height Monitoring System
AHMS	:	ADS-B Height Monitoring System
ANOVA	:	Analysis of Variance
ARD	:	Altitude Recording Device
ASE	:	Altimetry System Error
ATC	:	Air Traffic Control
CAA	:	Civil Aviation Authority
CFIT	:	Controlled Flight into Terrain
DCA	:	Department of Civil Aviation
EGM96	:	Earth Gravitational Model
EGPWS	:	Enhanced Ground Proximity Warning System
FAA	:	Federal Aviation Administration
FCS	:	Flight Control System
FCU	:	Flight Control Unit
FL	:	Flight Level
FOM	:	Figure of Merit
FTE	:	Flight Technical Errors
GM	:	Geodetic Mission
GMU	:	GPS-based Monitoring System
GNSS	:	Global Satellite Navigation System
GPS	:	Global Positioning System
GPS	:	Global Positioning System
HAMSL	:	Height Above Mean Sea Level

HKP	:	Height Keeping Performance
HMU	:	Height Monitoring Unit
HPL	:	Horizontal Protection Level
ICAO	:	International Civil Aviation Organization
ISA	:	International Standard Atmosphere
MCP	:	Mode Control Panel
MSL	:	Mean Sea Level
NAC	:	Navigational Accuracy Category
NAT	:	North Atlantic
NGA	:	National Geospatial-Intelligence Agency
NIC	:	Navigational Integrity Category
NUC	:	Navigational Uncertainty Category
PIRG	:	Planning and Implementation Regional Group
PTU	:	Port Transducer Units
QNH	:	Regional or airfield pressure setting
RMA	:	Regional Monitoring Agency
RVSM	:	Reduced Vertical Separation Minima
SLR	:	Satellite Laser Ranging
TAWS	:	Terrain Avoidance Warning System
TDOA	:	Time Difference of Arrival
TDRSS	:	Tracking and Data Relay Satellite System
TVE	:	Total Vertical Error
TVU	:	Total Vertical Error Monitoring Unit
WAAS	:	Wide Area Augmentation System

LIST OF APPENDICES

CHAPTER 1: INTRODUCTION

1.1. Research Introduction

The International Civil Aviation Organization (ICAO) globally implemented the Reduced Vertical Separation Minimum (RVSM) to accommodate growing traffic volumes in congested airspace. The aircraft altitude reported by the procedure stress on the aircraft avionics accuracy. RVSM is primarily focused on reducing the minimum vertical separation between flight levels 29000 feet (FL290) and 41000 feet from 2000 feet to 1000 feet (FL410).

Based on pressure altitude, air traffic and aircraft navigation are monitored and controlled by the controllers on the ground. This is also known as a flight level (FL), measured by an aircraft barometric altimeter. On the other hand, RVSM mandates that the aircraft's height-keeping performance be monitored (HKP).

The difference in altitude between the actual and pressure altitudes is called the Altimetry System Error (ASE) (McFadyen, Aaron; Martin, Terrence 2018). The nonstandard temperature and pressure of the atmosphere and instrument error can all contribute to the pressure altitude error. As per the ICAO recommendation, the ASE value must be less than 245 feet to ensure aircraft safety.

Presently, Height Monitoring Unit (HMU) has been installed on the ground by some airspace operators. This is to monitor the aircraft's performance in maintaining its altitude in the airspace. For the ASE measurement, the HMUs using geometric height derived from multi-literate technology. However, this method is low scalability, costly, and is challenging to cover the entire airspace.

1.2 Research Background

The primary motivation for this research is the high number of previous aviation incidents involving aircraft accidents and incidents caused by altimetry system error. Hence, it is significant to have an accessible tool and algorithm to calculate ASE and track the aircraft performances. Additionally, the existing methods for determining ASE are prohibitively expensive and complicated. Furthermore, Malaysia currently lacks an ASE monitoring system. Chapter 2 contains a detailed analysis of the accidents and their safety consequences.

1.3 Problem Background

1.3.1 Aviation Safety

The airspace is always congested as it is shared between many international flights, domestic flights, and jets. As the airspace usage demand snowballing every year, it is very crucial to enhance the safety features. The Reduced Vertical Separation Minima (RVSM) was implemented to accommodate increased air traffic in our airspace. The decrease of separation between aircraft increasing the safety risk. Thus, it is very significant to ensure the aircraft flying based on the flight region's pressure altitude at the flight time.

1.3.2 Requirements to Perform HKP Monitoring

ASE's presence causes the flight level observed by the pilot, and the controller could differ from the actual flight level. Hence, this might result in the aircraft deviating from the actual flight level and subsequently exposing the aircraft with a high risk to collide with another aircraft that shares the same airspace and flying at the same actual flight level. Thus, height-keeping performance monitoring needs to be done to avoid any fatal crash. The aircraft height-keeping performance can be verifying by check the difference between the aircraft pressure altitude against the aircraft geometric height.

1.3.3 Drawbacks of the Current ASE Monitoring Systems

Besides that, there are several shortcomings with the ASE obtained from existing monitoring systems such as Aircraft Geometric Height Measurement Element (AGHME), GPS-based Monitoring System (GMU/EPMU), and Height Monitoring Units (HMU). The HMU requires a wide area of coverage and installation on ground stations, which is costly. The GMU/EPMU requires a professional to be on board to operate the device and only applicable to that single flight. The AGHME only be used on aircraft equipped with transponder mode S, which can overfly AGHME stations for RVSM monitoring and require a wide coverage area.

1.3.4 Limited Study for Validation of ADS-Bs' Geometric Height

Geometric height is transmitted by aircraft using either the height above mean sea level (HAMSL) or the height above the WGS 84 ellipsoid (HAE), depending on the GPS receivers. It is frequently unknown, however, which of these geoid height references was used before the analysis. This leads to incorrect measures of ASE as a flight moves across the geoid contours. Thus, before ASE calculation, it is critical to validate the geometric height in the ADS-B message to develop an objective approach for maintaining and measuring the ASE.

1.3.5 Unavailability of ASE Monitoring System in the Malaysian Airspace

This research involves validation of ADS-B geometric height used for ASE monitoring is limited to Malaysia. The development of a method or tool that uses real-time aircraft state vector or post flight data could be a game-changer for Malaysia's Department of Civil Aviation (DCA) and Malaysian aviation industry.

1.4 Problem Statement

As stated in the problem background section, it is crucial to determine the ASE of the aircraft in order to track the aircraft performances and to maintains it for long run with a low cost and accessible integrated tool. By having an accessible integrated tool will supports the Regional Monitoring Agency (RMA) in general to monitor the safety of their airspace and in particular the aircraft maintenance personals to perform maintenance activity based on the flights' Height Keeping Performance (HKP) results.

1.5 Research Aim

This research mainly aims to develop and validate a computer algorithm with an accessible integrated tool to measure Altimetry System Error (ASE) using ADS-B data.

1.6 Research Objectives

Several objectives have been formulated as following to achieve the research aims:

- To identify a process, involve in measuring ASE values using the ADS-B dataset.
- To develop an algorithm and integrated tool to calculate the Aircraft Altimetry System Error with acceptable accuracy using the selected dataset.
- To validate the performance of the developed ASE algorithm and tool in terms of accuracy by benchmarking the existing methods.

1.7 Research Questions

The following research questions have been developed in response to the research objectives mentioned previously:

Objective 1: To identify a process, involve in measuring ASE values using the ADS-B dataset.

- What are the vital elements in the identified process?
- Why this process is crucial in calculating ASE values?

Objective 2: To develop an algorithm and tool to calculate the Aircraft Altimetry System Error with acceptable accuracy using the selected dataset.

- How are the algorithm to calculates ASE is built?
- How are the algorithm integrated to a tool?

Objective 3: To validate the performance of the developed algorithm and tool in terms of accuracy by benchmarking the existing methods.

- How are the ASE results validated to checks the accuracy?

1.8 Research Scope

The scope of the research is to determine the ASE values via algorithm developed by using data contained in the ADS-B message obtained from the airspace operators (NATS) based in the United Kingdom.

1.9 Research Significant

The tool will be a milestone in Malaysia Aviation since at the time of writing, there is no ASE monitoring system being implemented in Malaysia. One of the current ASE monitoring systems is based on the ground-based Aircraft Geometric Height Measurement Element (AGHME) stations located at a fixed position and require an aircraft to fly over it to capture geometric and compute the ASE. Virtually, it is impossible to install the AGHME stations in very different locations considering the cost and space to set up the station. The developed tool can be used by the local aviation authorities or RMA as a post check whenever the aircraft did not fly over the AGHME stations. As the ADS-B coverage provides continuous data, multiple independent ASE samples are to be collected and compared for the flight health checks.

1.10 Thesis chapter overview

The first chapter focuses mainly on introducing this research work, which consists of research background, problem statement, aim, objectives, scope and significance. The second chapter, on the literature review. This chapter discusses various terms, methods, formulas and other related inputs from the research and journal papers studied. Topics discussed include altitude terms used in aviation sector, Altimetry System Error (ASE), Automatic Dependent Surveillance-Broadcast (ADS-B) and undulation of geoid to understand the current implementations, limitations and opportunities to calculate ASE. ICAO and other aviation authorities in other regions related papers and publications were also studied to understand the regulatory requirements related to aviation safety especially related to RVSM and HKP.

Chapter 3 focusses on the methodology of the research. To begin with a research methodology flowchart was developed as a framework, and each stage of the flowchart is discussed in detail throughout Chapter 3. Design diagrams related to the research are also developed and elaborates on in chapter 3.

Chapter 4 consist of the research results and discussion. In this chapter, the outcome of each objective is observed and discussed. The flow and link between the objectives with each other can be observed throughout. The algorithms output is validated at the end of the chapter. Finally, chapter 5 is the conclusion. The summary of the work, limitations, implications, and recommendations of the current work and future work are discussed in these chapters.

CHAPTER 2: LITERATURE REVIEW

2.1 Introduction

Various ICAO documents, FAA articles, and journals were read as part of the literature review to better understand civil aviation operations and regulations. Besides that, the reading, especially recent research works related to ASE also helped to understand the fundamentals of Altimetry System Error (ASE), Automatic Dependent Surveillance-Broadcast (ADS-B) and Undulation of Geoid. The knowledge of algorithms basics required for development of tool to measure the ASE via the Geoid Undulation method highlights the software engineering domain contribution to this interdisciplinary research.

2.2 Altitudes in Aviation

The altitude values indicate an aircraft's vertical position. The aviation world has always depended on the onboard barometric / pressure altimeter to provide the barometric altitude (Avionics News,2005). Assuming that pressure decreases at a constant rate as altitude increases, a calibrated barometric altimeter can calculate the vertical distance. Generally, barometric altitude is referred to as either altitude or flight level (Mode C), depending on its application in a given situation.

Geometric altitude has been used as a secondary source altitude in the cockpit via a Global Positioning System (GPS) and broadcast to ground stations via the Global Navigation Satellite System's (GNSS) Automatic Dependent Surveillance-Broadcast (ADS-B) system.

Geometric altitude is the vertical distance between an aircraft and a reference ellipsoid (Ali & Taib, 2016). To derive the geometric altitude using the trilateration method, a constellation of at least four satellites must view the GPS receiver antenna. Figure 2.1 below illustrated the difference between barometric and geometric altitudes.

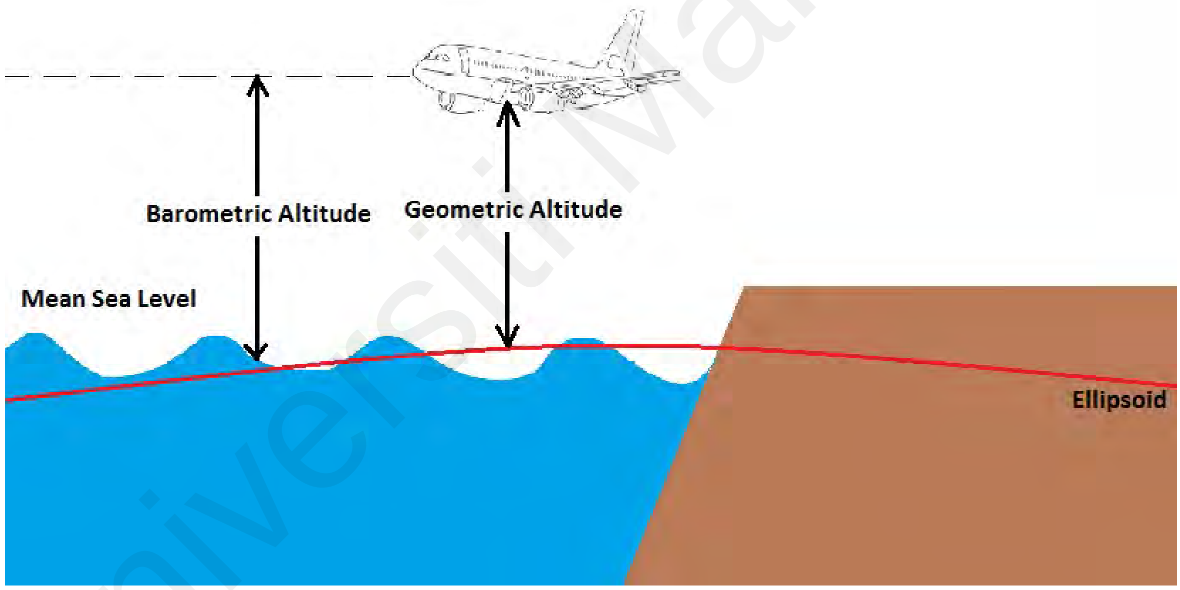

Figure 2. 1Barometric altitude and geometric altitude (Ali & Taib, 2016)

2.2.1 Barometric Altitude

The barometric altitude is derived from the barometric altimeter. The pressure changes at the aircraft static port are measured and converted into altitude in feet via the barometric method. A preset reference pressure level is used to determine the vertical height (Lehtinen,2013). QNH and QNE are two widely used and frequently used altimeter settings in modern aviation.

When the barometric altimeter is set to local QNH, an aircraft's altitude value is obtained as the vertical distance travelled above mean sea level (MSL). The mean sea level pressure at a particular place given by the air traffic controllers. A pressure altitude or flight level is the vertical height of an aircraft above a standard isobaric surface also known as the QNE standard sea level pressure of 1013.25 hPa/29.92 in Hg at 15°C) (ICAO, 2012).

Absolute altitude is another method of determining the altitude of an aircraft that is still used in some regions. Absolute altitude, or simply height, is measured in feet and is obtained from radar altimeters (IVAO, 2015). At touchdown, the altimeter should read zero if it is properly calibrated. Figure 2.2 below illustrates the different references for the barometric and absolute altitudes.

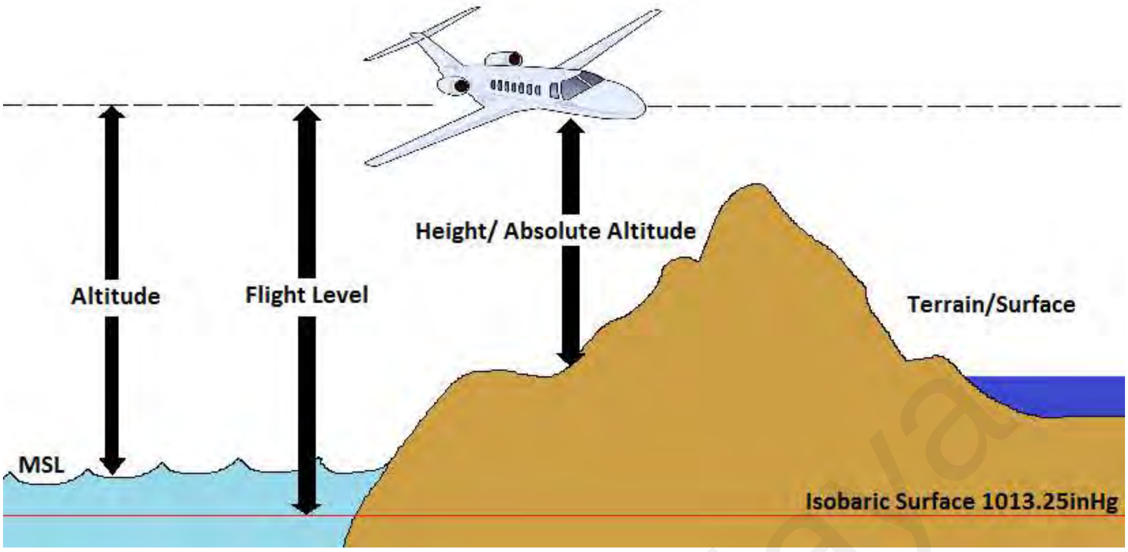

Figure 2. 2: References of barometric and absolute altitude (IVAO, 2015)

2.2.2 Geometric Altitude

Geometric altitudes are usually measured using GPS. It indicates the vertical distance of an aircraft from a reference ellipsoid or a reference geoid depending on the type of Global Navigation Satellite Systems (GNSS) receiver (Ali & Taib, 2019). GNSS provide the capability for aircraft to measure their altitude using satellite signals and is completely independent of barometric pressure (IFATCA Technical and Operations Committee (TOC), 2015).

The information is provided to ATC via ADS-B broadcast and provided to the pilot via a GNSS receiver. The ADS-B aircraft surveillance system uses INS (or GNSS) as its primary position source on the aircraft.

2.2.3 Utilization of Altitude

While the altitude values are fundamentally distinct, each one is fully utilized to perform critical tasks in modern aviation for navigation, safety, standards and procedures.

2.2.3.1 Aircraft Navigation

Pilots have long used barometric altitude to determine the aircraft's vertical position (Fisher, 2014). The pilot's altimeter setting must be adjusted to reflect the aircraft's position above or below the transition latitude (Jan, Gebre-Egziabher, Walter & Enge, 2002). As illustrated in Figure 2.3 below, an aircraft's vertical position is maintained by utilizing altitudes below the transition altitude and flight levels above the transition altitude. In the transition layer, no cruise phase is permitted.

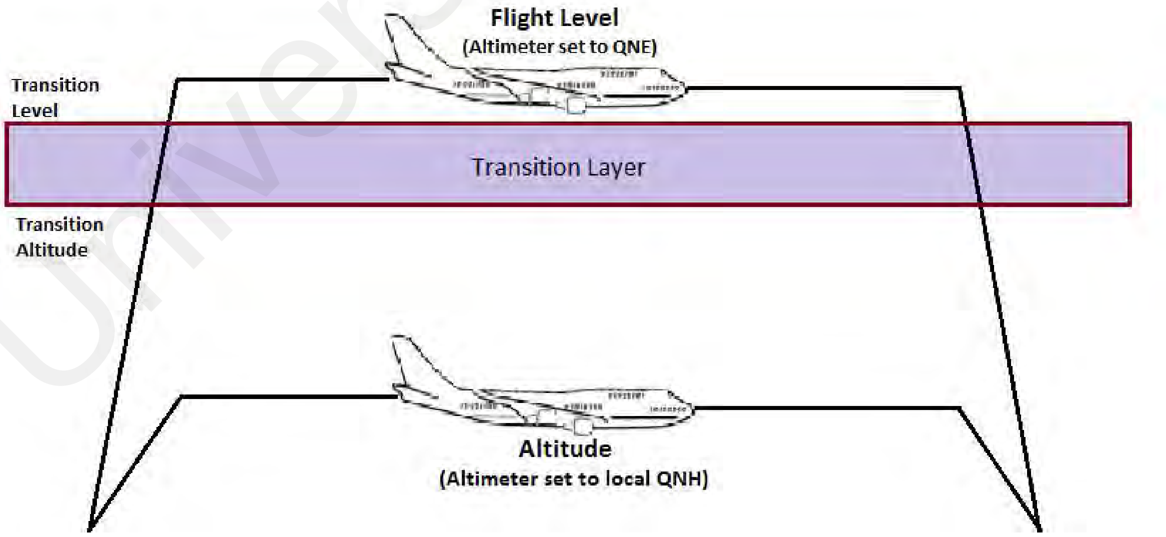

Figure 2. 3: Aircraft transition level and layer (Fisher, 2014)

When set to QNE, the altimeter displays aircraft flying above the transition altitude in flight level Mode C (pressure altitude). Except when the standard isobaric surface and mean sea level are identical, the flight level usually is inaccurate concerning the actual altitude above mean sea level (MSL). However, because all aircraft above the transition altitude is attuned using the same standard altimeter setting, temperature and atmospheric pressure variations will affect the aircraft equally (IVAO, 2015).

For aircraft flying below the transition altitude, the altimeter will be set to local QNH using the ATC-supplied local sea level pressure. Thus, the altimeter will display an aircraft's vertical elevation above the region's mean sea level. This altitude information is critical for the pilot, particularly for avoiding collisions during low-level flying because of terrain and obstacle elevations about the Mean Sea Level (Jong, 2010). The local QNH based on the lowest QNH value derived in the region, and it is based on the local altimeter pressure setting. Once the aircraft enters a new QNH pressure region, the altimeter will need to be updated.

2.2.3.2 Aviation Safety

Around two-thirds of Controlled Flight into Terrain (CFIT) accidents are caused by altitude error and a lack of vertical situational awareness (CFIT, 1999). In an accident involving Jetstream 31 the altimeter was set to 29.82inHg rather than 28.84inHg (ATSB, 1999). The pilot became aware of the setting error when he noticed a visual of nearby water waves. The aircraft was flying at a lower altitude of 400 feet than the intended 1400 feet. Geometric altitude is currently valuable for the Enhanced Ground Proximity Warning System (EGPWS) for situational awareness purposes. When combined with other air data signals such as absolute altitude, ground speed, pressure altitude, position, roll angle, and terrain and runway elevation data, the real-time accuracy of GPS-derived geometric altitude can be improved.

Geometric altitudes derived from multiple sources using this blending algorithm are more precise than those derived from a single source (AlliedSignal, 1999). Thus, extending the life of the EGPWS protects aircraft in the event of terrain conflict (Wiolland,2007) because geometric altitude is insensitive to temperature and pressure variations, particularly on long-haul flights, altimeter setting error, varying altimetry system standards and human error, all of which contribute to CFIT accidents, the EGPWS can continue to operate.

Additionally, geometric altitude can be used to cross-check for any barometric altitude deviations, such as those associated with severe weather conditions. This is necessary to ensure flight safety and the barometric altitude's validity.

The radar altimeter is a critical component of the Terrain Avoidance Warning System (TAWS). The absolute altitude information provided by radar altimeter technology may alert pilots to close terrain or to the fact that the aircraft is flying too low. When flying at low altitudes or in mountainous areas, the radar's absolute altitude is more critical than its elevation above mean sea level.

When down-linked by radar, the actual flight level (Mode C) and the selected altitude (level) are two different types of altitude data. The selected altitude is transmitted via the downlinked Mode S and is controlled by the Mode Control Panel (MCP) or Flight Control Unit (FCU), which also controls the aircraft's autopilot system. The altitude chosen should correspond to the altitude cleared by ATC (Barhydt & Warren,2002). The critical point is that the selected altitude represents the pilot's intended altitude, not the aircraft's actual altitude.

Historically, the only altitude used in ATC operations is the flight level (Mode C) in order to maintain the desired vertical separation between aircraft. To ensure that ATC can safely separate two adjacent aircraft vertically, regardless of their origin or destination, it is critical to use flight levels with the same standard altimeter setting.

It has been demonstrated that the intent information derived from Mode S selected altitude is reliable for enhancing flight safety, such as mitigating the risk of the level bust for aircraft that do not fly at their assigned level. When comparing the aircraft's altitude to the altitude specified by ATC for clearance altitude, apparent differences in altitude between the two altitudes can easily be spotted and communicated to pilots (Barhydt&Warren,2002).

2.2.3.3 Separation Standards of Aircraft

The daily average of flight passengers exceeded 9 million in 2014, and the figure has been steadily increasing each year (Kostas Iatrou, 2014). The North Atlantic (NAT) Region implemented the Reduced Vertical Separation Minimum (RVSM) on 27 March 1997 to accommodate a growing demand for air travel (Pilotext, 2008).

Between flight levels 290 and 410 inclusive, RVSM reduces aircraft vertical separation from 2000 to 1000 feet. As a result, six additional cruising levels were added, including FL300, FL320, FL340, FL360, FL380, and FL400, reducing in-flight delays while increasing air traffic capacity, fuel competence, and controller flexibility when rerouting aircraft in RVSM airspace (Pilotext, 2008).

RVSM has been implemented successfully on a global scale to date. With the adoption of the novel separation standard, all aircraft operating in RVSM airspace must adhere to the RVSM monitoring system outlined in ICAO Doc 9574 to ensure the security and viability of RVSM operations (Portugal,2003).

The monitoring system evaluates an aircraft's ability to maintain its assigned spacing interval with other aircraft, and calculate the aircraft's Altimetry System Error (ASE). The geometric altitude or height of the aircraft and the barometrically determined flight level are two critical components of ASE calculations.

Figure 2.4 below shows the The Flight Level Allocation Scheme (FLAS) of China RMA which also indicated the RVSM airspace.

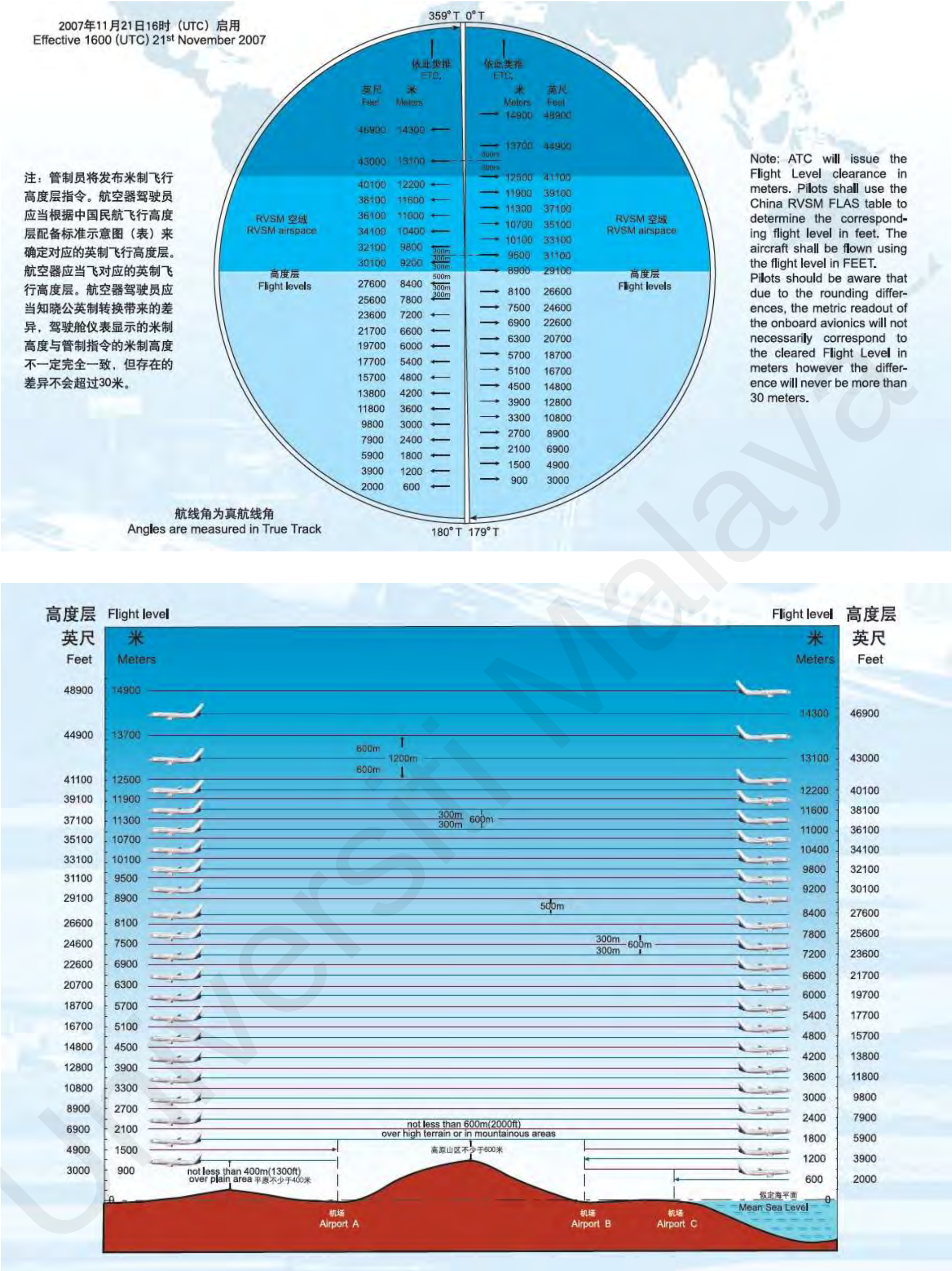

Figure 2. 4: The Flight Level Allocation Scheme (FLAS) (CHINA RMA)

2.2.3.4 In-Trail Procedure (ITP)

The Automatic Dependent Surveillance-Broadcast (ADS-B) In-Trail Procedure (ITP) application provides aircraft equipped with ADS-B receivers and onboard automation with flight level change flexibility (ICAO,2017). ADS-B ITP supports six different flight levels; leading the climb, following the climb, combining the climbs, leading the descent, following the descent, and combining the descents.

Aircraft flying below the recommended altitude require to request an ITP altitude. The altitude variation could be caused by information about the flight's altitude, identification, position, and ground speed received from nearby ADS-B-equipped aircraft. When the aircraft's altitude is adjusted appropriately, it can fly at a more competent level and save fuel. Figure 2.5 below illustrates the working principle of the ITP.

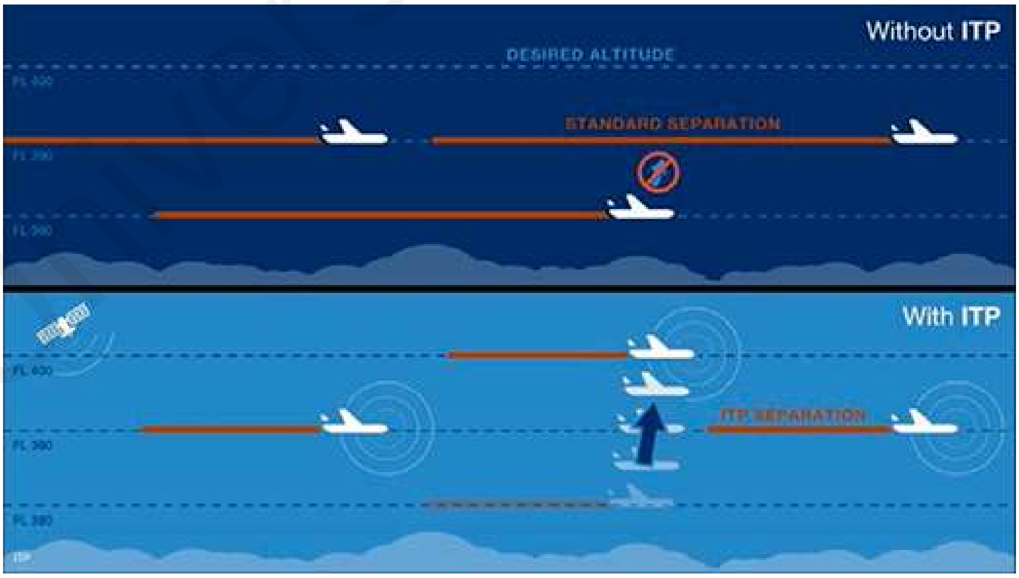

Figure 2. 5: Working principle of the ITP (FAA)

2.2.4 Barometric Altitude Limitation and Geometric Altitude Potentials

Many aircraft utilize barometric altimeters because they are common in aviation. However, it does have some remaining limitations that must be addressed. This has introduced many new research and ideas to utilize geometric altitude and avoid reliance on a single data source.

Calibrating the barometric altimeter whenever changing between standard and QNH pressure settings is necessary to prevent confusion. Furthermore, using the wrong altimeter setting could result in possible level busts (Jong, 2010). Higher QNH settings during takeoff and landing causes decreased levels at lower altitudes (IVAO,2015). Attained height can be calculated using GPS, and without needing an altimeter setting calibration, it will be free of human error or inaccurate setting.

In addition, the QNH altimeter setting is inaccurate close to the location where ATC broadcasts QNH information. When the aircraft is farther away from the QNH-measuring station, the accuracy will diminish (CFIT,1999). As geometric altitude is not subject to pressure levels and altimeter settings, its accuracy and sensitivity do not degrade (Jong,2010). Higher levels are always available when using the geometric altitude in RVSM airspace.

Furthermore, the altimeter has the formula from the ICAO's Standard Atmosphere hard-wired into it, and thus accuracy of the altimeter will be impacted whenever the atmospheric conditions are different from those assumed as the standard. The geometric altitude is overpowered over barometric altitude due to how it is dependent on atmospheric conditions. Thus, regardless of the weather conditions, the geometric altitude remains accurate (Jong, 2010). However, due to interference and multipath, GPS signals are vulnerable to interferences and multipath. It follows that total signal loss is not impossible (Wiolland,2010).

On the other hand, altitude data is readily available when using a barometric altimeter because it does not require satellites or power. Despite this, the accuracy of the barometric altimeter can be affected by the amount of humidity in the air due to the effect of humidity on the pressure lapse rate (Iatrou, 2014). While the conventional barometric altimeter is reliable, its reliability is negated by the routine monitoring and maintenance required throughout the surface area near the static port, condensation traps, and drains (Jong, 2010).

There is no technical reason why geometric altitude cannot be used by pilots and controllers in the future (Pilotext, 2008). One of the most crucial elements in calculating ASE is geometric altitude. The statistical analysis conducted by Portugal; N. (2003) compared the data of aircraft height from ADS-B with an Enhanced GPS Monitoring Unit (EGMU). The results proved that WAAS-enabled ADS-B data provides sufficient accurate geometric altitude information to calculate aircraft ASE (Portugal, 2003).

In 2008, as part of the follow-up investigation, the research team conducted a second study, the results demonstrated that using geometric altitude data from WAAS-disabled 1090ES equipment was sufficiently accurate for estimating aircraft ASE in uncontrolled conditions (AIS, 2008).

There is a new study done in 2010 that looks at the differences between the geometric altitude data from EGMU and ADS-B using an ANNOVA. Data are obtained from the EGMU and ADS-B sources simultaneously. The study found no significant difference between the altitudes given by each source.

Thus, ADSB geometric altitude fulfils the criteria for HKP monitoring (AIS, 2011). Some countries such as Australia use ADS-B geometric altitude to calculate aircraft's Altimetry System Error (ASE) for HKP monitoring (ICAO, 2002).

Geometric altitude is helpful for situational awareness purposes, and when combined with other air data, GPS-derived geometric altitude can be improved. When combined with other air-data signals, the geometric altitude is also more accurate than any single source (FAA, 2009).

Additionally, it was discovered that the geometric altitude is helpful in verifying the reasonableness of altitude data, such as the barometric altitude (FAA, 2009). Finally, geometric altitude may be beneficial for performing a cross-check on the safety and the validity of barometric altitude, for example, during extreme weather conditions.

2.3 Altimetry System Error (ASE)

The term "Altimetry System Error" has numerous definitions. According to ICAO Doc 9574, the Altimetry System Error (ASE) is the difference between the indicated altitude on the altimeter display and the pressure altitude equivalent to continuous ambient pressure (ICAO,2020).

In a simplified word, ASE is the difference between altitude, which air traffic controller, pilot and aircraft monitoring system believe the aircraft to be and the actual altitude (ICAO, 2020). Additionally, the Federal Aviation Administration (FAA) defines ASE as an "invisible risk" that occurs when the pressure altitudes displayed to the aircraft crew differ from the International System of Units (1013.25 hPa) (FAA, 2019). The ASE evaluates an aircraft's capability to convert still pressure to an equivalent height in feet to the ISA model (Martin et al., 2008).

The relationship between various aircraft technical error components is depicted in Figure 2.6 below. The Total Vertical Error (TVE) is calculated as the sum of the aircraft's Flight Technical Errors (FTE) and Aircraft Specific Errors (ASE). FTE is the variance between the altimeter reading and the cleared altitude assigned by the ATC in terms of displayed altitude. The Assigned Altitude Deviation (AAD) is the variance between the assigned altitude and the pressure altitude of the ATC's transponder. ASE values can differ significantly for a single aircraft or an entire group of same type aircraft.

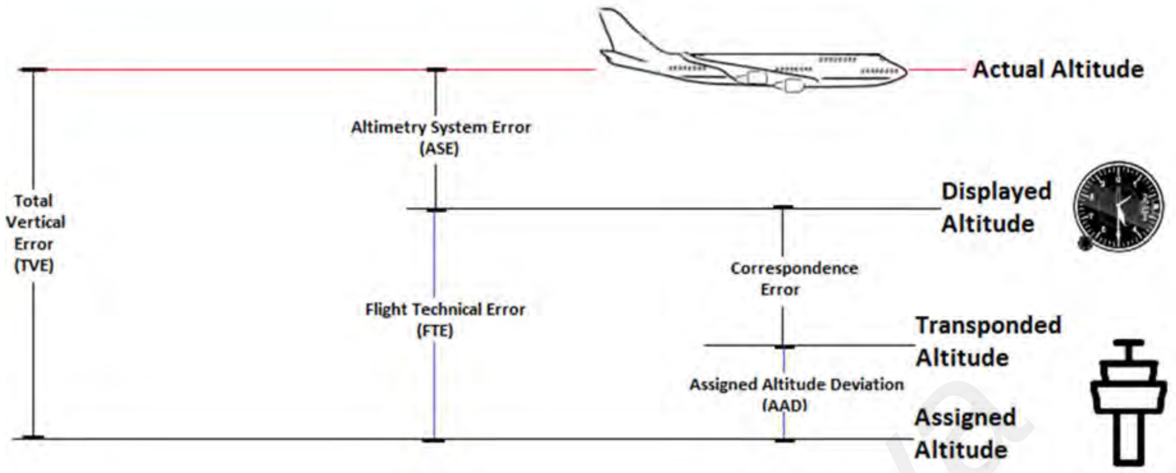

Figure 2. 6: Various aircraft technical error components (Falk et al., 2010)

2.3.1 Error sources for ASE calculation using ADS-B

The altimeter is a pressure-sensitive pitot-static system instrument. It calculates the aircraft's altitude about static pressure, also known as ambient pressure. Static pressure exists regardless of whether the aircraft is in flight or at rest. It is typically equivalent to the local barometric pressure in the area (FAA, 2003)

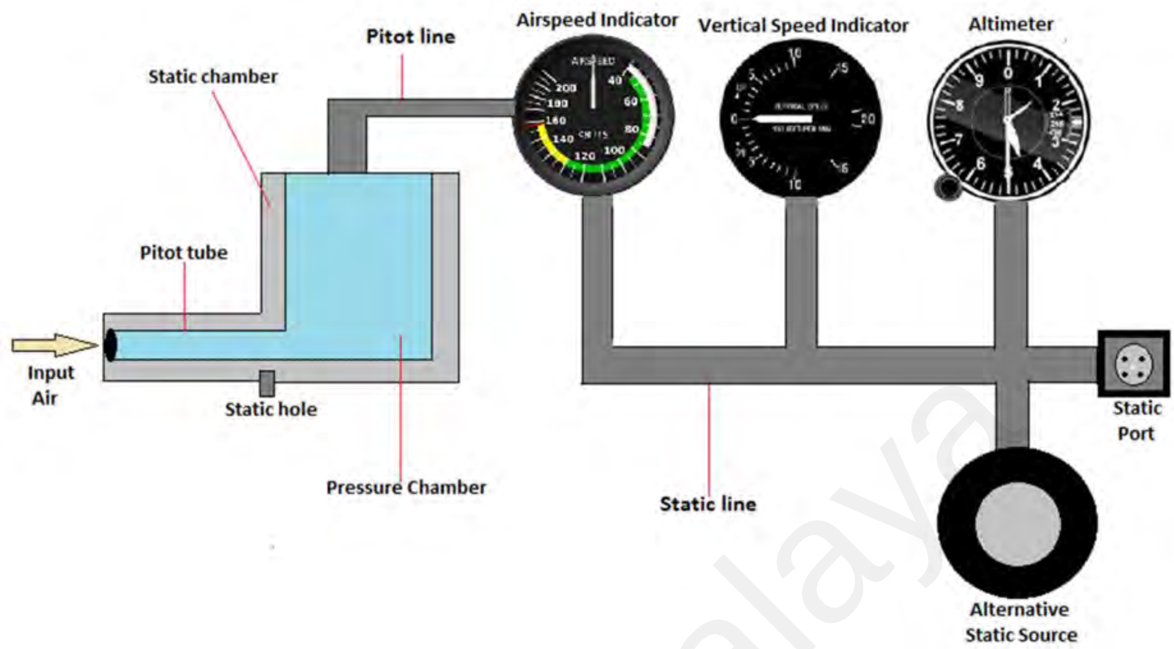

Figure 2. 7: Pitot-static system schematic (AOPA,2018)

The pitot-static system is schematically depicted in Figure 2.7. The static port, typically placed on the aircraft's fuselage side, is used to obtain static pressure. The static line is used to introduce static pressure into the altimeter. As a result, any impediment or damage to the static port distorts the flow of air past the static port, impairing the static probe's ability to accurately detect the actual static pressure, resulting in incorrect altitude readings. Certain modifications to the airframe, such as painting or mounting accessories near the static port, may impair the delicate airflow (Abdullah, 1995).

Additionally, the static port can become blocked for various reasons; the most frequently identified issues include foreign material entry into the system, such as water or insects, and airframe icing during cold temperatures, causing the static port static line to freeze over. Any deformations to the aircraft's fuselage skin around the static port area also affect the aircraft's ability to detect static pressure properly due to the obstructed airflow. The damage could have occurred during regular flight operation or could have occurred simply due to the inevitable failure of any component of the static-pitot system. Other factors, such as aerodynamic loading during flight, temperature variations, and humidity, may also contribute to pressure sensing being inaccurate (FAA, 2014).

This type of error is called Altimetry System Error (ASE) because it is not visible to pilots. An aircraft's ASE value is not always stable. Thus, unchecked aircraft will inevitably degrade their ASE value over time, which, if not corrected, will cause the aircraft to diverge from its intended flight level without the pilot's or ATC's knowledge (Australia, 2011). There are numerous errors can result in the ASE. Three primary sources of error exist are quantization error, meteorological error, and incorrect height datum.

2.3.1.1 Quantization Error

The pressure altitude and geometric height fields in an ADS-B data message have a finite bit length, which causes quantization error. Both sets of data are broadcast in a 25ft quantization format. A rounding error can occur as a result of the error. During takeoff, this mistake can be reversed.

2.3.1.2 Meteorological Error

Meteorological error, defined as a poor fit of the actual atmosphere to predicted meteorological data, is almost certainly the cause of an aircraft's ASE time series. The mean of a statistically large number of data may be used to predict ASE. However, in some geographical regions, local error due to disruption of meteorological data and error due to diurnal/seasonal changes in the atmosphere can be a root cause of error for ASE estimation.

The pressure altimeters have been set to ISA specifications. Errors will occur if the ISA norm is not followed. The measured minimum safe altitudes / heights must be modified when the atmospheric temperature on the surface is far lower than that expected by the standard atmosphere, according to ICAO PANS-OPS (Doc 8168).

An aircraft would be lower than the altimeter reading when the temperature is less than ISA. For example, if the OAT is - 40 °C, the true altitude for a 2000 ft indicated altitude is 1520 ft, resulting in less terrain separation than predicted and posing a danger of obstacle clearance. The pilot in charge of applying the corrections must notify ATC of the corrections he or she plans to apply. If the pilot fails to apply the correction, ASE can result.

2.3.1.3 Incorrect height datum

The geometric height derived from GPS in an ADS-B message can be HAE (Height Above Ellipsoid) or HAMSL (Height Above Mean Sea Level), depending on the GPS receiver installed on an airframe. The height datum information is not found in ADS-B message. Hence, the methodology to distinguish the height datum using geometric height is missing.

The difference between HAE and HAMSL is Earth's gravitational field. Generally, when a flight crosses geoid contours, the appropriate datum height can be chosen. Additionally, it can be challenging to discern the correct route on which flights follow geoid contours consistently. According to statistics, the distribution of ASE data with an incorrect height datum is wider than the distribution of ASE data with the precise one.

2.3.2 Height Keeping Performance Monitoring in detecting ASE

With the current global use of RVSM, airspace has become even more congested, and aircraft are at an increased risk of colliding due to their proximity. This emphasizes the critical nature of performing height-keeping performance (HKP) monitoring to determine the aircraft's ability to maintain the cleared altitude assigned by the ATC.

The Altimetry System Error (ASE) is a metric used to determine an aircraft's ability to maintain its altitude. According to ICAO, aircraft flying in RVSM airspace must have an average ASE value of fewer than 80 feet in magnitude and less than 245 feet in absolute value (Martin, Falk & Perez,2008). In comparison, a group of identical aircraft must have an average ASE value of fewer than 80 feet and a total value plus three standard deviations of a lesser than 245 feet (Falk, Gonzalez & Perez,2010).

If aircraft do not adhere to the stringent ASE requirement, they will be denied access to RVSM airspace. The Regional Planning and Implementation Group (PIRG) of the International Civil Aviation Organization (ICAO) establishes the Regional Monitoring Agency (RMA) to ensure the safe implementation and continued operation of RVSM in the regions where it is used. All RVSM height-keeping performance monitoring programs are the responsibility of RMAs (ICAO,2002).

2.3.3 Regional Monitoring Agency (RMA)

Regional Monitoring Agencies (RMAs) have been established in all regions where RVSM has been implemented. Data monitoring was conducted by RMA every month by exchanging the monitoring data. Every successful monitoring is merged with AGHME and can be found on the web under RVSM approvals.

The Regional Monitoring Agency (RMA) is in charge of aircraft that operate within the RVSM. Additionally, the RMA is responsible for enforcing RVSM requirements and conducting airspace safety evaluations in accordance with the ICAO Regional Planning Group's directives (ICAO, 2011).

The height-keeping performance data captured continuously and closely monitored for any ASE events. RMA develops and maintains a database of aircraft authorised to operate in RVSM airspace in that zone. In the following circumstances, the aircraft was found to be non-compliant:

i. TVE ≥ 90 m (300 ft.)

ii. ASE ≥ 75 m (245 ft.)

iii. AAD ≥ 90 m (300 ft.)

RMA plays a critical role in this process by taking appropriate action to ascertain the probable cause of the height deviation and verifying the operator's approval status. The data is being analysed to determine trends in height deviation. The risk level under surveillance establishes a mechanism for collating and analysing all reports and deviations of 300ft—the root cause of each deviation and its size and duration are determined.

The occurrence frequency is determined. The risk assessment of the system compares its performance to the system's overall safety objectives. RMA verifies that only approved aircraft operate in applicable RVSM airspace; it identifies and notifies unapproved operators and aircraft operating in RVSM.

2.3.4 Existing Methods Used to Measure ASE

The ASE value indicates the aircraft's altimetry system's accuracy (MAAR,2015). ASE is not detectable during normal aircraft operations, and calculating aircraft ASE requires a specialized height monitoring system.

At the moment, several specialized types of equipment are available for independently measuring ASE to monitor height-keeping performance that includes the Height Monitoring

Unit (HMU), GPS Monitoring Unit (GMU) ,Aircraft Geometric Height Measurement Element (AGHME) and ADS-B Height Monitoring System (AHMS).

The most novel technique is the ADS-B Height Monitoring System (AHMS), which is currently being extensively tested to determine its suitability for monitoring HKP. These monitoring systems rely on aircraft being in the air to monitor the HKP (FAA,2014). Meteorological data is also required to determine the geometric height of the assigned flight level that corresponds to the time and location of the aircraft's ADS-B reports (Falk et al., 2010).

In 1997, a study compared HMU and GMU as HKP monitors (Martin et al., 2008). The results indicated that both units' geometric height and flight level values were on average 10 and 50 feet apart. As a result, the TVE of the two monitoring units varied by an average of 40 feet. The variances were caused by each system's unique meteorological data and processes. In general, the two systems performed similarly to the height-keeping performance monitoring tool.

Table 2.1 below shows the summary of existing methods being applied for monitoring the ASE value.

Table 2. 1 : Methods being applied for monitoring the ASE value.

No.	Method	Country
No. 1	**Method** Height Monitoring Unit (HMU) (CAA, 2014)	**Country** Austria, Germany, Switzerland
	Description The HMU determines an aircraft's geometric height and position based on the signals received from the aircraft's SSR transponder, which responds to radar station interrogations. The data collection process will result in TVE (Total Vertical Error), AAD (Assigned Altitude Deviation), and ASE (Altimeter System Error) readings for each aircraft measured.	
	Limitations • Need a wide area of coverage, but the installation of ground stations is costly. • Sometimes, an aircraft needs to fly a long distance to overfly the HMU station. • Fixed site requires meticulous planning on the locations selected.	
No. 2	**Method** GPS Monitoring Unit (GMU) / Enhanced GPS Monitoring Unit (EGMU) (Authority, 2002)	**Country** USA, Australia, China, Thailand
	Description The GPS monitoring unit collects data from the aircraft's systems directly. To determine ASE, flight data was processed with GPS differential corrections and meteorological data.	
	Limitations • A professional must be onboard to operate the device • Not very effective in terms of cost and time • Can only measure a single flight.	
No. 3	**Method** Aircraft Geometric Height Measurement Element (AGHME) (Martin et al., 2008)	**Country** USA, Canada
	Description Aircraft equipped with Mode S transponder. The AGHME system estimates only aircraft geometric height through post-processing using meteorological and mode S data to estimate TVE, ASE and AAD.	
	Limitations • Only able to read aircraft with Mode S transponders • Need a wide area of coverage • Sometimes, an aircraft needs to fly a long distance to overfly the AGHME station	

No.	Method	Country
4	ADS-B Height Monitoring System (AHMS) (CAA, 2014)	United States, Australia, China, and Asian RVSM regions
	Description It utilizes ADS-B receivers to obtain geometric height data from ADS-B-equipped aircraft in order to calculate ASE.	
	Limitations • Aircraft needs to flies within coverage area.	

2.3.4.1 Height Monitoring Unit (HMU)

The Height Monitoring Unit (HMU) is a ground-based monitoring system that consists of two major components: a height monitoring element (HME) computer and a total vertical error monitoring unit (TVU) computer. Due to their wide operational area of coverage, Height Monitoring Units (HMUs) can locate multiple aircraft concurrently. The HMU monitoring system measures aircraft height in a circular area using a central site with several fixed ground stations and four additional receivers arranged in a square. The typical HMU station elements are illustrating in Figure 2.8.

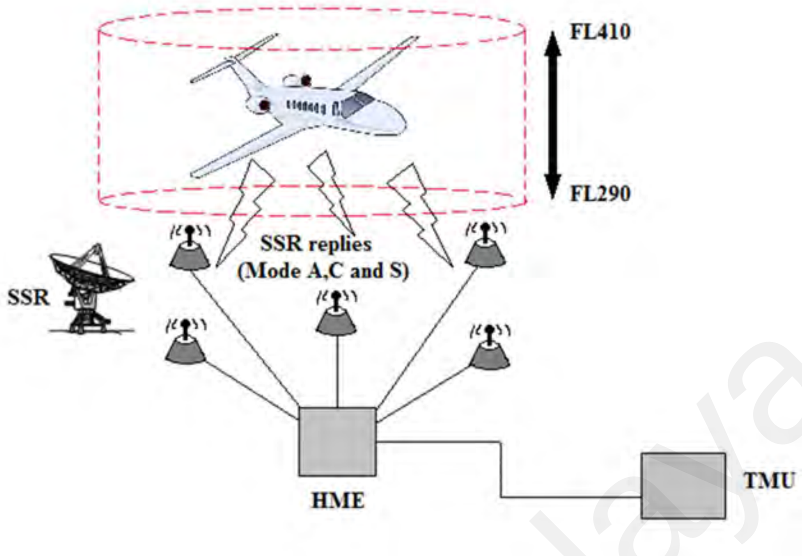

Figure 2. 8: Height Monitoring Unit (HMU) station (CAA, 2014)

In controlled airspace, aircraft that radar stations question activate the HME, which detects and extracts signals from the aircraft's SSR transponder whenever the aircraft is flying at RVSM levels and passes over the HMU coverage area. The aircraft's three-dimensional position, including its geometric height, is determined using a multi-lateration technique in conjunction with HME signals containing data from S and A/C transmissions. The time difference of arrival (TDOA) method determines the date and time of receipt of reply signals from multiple receiver locations (CAA, 2014).

Before determining the aircraft's position, the transponder signals will undergo a complex process that includes rejecting both multipath and garbling effects and statistically removing irrelevant signals. Then, using data collation, the track histories of each aircraft that passes through the coverage area are transmitted to the TMU as one plot per second. For calculations of Total Vertical Error (TVE), Assigned Altitude Deviation (AAD), and Altimetry System

Error (ASE), the actual geometric altitude or geometric height, assigned flight level geometric height, transponder altitude, and cockpit altitude are required.

Under the assumption of zero correspondence error, the altitude transmitted by the transponder is equivalent to the altitude indicated in the cockpit (i.e., FTE equals AAD) (Garrigues,2002). Within the HMU coverage area, the meteorological station transmits the geometric height of the allocated flight level using a predefined grid. The data is updated four times per day and is only valid for one day. The HME determines the geometric height relative to the WGS84 ellipsoid when the aircraft flies over the HMU detection area.

The Total Vertical Error (TVE) is calculated by combining the pressure altitude of available meteorological data with the final track information. After the process, all required values such as Total Vertical Error (TVE), Assigned Altitude Deviation (AAD), and Altimetry System Error (ASE) will be obtained. The height monitoring reports will be shared with the appropriate RMAs to verify the aircraft's performance in preparation for RVSM approval. A dedicated database of RVSM approval records is created and maintained, which is entirely comprised of results shared among RMAs (PARMO, 2015). On request, the monitoring report can be shared with operators.

The ASE calculation is carried out entirely within the HMU coverage area, and no geometric height values are retained until the RMAs receive the final monitoring results (PARMO, 2015). Additionally, because the HMU can simultaneously detect multiple aircraft, it can monitor groups of aircraft rather than individual aircraft. Figure 2.9 illustrates the procedure for monitoring with the Height Monitoring Unit (HMU).

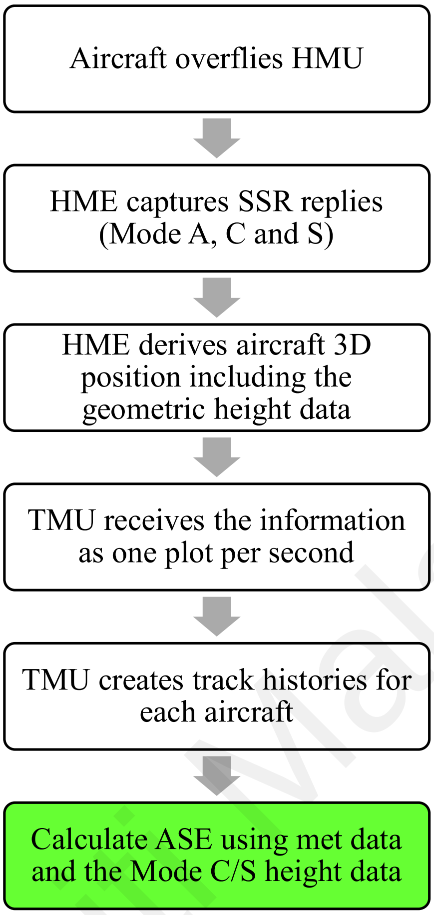

Figure 2. 9: Height Monitoring Unit (HMU) monitoring process (CAA, 2014)

Extensive planning and study are required for the HMU installation. To meet the coverage specification for the ground station, it must be easily accessible for installation and maintenance and free of radio interference at the high point. Additionally, the proposed site must be evaluated for its air traffic density, transition area, and geographic layout.

2.3.4.2 Global Positioning System (GPS) Monitoring Unit (GMU)

Monitoring an entire fleet of aircraft using HMU alone is not possible as this would require the installation of hundreds of HMU stations, which would be prohibitively expensive financially. The GPS Monitoring Unit (GMU) is a portable device mounted on a single aircraft. GMU is a digital recording and monitoring system capable of collecting geometric height data about the WGS84 ellipsoid during flight.

The GMU can be fitted in the cockpit or cabin, depending on the aircraft type, and installation takes about 15 minutes. A professional GMU operator must install and operate the GMU in the aircraft, and the entire process takes up to 45 minutes. Typically, the GMU in an aircraft will include a GPS receiver and two GPS antennas with suction pads that will be temporarily attached to the aircraft's interior windows in order to collect data (Authority, 2002).

Since the GMU is a stand-alone unit, it does not require integration with any other aircraft system. The unit will draw between two and four amps from the aircraft's plug-in power when monitoring via the GMU, the geometric height, pressure altitude (Mode C), and meteorological data are required. After applying discrepancy corrections from ground stations to the GPS data received via the GMU, an accurate three-dimensional position of the aircraft is obtained (Authority, 2002).

The corrected GPS geometric height is attuned to the aircraft's actual GPS geometric height at the assigned flight level flown post-flight using meteorological data (Martinet al., 2008). The technique is similar to that used by HMU. The Digital Flight Data Recorder (DFDR) is used to collect Mode C data, combined with meteorological and GPS geometric height data (FAA, 2015). The AAD is calculated using the Mode C data that was collected.

As a result, TVE values are computed during the final processing of the ASE's output. Monitoring results in their entirety are forwarded to the appropriate RMAs. Finally, aircraft operators are provided with a copy of the monitoring data. The monitoring process with a GMU is depicted in Figure 2.10.

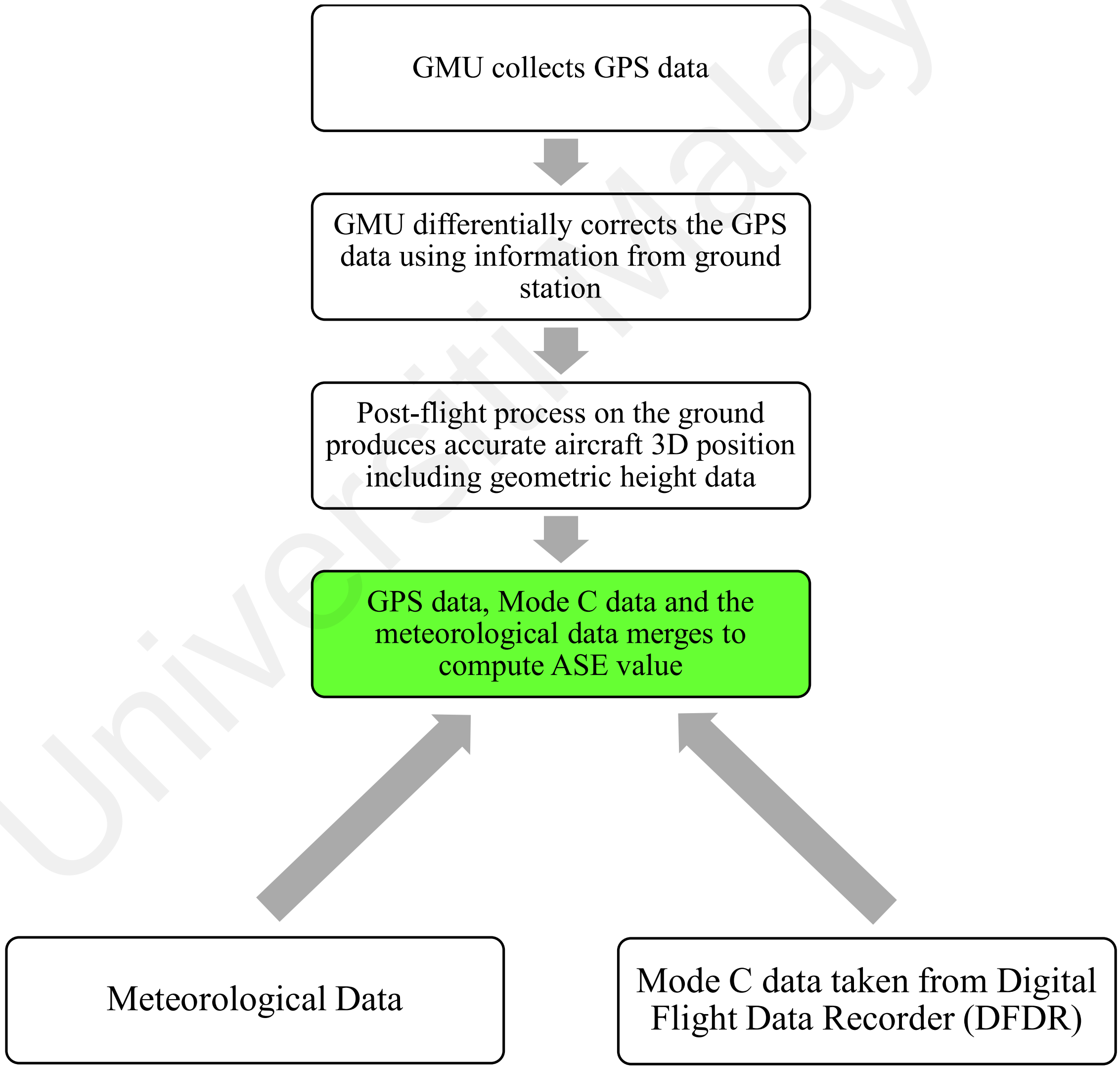

Figure 2. 10: GPS Monitoring Unit (GMU) (Authority, 2002)

Currently, an Enhanced GPS Monitoring Unit (EGMU) is available, which includes a GPS receiver, two shielded mobile GPS antennas, and an additional Altitude Recording Device (ARD) for collecting pressure altitude (Mode C) data from the aircraft transponder. Additionally, the unit contains an internal battery, which eliminates the need for external power. However, the monitoring process will be identical to that of the previous GMU.

2.3.4.3 Aircraft Geometric Height Measurement Element (AGHME)

Aircraft Geometric Height Measurement Element (AGHME) is a ground-based height monitoring system similar to the HMU. At the moment, AGHME is used in four locations in the United States and two locations in Canada, a total of six locations. Automatic activation of the AGHME is possible whenever an aircraft flies over the coverage area. However, a Mode S transponder is required to maintain visibility of the aircraft during the AGHME monitoring process.

When an aircraft installed with a Mode S transponder fly over the AGHME stations, the AGHME calculates the aircraft's geometric height instantly using the multi-lateration method. AGHME can determine the aircraft's TVE based on its geometric height, and post-processing can estimate an ASE-like EGMU monitoring system (Martin et al., 2008). The AGHME stations' total coverage area enables the ASE monitoring of aircraft groups.

2.3.4.4 ADS-B Height Monitoring System (AHMS)

The ADS-B Height Monitoring System (AHMS) is the most current ground-based monitoring system. It utilizes ADS-B receivers to obtain geometric height data from ADS-B-equipped aircraft in order to calculate ASE. The ADS-B Height Monitoring System (AHMS) is the most recent ground-based monitoring system, relying on ADS-B receivers to provide geometric height data from ADS-B installed aircraft to calculate ASE. ADS-B is currently being used to monitor aircraft height-keeping in the United States, Australia, China, and Asian RVSM regions (CAA, 2014).

Every second, whenever an aircraft flies within the coverage area, an ADS-B message comprising all the required data for ASE estimation is broadcast to the ground stations. To estimate the ASE, pertinent data such as the geometric height, barometric altitude, and meteorological data are extracted and later processed in the ASE processing software.

2.3.5 Aircraft accidents due to ASE

The following table2.2 below summarizes past aircraft accidents, contributing factors and safety impacts that occurs due to altimeter system errors.

Table 2. 2: Aircraft accidents involving ASE

#01	Aircraft Type	Aircraft Boeing 737-800/BAE125
	Airline	Ceiba International 737/British Aerospace 125
	Date	5 September 2015
	Summary of the Accidents/Incidents	The accident occurs on 5 September 2015 involving Aircraft Boeing 737-800/BAE125 from airline Ceiba

		International 737/British Aerospace 125. The aircraft HS 125-700 departure from Ouagadougou had climbed at FL340 and cleared to FL380 for weather avoidance. They later requested FL340 and maintained it. The 125 collided with 737 at FL 350. Although the 125 crew had correctly read their cleared level as F340, they were at FL350 when the collision occurred. The HS125-700 suspected crashed into the ocean.
	Contributing factors	The altimetry problems on the HS125 may have contributed to the collision. A minor discrepancy (200 feet) was reported between the altitudes displayed on the two primary altimeters.
	Safety Impact	With the availability of the algorithm, the HKP measurement of the aircraft could have been done regularly or at the desired interval. This could have detected any fault of the flight's altimeter.
#02	Aircraft Type	Aircraft Boeing 737-800/BAE125
	Airline	Arik Air/British Aerospace 125
	Date	23 July 2015
	Summary of the Accidents/Incidents	The Arik jet flying at 31,000ft, and its crew expressed concern to an air traffic control that BAe 125 was approaching from the opposite direction at the same altitude. However, the controller assured the Arik crew that the BAe 125 was at 32,000ft. Unconvinced, the Arik pilots asked to climb to 39,000ft, but this was denied owing to traffic above. The controller contacted the BAe 125's pilots, who confirmed the aircraft's altitude as 32,000ft. Not until radar information identified the BAe 125 as being at 31,000ft. As a result,the British Aerospace 125 jet involved a fatal mid-air collision with a Boeing 737-800.
	Contributing factors	Altimeter discrepancy of the Bae125.
	Safety Impact	With the availability of the algorithm, the altimeter checks could have performed by the aircraft maintenance engineer during the aircraft maintenance. The flaw of the altimeter could have detected earlier.
#03	Aircraft Type	Aircraft Antonov 72
	Airline	Transport Plane
	Date	25th Dec 2015
	Summary of the Accidents/Incidents	The airplane flies to Shymkent Airport (CIT) from Astana Airport (TSE) at 16:52. However, the autopilot failed shortly after takeoff, and the flight has been flown manually by the captain. The radio altimeter also failed after two minutes and 40 seconds of takeoff. The altitude is reducing from 696 to -1375 meters. In 3 minutes of intervals, the

		altimeter again hit 2672 m from 749 m. The airplane crash into the slope of a ravine of the runway and broke up.
	Contributing factors	The investigation commission found out that the autopilot and radio altimeter's failure, combined with low visibility and the pilot failing to follow instructions to use the barometric altimeter, caused the crash.
	Safety Impact	With the availability of the algorithm, used in real-time as suggested as future improvement, the tool can be used as an alternative for the altimeter reading.
#04	Aircraft Type	Aircraft Airbus A318/Pilatus PC-12
	Airline	France Airlines/Jets
	Date	2nd June 2010
	Summary of the Accidents/Incidents	The A318 preparing to land at Bordeaux, France. The oscillations can be felt, and the aircraft was in close visual contact when the copilot looked through the aircraft windshield. The aircraft instantly disconnected from the autopilot mode and descended to the left. The airbus descends to 200ft. The traffic alert collision avoidance system (TCAS), when checked by the copilot, specifies that the aircraft at 2000 ft below does not notice that it is the same flight that had just crossed. The A318 had passed, and the separation was estimated approximately 100 ft vertical. The collision occurred at 290 FL. The Pilatus noticed a trivial discrepancy on the two altimeters as they departed. The variance started to surge as the aeroplane ascends to the assigned altitude of 270 FL. The first altimeter displayed FL270, and the second altimeter displayed FL290. The pilot contacted ATC, and the controller confirmed the flight altitude at FL270. The pilot of both airplanes reported the incidents to ATC. The PC12 Mode C data had incorrect flight level, FL270 and A138 shown correct flight level, FL290.
	Contributing factors	The contributing factor is an outflow in a connector between the cabin differential pressure indicator and a static pressure line of the altimeter, airspeed indicator, and vertical speed indicator. As the cabin was pressured, the altimeter on the pilot's side shown an altitude lower than an actual.
	Safety Impact	With the availability of the algorithm, the altimeter health checks could have performed by the aircraft maintenance engineer. The flaw of the altimeter could have detected earlier.
#05	Aircraft Type	Aircraft Boeing 737-8F2
	Airline	Turkish Airlines
	Date	25th February 2009

	Summary of the Accidents/Incidents	The Boeing 737 departed from Istanbul-Ataturk for a flight to Amsterdam. While descending through 1950 feet, the left-hand primary flight display shows -8 feet. However, the right-hand main flight display indicating the correct height. The left-hand radio altimeter system is taking the incorrect altitude as the correct one. This error reading was used by various aircraft systems, including the aircraft autothrottle. The aircraft started to follow the glide path due to the incorrect altitude reading, and the autothrottle moved to 'retard flare' mode, which was generally activated during landing. The right-hand autopilot system is receiving correct altitude information from the right-hand radio altimeter system. The autopilot tries to keeps the aircraft on the glide path for as long as possible. The airspeed reached 126 knots; the frame of the airspeed changed colour and started to flash. The crew did not respond to the warnings. The aircraft started a rapid reduction in speed, and high pith altitude and stall warning went off at an altitude of 460 feet. The captain takes over the aircraft, and the autothrottle disconnected—the aircraft already at 350 feet at that point and insufficient for recovery. The aircraft impacted farmland. A total of nine fatalities were reported out of 7 crew members and 135 passengers.
	Contributing factors	The left radio altimeter showed an incorrect value -8 resulted in activation of the autothrottles restard flare' mode. As the speed continued to drop, the aircraft pitch altitude kept increasing. The crew failed to spot the aircraft speed decay, and pitch increase still sticks shaker activated.
	Safety Impact	With the availability of the algorithm, the HKP of the aircraft could have been monitored and could have taken necessary action to prevent the accidents.
#06	Aircraft Type	Aircraft B-2 Bomber
	Airline	Air Force Aircraft
	Date	25 February 2008
	Summary of the Accidents/Incidents	During flight pre-check, the flight crew received instructions that the Air Data needed to be altered. The pilots and flight control experts are not aware of the pitot heat technique. They adjusted the Air Data System without enabling the heat to dry the PTU (Port Transducer Units). This created a significant difference in 3 of the 24 PTUs. The crew has enabled the pitot heat as per the checklist while preparing for takeoff. The moist sensors dried once to enable the pitot heat. The altimeter showed an error of 136 feet above the actual elevation due to the incorrect data. The aircrew did not notice this error. The pilot takes off the aircraft. The FCS (Flight Control System) calculated the negative angle of attack based on the skewed ADS data.

		One of the pilots tried to recuperate the control, but the aircraft irrecoverable.
	Contributing factors	The US Airforce accident board concluded that moisture in PTUs caused notable differences to be programmed into the ADS during setting. The flight computers calculated an inaccurate speed and negative angle of attack. Based on the skewed data, inadequate altitude, and airspeed due to the partial data spilt and was unable to recover the aircraft.
	Safety Impact	With the availability of the algorithm, the altimeter inaccuracy could have spotted earlier and corrected, and the accidents could have prevented.

2.4 Automatic Dependent Surveillance-Broadcast (ADS-B)

Automatic Dependent Surveillance-Broadcast (ADS-B) is the latest state-of-the-art aircraft surveillance system that employs satellite technology instead of the conventional ground-based radar system. It will continuously broadcast aircraft position and other data by using either the 1090 Extended Squitter (1090ES) datalink or the Universal Access Transceiver (UAT) datalink regardless if the aircraft is airborne or on the ground.

The ADS-B system is comprised of two main components, namely the ADS-B Out component and ADS-B In component. ADS-B Out includes a transmitter that permits the sharing of precise aircraft position along with additional information via datalink capability and allows ground stations to receive the aircraft's ADS-B transmission whenever the aircraft flies within the ADS-B ground stations coverage area. Ground stations will subsequently relay the information to ATC to provide air traffic services. On the other hand, the ADS-B In component, which consists of a receiver and data link that can enable aircraft to receive ADS-B messages from neighbouring ADS-B Out aircraft and ground stations.

Ultimately, both ATC and pilots can use the information in the message to further enhance flight safety, collision avoidance, and the pilot's situational awareness by increasing aircraft visibility via cockpit display of traffic information (CDTI). Nevertheless, it should be noted that the 'see-and-avoid procedure should not be superseded as ADS-B may not give a complete depiction of aircraft traffic simply because not every aircraft is equipped with ADS-B yet (Authority, 2002). ADS-B is depicted schematically in Figure 2.11 below.

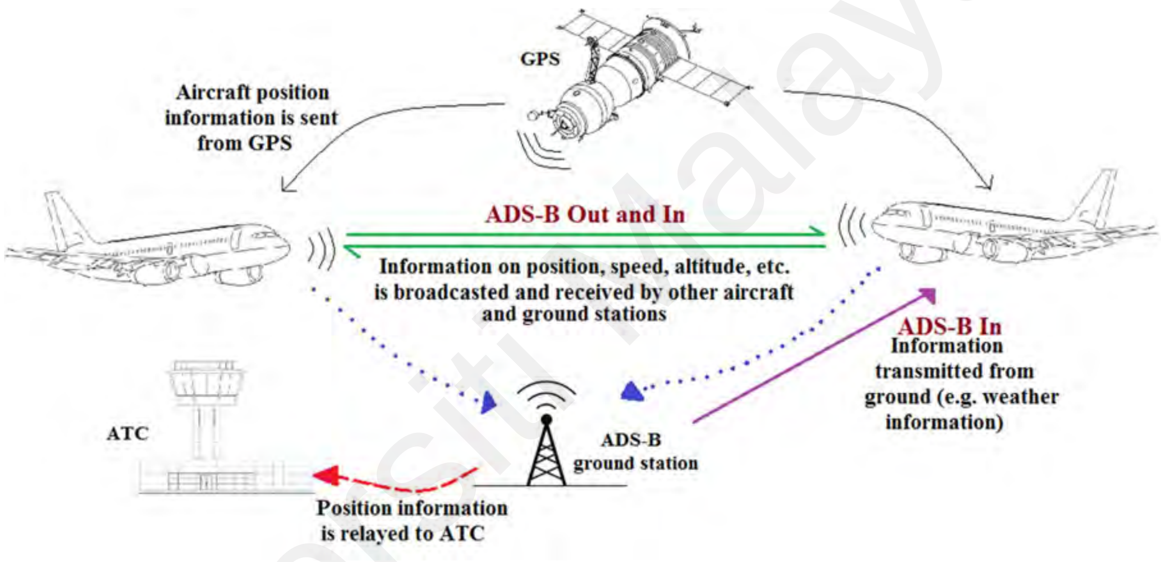

Figure 2. 11: Schematic depiction of ADS-B (FAA, 2020)

2.4.1 Principles of ADS-B Operation

The onboard GPS receiver supplies aircraft position, speed, time, the horizontal figure of merit (FOM), and horizontal protection (HPL). In contrast, flight level (Mode C) is provided by the barometric altimeter. Pilots will punch in the flight identification, which is equivalent to the aircraft call sign.

The information is forwarded to the ADS-B transceiver, a single unit comprising both the transmitter and receiver, where the ADS-B message will be assembled and encoded into the required ASTERIX category 21 message format (Kunzi & Hansman, 2011). The process produces a position integrity indicator called the Navigational Accuracy Category (NAC) derived from the GPS available HFOM value and Navigational Integrity Category (NIC) derived from the HPL value (Ali et al., 2015).

Eventually, the ADS-B message will be transmitted to the ground station and other aircraft equipped with ADS-B in the vicinity through an installed antenna via a digital data link (i.e., 1090ES or UAT). The ADS-B transceiver can also receive and decode ADS-B In messages when the transceiver is ADS-B incapable. Figure 2.12 below illustrates the source and flow of ADS-B data.

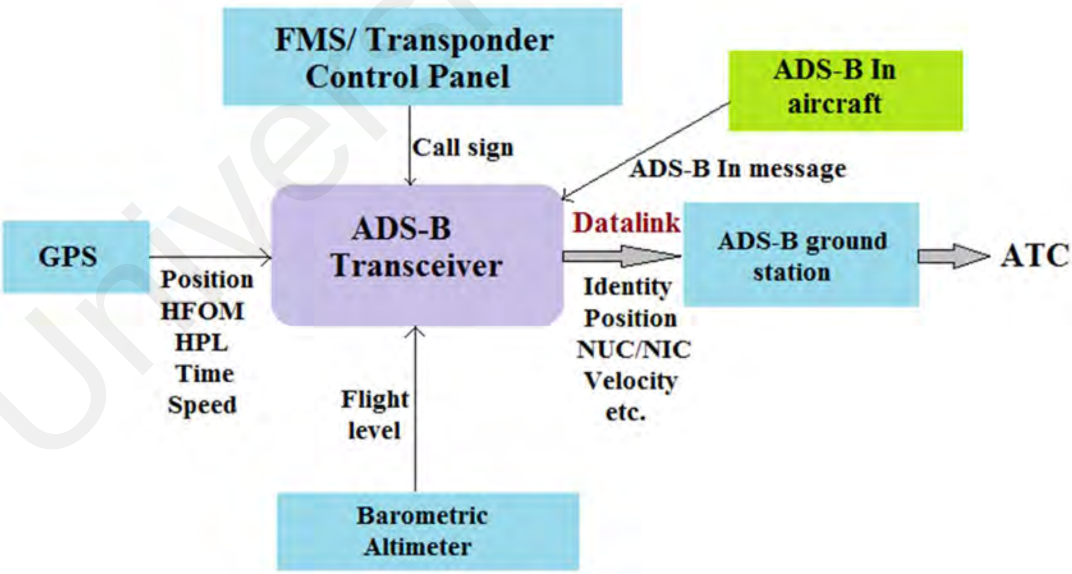

Figure 2. 12: Source and flow of ADS-B Out and ADS-B In a message (FAA, 2020)

2.4.2 Data in ADS-B Messages

The ADS-B data contains several types of ADS-B messages; each message contains different information depending on the message type number. The airborne position message, the surface position message, the airborne velocity message, the aircraft identification and category message, the target state and status message, and the aircraft operational status message are all examples of these message types.

The message will be decoded in order to extract the relevant information, which includes aircraft identification (call sign), aircraft position (i.e., latitude and longitude), airborne position (i.e., geometric altitude/geometric height and barometric altitude), position integrity, and accuracy, vertical climb rate, heading, ground speed, time and ADS-B ground station identification.

The information is real-time download via a data link (Kexi, Jun & Xuejun, 2010). Navigational Uncertainty Category (NUC) is also available in the ADS-B message typically used to exclude the insufficient ADS-B data, and this happens when the NUC value less than 5. Other possible information includes conflict alert information and flight path angle.

2.4.3 Potential of ADS-B Data in ASE Measurement

ADS-B has shown great potential to be used as another means for aircraft height, keeping performance monitoring. This is because relevant data such as aircraft altitude, longitude, geometric height, barometric altitude, and time is readily available in the ADS-B message.

Unlike HMU, ADS-B does not need to measure aircraft geometric height since altitude information is sourced directly from GNSS. Also, no professionals are required onboard to operate the system. Therefore, surcharge for a professional operator can be eliminated, providing a more cost-effective solution in the long run.

Since ADS-B stations are cheaper and easier to install than radar, the greater coverage area is available as more ground stations can be set up. Each ADS-B ground station's detection area can cover almost 200 nautical miles in terms of the radius at flight level 300. The overlapping coverage from all ground stations further generates an overall wide area of ADS-B operational coverage network (FAA, 2011).

Due to this reason, the ADS-B aircraft tracks are comparatively more prolonged than those from HMU, GMU, and AGHME, which in turn produces an extensive amount of ADS-B data; therefore, this not only allows for repeated measurement on single aircraft but monitoring of aircraft groups can also be made possible. The large volumes of data sets can further assist RMAs in determining any unusual ASE trends and behaviours.

2.4.3.1 China RMA ASE Evaluation Using ADS-B Data

China identifies a problem with recognizing actual flight altitudes that differ from those reported by the pilot or ATC. As a result, ASE is a well-known risk. To ensure the safety of RVSM operations, high-accuracy altimetry systems are required. China RMA is equipped with two EGMU and two E2GMU. However, EGMU surveillance is limited to basic MMR. As part of its efforts to improve civil aviation safety, China's Regional Monitoring System (RMA) studied and developed methods for monitoring the Altimetry System Error using ADS-B data (ASE).

China RMA received training from an FAA center in 2008 to use the FAA's Enhanced GPS Monitoring Unit (EGMU) calculation software. China RMA began developing software and comparing aircraft ASE results with AAMA and MAAR in 2012. (ICAO,2013).

China ADS-B track data was submitted for validation to AAMA HAE Geometric Assigned Flight Level Conversion. The results were compared to those obtained from China RMA ASE, which was processed manually. Compared to AAMA and MAAR, China RMA ASE estimation can produce ASE values comparable to those generated by the FAA's ASE software (ICAO,2013).

2.4.4 Existing Research in the Viability of ADS-B Geometric Height for ASE Estimation

The aircraft geometric height is one of the critical components in calculating the Altimetry System Error (ASE). Therefore, it is paramount that the ADS-B message's geometric height data is validated before it can be used for ASE monitoring purposes. Table 2.3 below summarizes studies conducted to utilize ADS-B data for ASE calculation.

Table 2. 3: Summary of the feasibility of ADS-B Geometric Height for ASE Estimation

#01	**Title**	ADS-B Geometric Height Validation
	Author	Lauren Martin et. al.
	Year	2008
	Summary of the Study Three test flights using research aircraft were performed by the Federal Aviation Administration (FAA) in 2008, involving four flight segments within the U.S. domestic airspace. Comparisons were made on the aircraft geometric height from ADS-B (using both UAT and 1090ES data link) with the Enhanced GPS Monitoring Unit (EGMU. The differences values from the three sources were compared using the Analysis of Variance (ANOVA) method. After removing the rounding errors, results from the ANOVA test showed that aircraft geometric height estimates from both the ADS-B sources were not significantly different from those obtained from an EGMU.	
	Method Enhanced GPS Monitoring Unit (EGMU) Analysis of Variance (ANOVA) method	
#02	**Title**	Latitude-Longitude Effect of Altimetry System Error
	Author	Christine Falk et. al.
	Year	2010
	Summary of the Study Air services Australia and the FAA have joined forces to evaluate ADS-B geometric height for use in ASE estimation. The ADS-B data was collected from the Australian ADS-B network. Simultaneously, the estimation process of ASE was done through FAA's processing software. It was observed that there is a notable variation in initial ASE values with latitude and longitude from different ADS-B ground stations (Falk, Aldis & Butcher,2010) (Falk, Gonzalez & Perez,2010). ASE will need to be calculated based on both height references first	

	before the correct ASE results can be selected later through knowledge on the aircraft GPS fitment from an ADS-B approvals database.	
	Method FAA's processing software	
#03	**Title**	ADS-B Geometric Height Validation
	Author	Zhang Kexi et. Al.
	Year	2010
	Summary of the Study Compares the geometric altitude data from EGMU and ADS-B directly using the ANOVA test. In several flight tests conducted in China, both the geometric height data from the EGMU source and ADS-B source were taken from the same aircraft, simultaneously minimising the potential random error. As such, the possible error from both data will occur mainly due to altimetry system error. The ANOVA test results showed no significant difference between the geometric altitudes from the two sources.	
	Method Analysis of Variance (ANOVA) method	
#04	**Title**	Determination of Height reference using Geoid Height
	Author	Australian Airspace Monitoring Agency (AAMA)
	Year	2013
	Summary of the Study AAMA has found a method to determine which height reference is used in the transmitted aircraft geometric height using statistical analysis. The average ASE value for an aircraft over each different geoid height is plotted. Theoretically, the ASE value using the correct height reference should not vary with different geoid height values; thus, the slope will be zero graphically. Further, the Asian Region (MAAR) obtained ADS-B data from the Bangkok ADS-B station from November 2011 to June 2012. According to a study previously done by AAMA, a GPS receiver may transmit geometric altitude data as either height above means sea level (HAMSL) or height above ellipsoid (HAE), in which prior knowledge regarding the height datum used is not available (Barry, Aldis & Jason-Jones, 2013). The more significant variations of geoid height eventually have made it possible to determine the correct height reference through further analysis done similarly as AAMA'S.	
	Method Statistical analysis	

#05	Title	China RMA's Evaluation of Altimetry System Error using ADS-B
	Author	China Regional Monitoring Agency (China RMA)
	Year	2013
	Summary of the Study To ensure the safety of RVSM operations, high-accuracy altimetry systems are required. As part of its efforts to improve civil aviation safety, China's Regional Monitoring System (RMA) studied and developed methods for monitoring the Altimetry System Error using ADS-B data (ASE). China RMA received training from an FAA center in 2008 to use the FAA's Enhanced GPS Monitoring Unit (EGMU) calculation software. China RMA began developing software and comparing aircraft ASE results with AAMA and MAAR in 2012. (ICAO,2013). China ADS-B track data was submitted for validation to AAMA HAE Geometric Assigned Flight Level Conversion. The results were compared to those obtained from China RMA ASE, which was processed manually. Compared to AAMA and MAAR, China RMA ASE estimation can produce ASE values comparable to those generated by the FAA's ASE software (ICAO,2013).	
	Method Software Development	

2.5 Undulation of Geoid

Gravity, essentially caused by Earth's gravitational pull, has always shaped our planet (Hofmann-Wellehof & Moritz, 2006). Earth Gravitational Model 1996 (EGM96), and Earth Gravitational Model 2008 (EGM 2008) are the most popular earth gravity models used in the field of remote sensing due to their high utilization in open-source Digital Elevation Model (DEM) and other photogrammetric products (Bhardwaj, 2020).

Orthometric height (H) is defined as the vertical distance between the physical surface / terrain of the earth and the surface of the geoid. The ellipsoidal altitude (h), on the other hand, is the distance between a terrain point and the reference ellipsoid measured along the normal (Rodriguez-Gonzalvez et al., 2020). Currently, the Global Navigation Satellite System

(GNSS) has been used with reasonable success for ellipsoidal height (h) determination. However, the ellipsoidal height does not have a physical meaning. Hence, the orthometric heights are used in practice (Kaloop et al., 2019). Figure 2.13 below illustrates the components required for undulation of geoid computations.

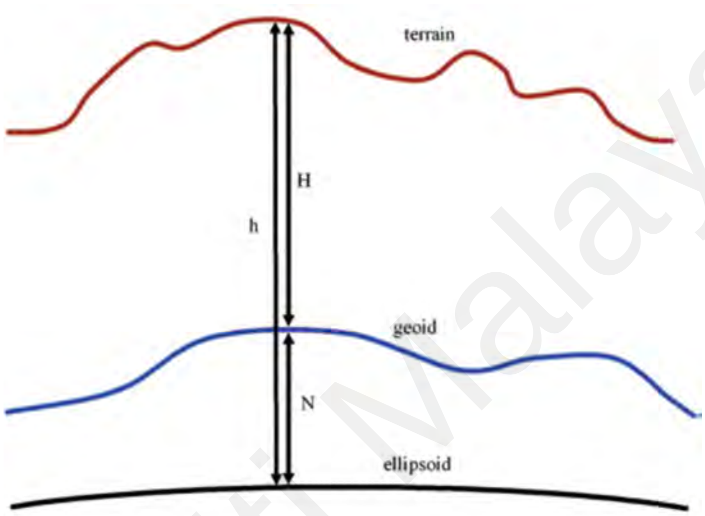

Figure 2. 13: Terrain/earth surface, geoid and ellipsoid heights (Oluyori, P. D. et al., 2018)

Consistency is an important characteristic in height systems which the mean sea level (MSL) surface cannot guarantee. Only a geoid surface can provide height consistency (Oluyori et al., 2018). The Geoid is defined as the equipotential surface of the Earth's gravity field which coincides with the Mean Sea Level (MSL) in the absence of disturbing factors like ocean currents, salinities, wind, etc., and it extends through the continents (Uotila, 1971). The geoid is continuous and much smoother than the actual earth surface, unlike the ellipsoid, it is still a closed, too complicated to serve as the computational surface on which to solve geometrical problems, but it is suitable as a vertical datum (Becker, 2012).

The geoid undulation, N is the difference between ellipsoid and geoid surface used for the conversion of ellipsoidal height to orthometric height. The N is given as (Heikanen & Motitz, 1967) and (Eteje et al, 2018);

$$N = h - H \tag{1}$$

2.6 Computer Algorithm

An algorithm is any well-defined computational procedure that takes some value, or set of values, as input and produces some value, or set of values, as output. An algorithm is thus a sequence of computational steps that transform the input into the output. (Cormen, T.H., et al, 2009).

Algorithms are used as specifications for performing calculations, data processing, automated reasoning, automated decision-making and other tasks. In computer systems, an algorithm is basically an instance of logic written in software by software developers (Wikipedia, (n.d.), Algorithm).

An algorithm needs to have the following six characteristics (GeeksforGeeks (2020), Introduction to Algorithms):

1) Clear and Unambiguous: Algorithm should be clear and unambiguous. Each of its steps should be clear in all aspects and must lead to only one meaning.
2) Well-Defined Inputs: If an algorithm says to take inputs, it should be well-defined inputs.

3) Well-Defined Outputs: The algorithm must clearly define what output will be yielded and it should be well-defined as well.
4) Finite-ness: The algorithm must be finite, i.e. it should not end up in an infinite loops or similar.
5) Feasible: The algorithm must be simple, generic and practical, such that it can be executed upon will the available resources. It must not contain some future technology, or anything.
6) Language Independent: The Algorithm designed must be language-independent, i.e. it must be just plain instructions that can be implemented in any language, and yet the output will be same, as expected.

CHAPTER 3: METHODOLOGY AND SYSTEM DESIGN

3.1 Introduction

This chapter details the methods and procedures used to complete the dissertation to meet the specified objectives. The flow chart for this research's methodology is shown in Figure 3.1 below.

3.2 Description of Methodology Flow Chart

3.2.1 Literature Review

The research work is begun with a literature review of journal papers to gather the fundamental knowledge on and theoretical knowledge of altitude values and its application in aviation, limitations of barometric altitude and potentials of geometric altitude, Altimetry System Error (ASE), and existing methods to measure ASE, and Automatic Dependent Surveillance-Broadcast (ADS-B) data and existing research on the viability of ADS-B data for measuring ASE. Additionally, references are made to various standards and regulations of the International Civil Aviation Organization (ICAO) to understand aircraft altitude specification requirements and air traffic control operations. Various aircraft related journals and researches from ICAO studied to understand aircraft accidents related to ASE. All the accidents related information is collected and summarized into a table by year, country and date.

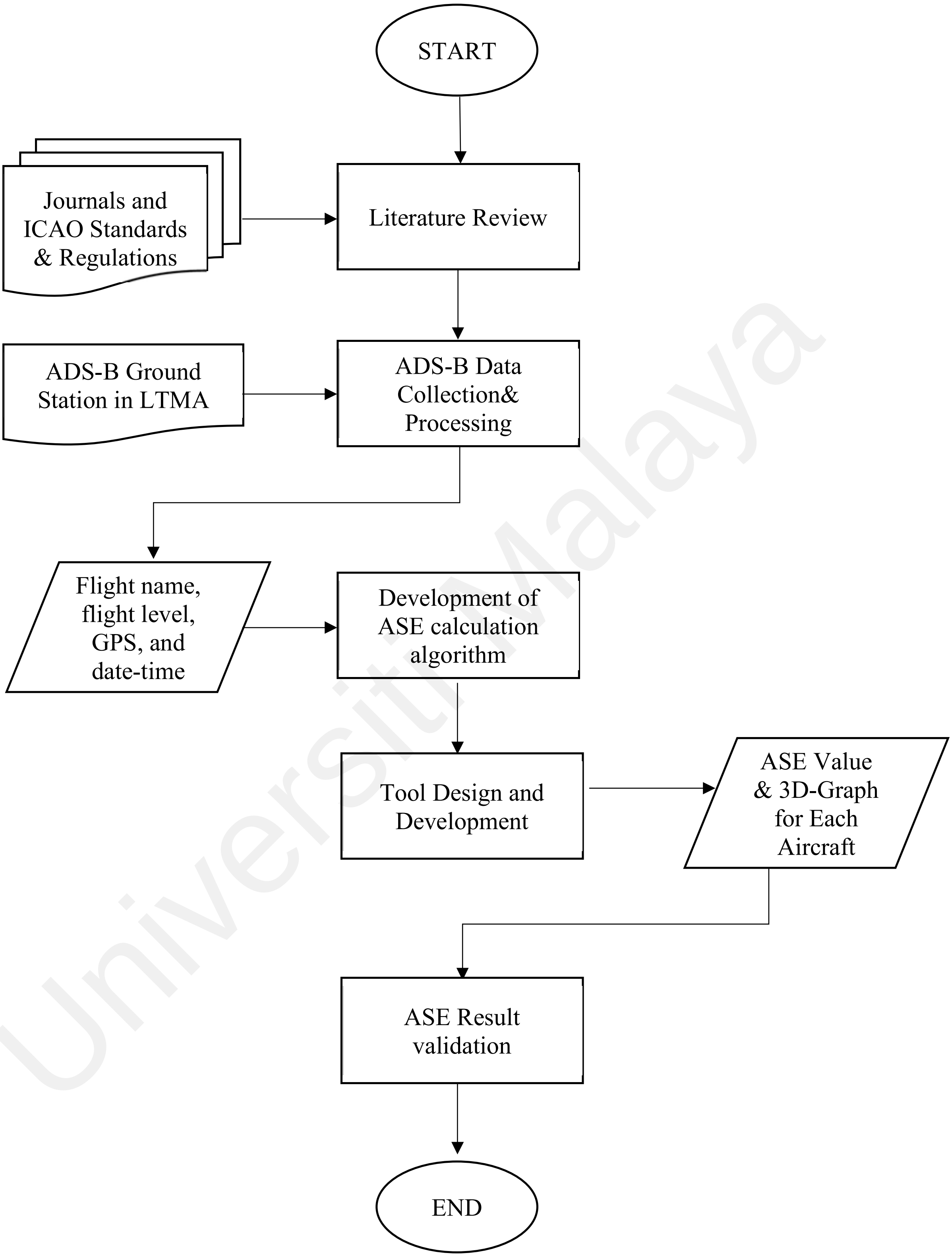

Figure 3. 1: Research Methodology

3.2.2 ADS-B Data Collection & Processing

This research starts with data analysis using ADS-B data from London Terminal Area for 38 British Airways aircraft. The data is obtained from airspace operators (NATS) based in the United Kingdom.

This data is classified as primary data as the data directly collected from ADS-B, and it is not published yet and is more reliable. The advantages of using the ADS-B data are specific to the research objectives aircraft data, and all the fields satisfy the research objective.

The collected data is based on an instance, traffic during a specific duration. The ADS-B is a surveillance method used to broadcast aircraft identity and position through the GNSS system. The ADS-B data includes latitude, longitude, quality indication, and aircraft identifications.

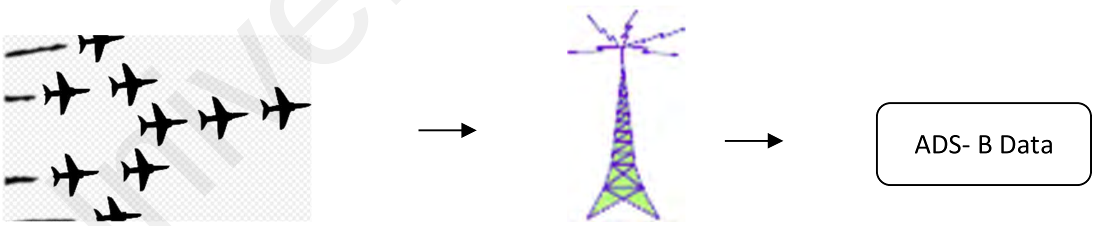

Air Plane Data ADS-B Ground Station

Figure 3. 2: ADS-B Data Acquisition

The data flow into the ADS-B file is depicted in Figure 3.2 above. ADS-B is an acronym for automatic dependent surveillance broadcast. It is a cooperative surveillance technology in which an aircraft determines its location. This data is broadcast periodically via satellite navigation, allowing it to be tracked to ground station and other equipped aircraft Schultz, Olive, Rosenow, Fricke and Alam,2020). The information can be used in place of secondary radar by air traffic control at ground stations. Other aircraft operating in the same airspace can also receive the same information, providing situational awareness and enabling self-separation. Benefits using include increased flight safety and efficiency and information on traffic, weather, terrain, flight information, and expenses.

Figure 3.3 is the descriptive statics of the data collected. Most of the field variables are having an accuracy level of 100. Since the data has 100 accuracies, there is no data clean-up activity required as part of the processing.

Figure 3. 3: Breakdown of the data collected

The collected data is in an excel format and contains data collected in a single day. There are total of 4999998 rows. The data contains unique identifier for each aircraft with latitude and longitude information. The data collected contains 25 columns in total. The data analyzed and identified all the required fields for the algorithm processing. However, there is no any modification made to the file manually. The algorithm built to read and only processed the required fields for the algorithm calculations. The sample data has been included in the Appendix section.

The collected ADS-B data needs pre-processing to extract required fields using the MATLAB read table function that have to be used to input the ASE calculation algorithm using the ADS-B Data Altimetry System Error method. The extracted data contain variables such as Velocity Accuracy, GPS, Time of Day, Longitude, Latitude, flight name, and Flight Level are identified. These variables are identified as dependent variables as they will be used to epitomize the ASE calculation outcome. Pre analysis of the data is conducted by evaluating the data to improve the research's validity and reliability.

It is not necessary to transmit data in real-time, and post-flight availability data is sufficient to operate the tool. As this tool, mainly for aircraft maintenance activity it is relevant to use the post-flight ADS-B data.

3.2.3 Development of Altimetry System Error (ASE) Calculation Algorithm

The algorithm designed based on the standard six properties of the algorithm. Each property validated and ensured the algorithm met all the characteristics of algorithm such as input, output, finiteness, clear and unambiguous, feasible and language independent to deliver the expected and seamless solution.

The algorithm has been designed in a clear and unambiguous way. Each of the steps which is require as part of the algorithm processing has been clearly identified to meet the expected results. The algorithm requires an input file which must contains all the mandatory variables which needed for the ASE value calculation process. The algorithm has been designed in a way that will be prompted for an input file and will not able to proceed further if failed to provide an input file. The algorithm also has been designed to be able to read and process the input file.

The expected output is well defined, in this algorithm the expected output is a plotted graph which will illustrates the ASE value against flight level by datetime stamp. The algorithm has been designed in a finite-ness way to ensure not faced any infinite loops. The algorithm also designed in a feasible way as this algorithm is a simple, generic and do not rely on any future or special technologies. The algorithm is a language independent as this algorithm can be adapted to any programming language and there is no reliant on any specific language.

3.2.3.1 ASE Calculation Algorithm Flow Chart

The flow chart shown in Figure 3.4 describes the process or method chosen to build the ASE calculation algorithm. The input file will be the ADS-B data file. This file is raw data of ADS-B, which transmits to the ADS-B ground station. The required data will be extracted and constitute the data formatted for processing.

Once the input file is keyed in, the process starts processing an input file by extracting the required fields extracted from the input file. The value stores in a table. The only required fields include aircraft names, Date-Time, latitude, longitude, GPS level, and Level extracted from the input file. The fields are identified based on the column position in the file. The file read through and requires the data's position marks columns, and those data extracted and stores into a table for further processing.

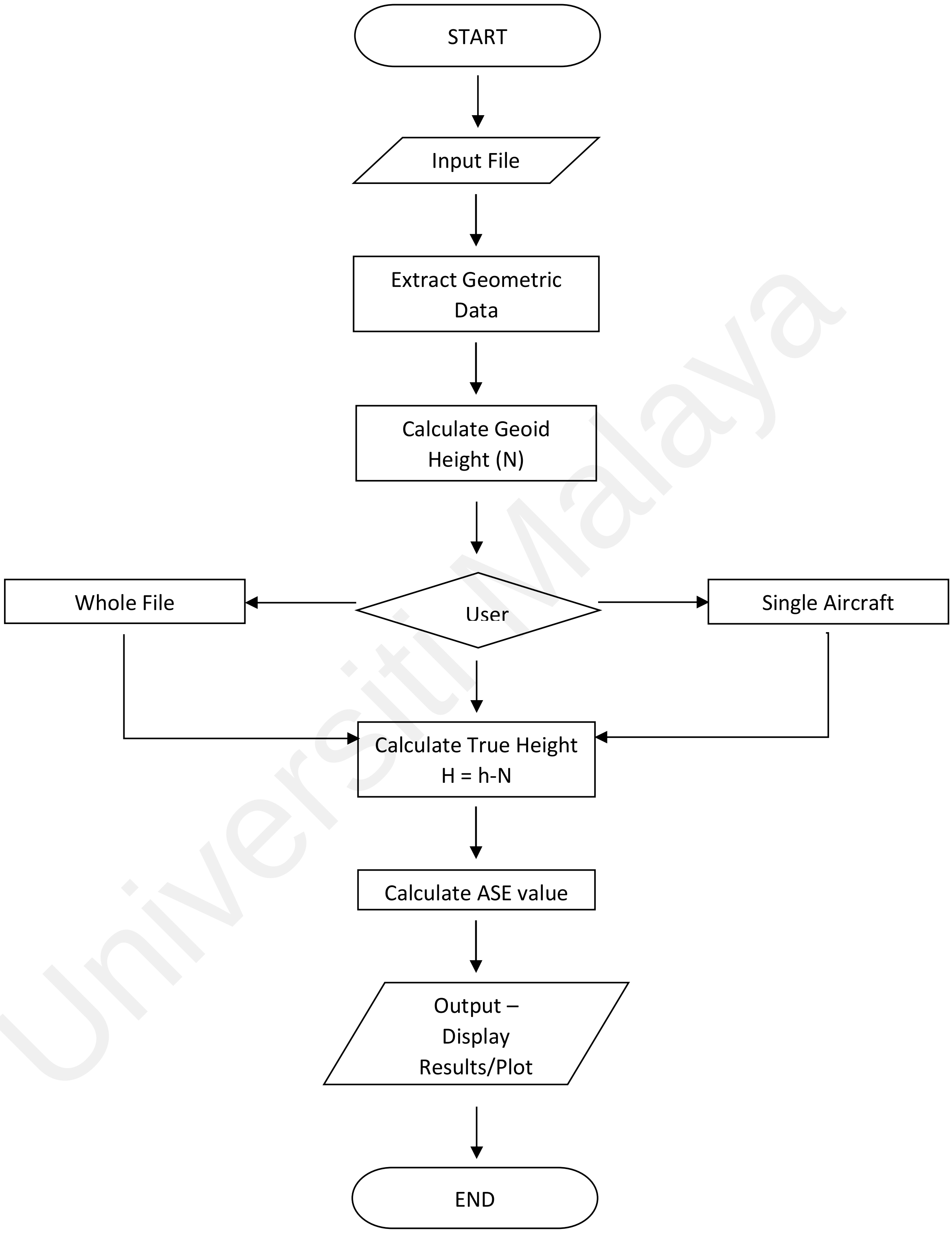

Figure 3. 4: Flow Chart of ASE Calculation Algorithm

The Geoid Height (N) was calculated for each aircraft using the EGM96 (Earth Gravitational Model) Geopotential Formula. EGM96 geoid is a vertical datum first defined in 1996-01-01 and is suitable for use in World. The origin of the EGM96 geoid is derived from the EGM84 geoid undulation model, which consists of spherical harmonic coefficients to degree and order 360 applied to the WGS 84 ellipsoid. Figure 3.5 below shows the illustration of Geoid Height, Geometric Height, and Barometric Height.

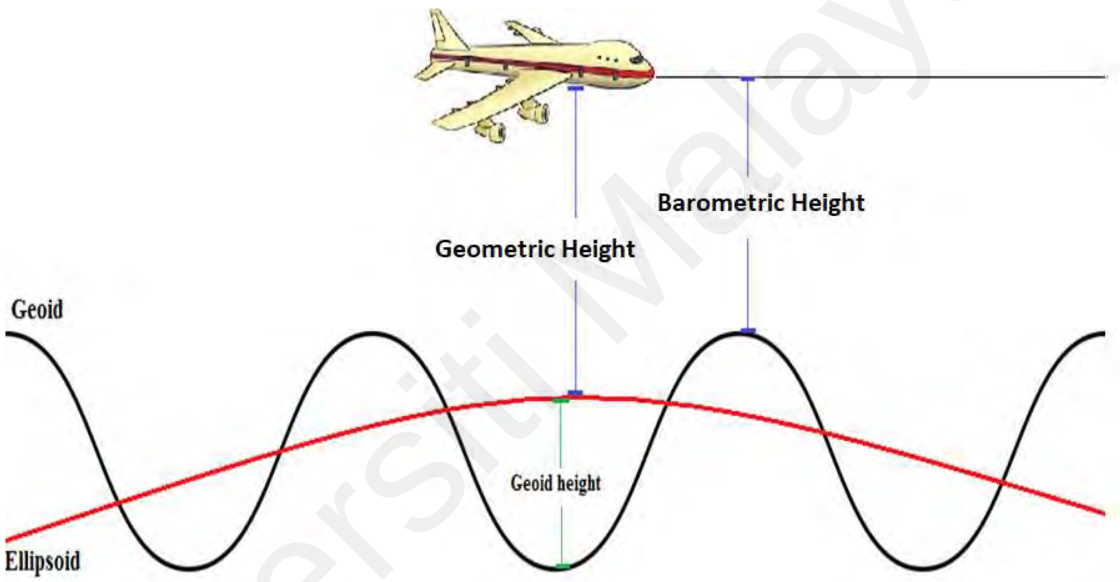

Figure 3. 5: Relationship between Geoid Height, Geometric Height, and Barometric Height

The EGM96 geoid is a vertical datum for Geodesy. The EGM96 incorporates improved surface gravity data and altimeter-derived gravity anomalies from ERS–1. The GEOSAT Geodetic Mission (GM), extensive satellite tracking data, includes data from Satellite Laser Ranging (SLR), the Global Positioning System (GPS), NASA's Tracking and Data Relay Satellite System (TDRSS), the French DORIS system, and the US Navy TRANSIT Doppler tracking system—as well as direct altimeter ranges from TOPEX/POSEIDON (T/P), ERS-1, and GEOSAT. T.

Once the Geoid Height (N) is calculated, the user can choose between processing the ASE value for specific aircraft or the entire file by entering the dialogue box prompts option value. The actual height or orthometric height of the aircraft calculated using the following formula.

$$H = h - N \qquad \textit{(1) (Li \& Gotzez, 2001)}$$

Flight GPS level (h) subtracted with Geoid Height (N) to obtained flight true height or orthometric height. The difference between flight level (FL) and true height (H) is calculated as the ASE value. ASE value of the flight calculated using the following formula.

$$ASE = FL - H \qquad (2)$$

Flight ASE values for the aircraft are displayed in the table and graph plotted to display the pattern of the ASE values used by aircraft engineers for the flight's health checks.

3.3.2.2 Design Diagram

Several UML diagrams are designed to specify, visualize, construct, and document the tool's artefacts. The design diagram function is to explore potential designs and validate the architectural design of the tool. The visual representations allow for understanding possible flaws or errors in the tool. The behavioral UML diagram and structural UML diagram designed to help visualize the ASE calculation tool.

3.3.2.2.1 Use Case Model

The Use Case Model shown in figure 3.6 describes the superior functionality provided by the ASE measure tool. The aircraft maintenance, repair, and operations (MRO) are the primary actor for the ASE measure tool. They are the primary role to troubleshoots, predictive maintenance, and perform health checks on the aircraft periodically to ensure that the aircraft is optimal and, most importantly, safe for flying. The aircraft maintenance engineers and technicians could enter the input file wish to be processed and choose the data set that needs to be processed.

The set of data sizes could be for specific aircraft or the entire file. The aircraft maintenance engineer and technician could view each aircraft's ASE value and view the ASE pattern graph. The air aircraft maintenance engineers and technicians could view the Geoid Height, N value of each aircraft. This activity could perform yearly once or six months to validate aircraft barometer data against the ASE measure tool to check whether the aircraft is still in good condition.

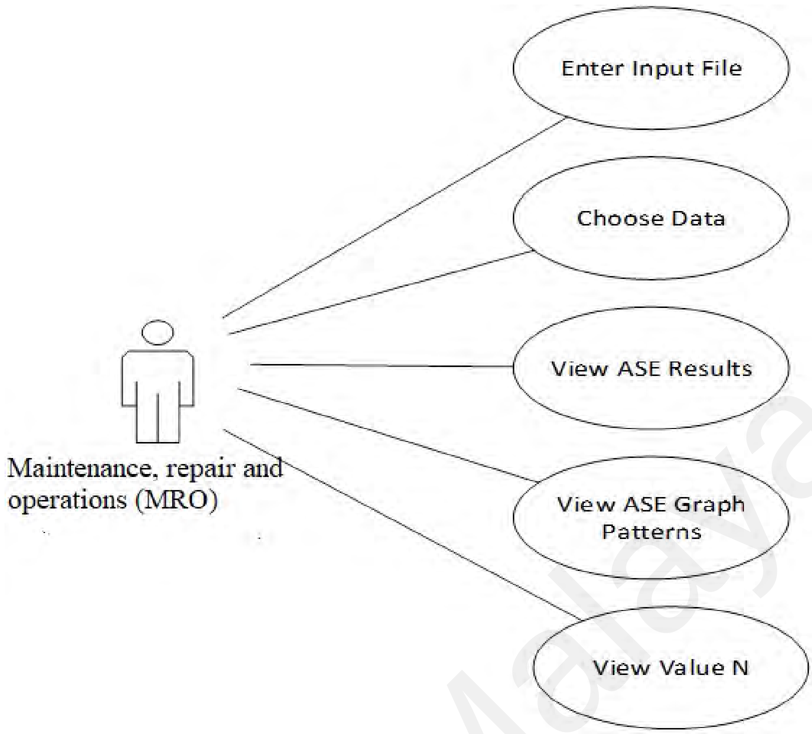

Figure 3. 6: Use Case Model of ASE Algorithm

Table 3. 1: Use Cases - Aircraft Maintenance

Description	Collect, analyse, and store aircraft systems, engine data for maintenance. The reliability of an A/C can be significantly increased by detecting and replacing attired parts.
Scenario	Troubleshooting is a line maintenance activity that focuses on resolving technical aircraft issues that are not directly addressed in the aircraft mechanics procedures. After the aircraft touches down, spare parts and tools can be prepared. The time required to resolve the issue and return the aircraft to service is significantly reduced.
User groups	Maintenance; MRO.
Benefit	Increase in A/C safety; High reliability for A/C dispatch; Accurate aircraft information.
Required data	Various aircraft systems, engine systems data.
Data Sources	ADS – B Data
Special Considerations	Data Security, integrity, and reliability.
Transmission Technologies	GNSS Satellite

3.3.2.2.2 Class Diagram

In object-oriented design, the class diagram is the primary diagram that we create. Its significance stems from the fact that its contents contain the primary components of our program's code. A class diagram design depicts the various types of objects in a system and their relationships. A class diagram can be viewed as an abstraction for any number of possible object diagrams. Consistency is required between class diagrams and collaboration/object diagrams.

Additionally, a class's set of attributes and operations is documented. The attributes define the set of values that each instance of the object stores as its state. The set of operations refers to the messages that a class object may receive.

When an Aircraft Maintenance Engineer or Technician object sends a message to enterInputFile, the File class defines this operation. We extract all required fields from the input using the extract data method and calculate the N value using the calculateN method. When the message is sent to the input file, the appropriate definition of the operation is executed based on the class of the object being received. In practice, the receiving object recognises the class to which it belongs and calls the appropriate method. Thus, when the Results class receives the calculateAse message, the redefined version of the class method is invoked.

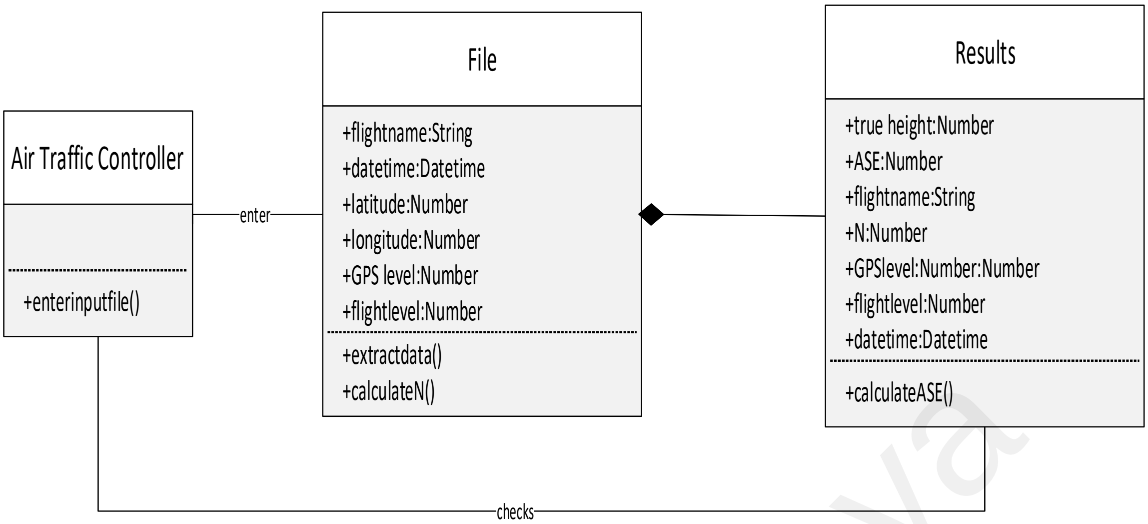

Figure 3. 7: Class Diagram of ASE Algorithm

3.3.2.2.3 Activity Diagram

The activity diagram can be used as a flowchart that consists of a list of activities performed by the system's system and dynamic behaviors. Using the activity diagram, we visualized the system's nature and constructed the executable system by using forward and reverse engineering techniques.

The activity diagram is used to model the activity flow of the ASE tool. The activity diagram is used to draw from a very high level of the ASE tool, which can be used by a business or another user who is not a technical person. Figure 4.8 illustrates the activity that needs to be performed by the user while using the ASE tool.

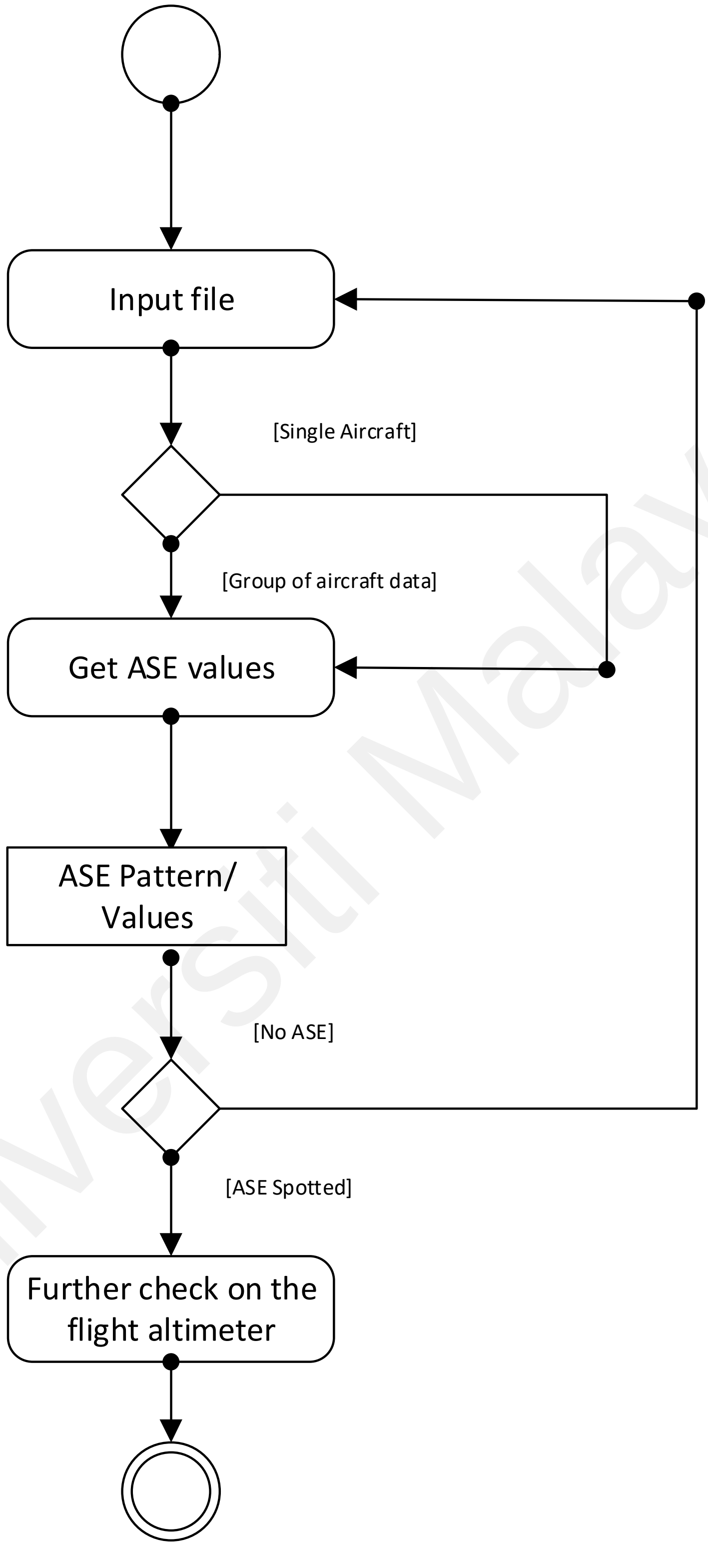

Figure 3. 8: Activity Diagram of ASE Algorithm

The very first activity will be preparing the input file and input the file to the ASE tool. Next, the user must decide whether single aircraft data and the entire file need to be processed. The ASE tool will process the data accordingly based on user choice. The ASE patterns and values will be displayed to the user. The user needs to check the output data and decide whether any significant ASE values are spotted. If there is, then further checks require to be performed against the respective flight altimeter.

Even though the activity lessens, it can be the best way to replace current health checks activity, depending on the hardware installed at the ground station, which is typically massive and requires much effort.

3.4 Tool Design

The MATLAB language is used for the tool development. A simple home page has been built using the MATLAB GUI features. A background image added to the page by using imread function of the MATLAB. A button function included in the home page which will direct to the next screen upon click on the button. A MATLAB pushbutton function has been used for the button function.

The MATLAB uigetfile function has been used to read the file from local directory. A sub table created on selected columns from the file. The Geoid Height (N) derived using the EGM96 Geopotential Model for every latitude and longitude which available in the file. The derived N value converted from meter to feet by using the convlength function. The selected columns are stored into MATLAB table. A prompt box created using questdlg function which will allow the user to choose whether to process the whole file or specific aircraft. All the column gets iterate using the column number. The Orthometric height calculated using the equation. The ASE value calculated using the formula and negative value converted abs function. All the values summarize into a single table. The graph plotted using the scatter function. The detailed algorithm included in the Appendix section.

This tool has been designed as a standalone program. The perquisition to use this tool is to have MATLAB software to be installed. The tool can be launch within the MATLAB. This tool's target user is the MRO team, and minimalize features will help the target user use the tool effortlessly.

3.4.1 Main Screen

The main screen of the ASE tool is shown in Figure 3.9. The main page is designed with a tool label and instruction text to use the tool. A push button has been placed in the middle of the home page. A simple home page created using MATLAB GUI to guide the user use the tool upon launch as simple descriptive text has been provided in the homepage.

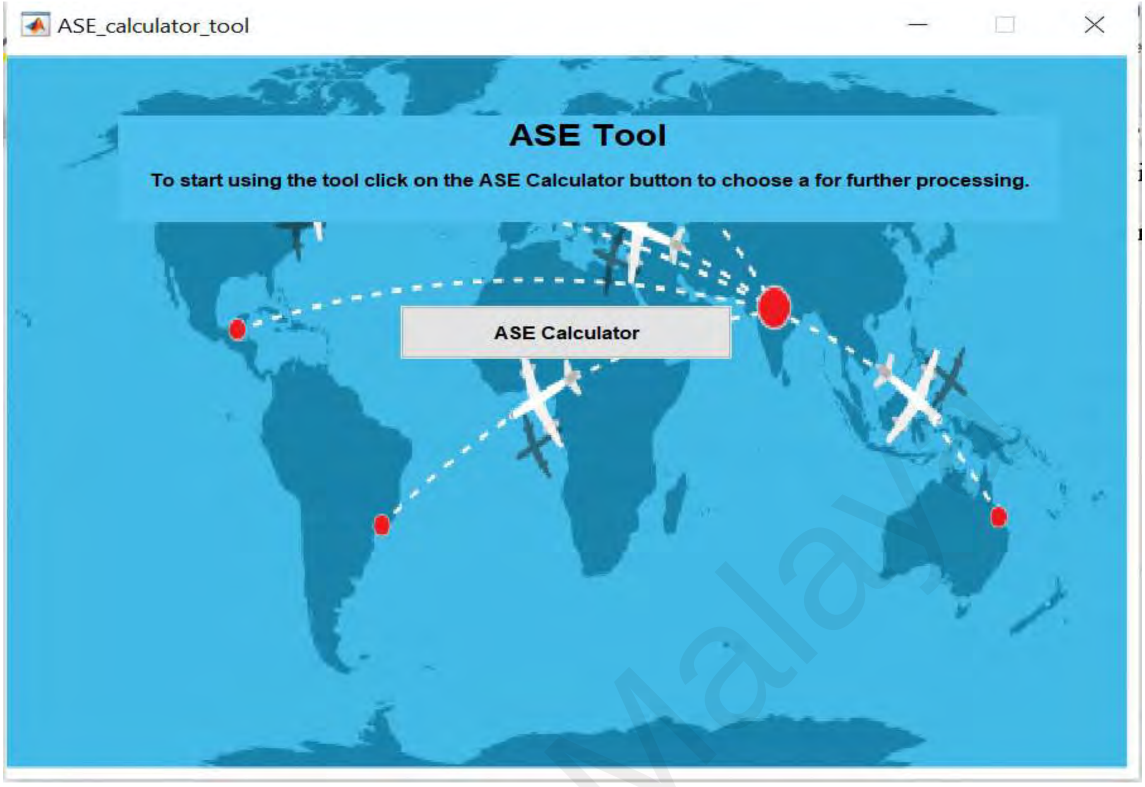

Figure 3. 9: Main Screen of the ASE calculator tool

3.4.2 File Browsing Screen

When the user clicks on the 'ASE Calculator' button, the file browsing screen, as shown in Figure 3.10, is prompted, allowing selecting the desire input file to process.

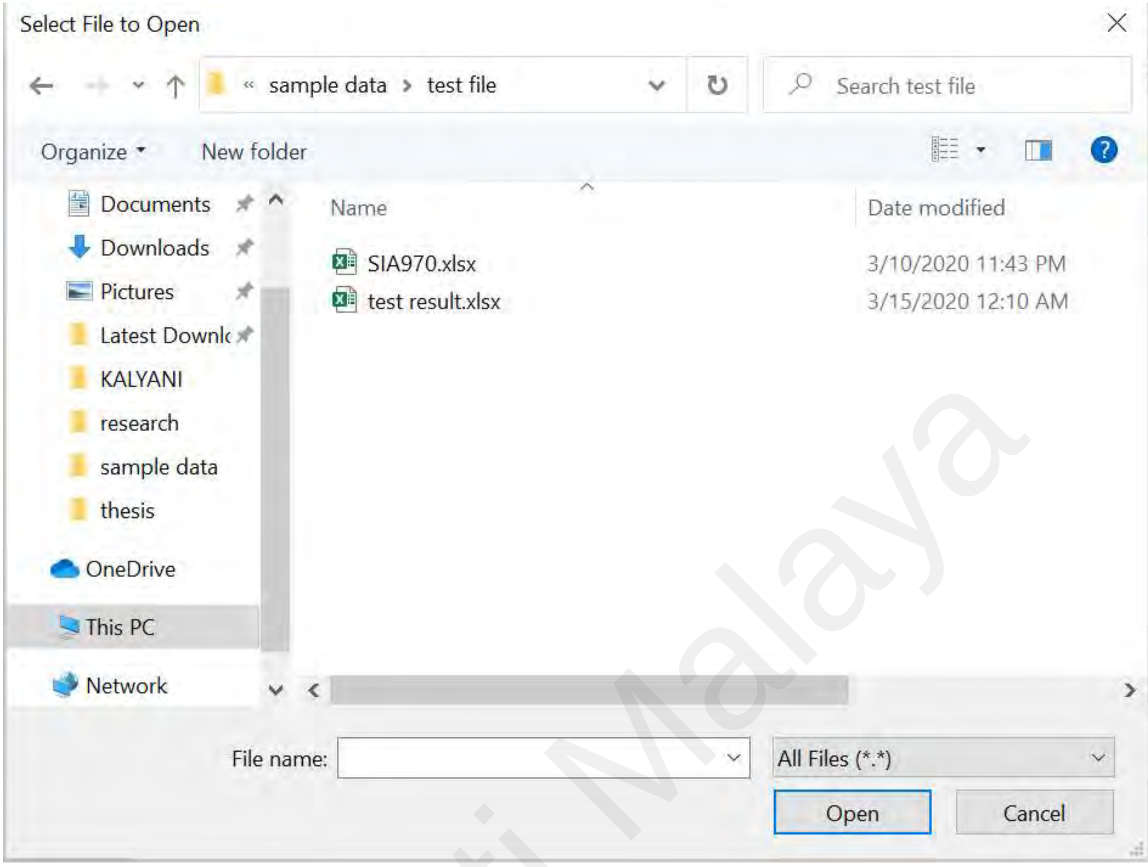

Figure 3. 9: File Browsing Screen of the ASE calculator tool

3.5 Validating Method of the ASE tool

The validation of ASE value accuracy is achieved by comparing the ASE values obtained from the algorithm of this paper with the method adopted by China RMA (ICAO,2013) with references to The National Geospatial-Intelligence Agency (NGA) for calculation of geoid based on EGM 96 (NGIA).

One flight path will be chosen and those data is processed using both the tool developed and China RMA method. Subsequently, the mean ASE value obtained from these two methods is compared and the developed tools' accuracy is measured in relative to the China RMA method.

China RMA is chosen since its method is currently in implementation, developed recently, and the method adopted and the availability of journals and references. Additionally, China RMA validated their findings against AAMA and MAAR, demonstrating the efficacy of the outcome. The ASE results from China RMA were consistent with those from the FAA's code ASE. Due to the unavailability of FAA's code results, China RMA is the available alternative for comparing the algorithm results' accuracy. The result validation enables the MatLab tool developed to demonstrate its accuracy and reliability.

This methodology for the ASE results validation is divided into 4 phases as the following;

Phase I Creating a standard dataset of a chosen flight for comparison between the algorithm used in this paper and the China RMA method

Phase II Computing the ASE value of the dataset based on China RMA procedure.

Phase III Computing the ASE value of the dataset based on the developed algorithm of this paper.

Phase IV Compare the pattern and accuracy of both values.

In the phase I above, one flight path is chosen from the available 38 flights that fulfills criteria to enable it to be compared using both the tool developed and China RMA. The criteria are a segment of a flight's ascent or descent into a Flight Level allocated in China RVSM FLAS table as shown in figure 4.6. Based on these criteria, Flight 9MSPG is chosen as one segment of the flight ascended to a flight level of 2000 feet.

In phase II and phase III, each row of the data from this flight will be evaluated to calculated its points ASE value using the China RMA method and the tool developed respectively. In Phase II, ASE values of these data is obtained by replicating the China RMA method shown in Section 3.5.1.

Meanwhile in Phase III, ASE values are obtained from the developed tools' output file. The same dataset utilized in Phase 1 to be used as an input into the algorithm and tool developed for this research. The output data will be used to compare the HKP values from the China RMA. It is to be noted that the algorithm returns the geoid value in meters and need to be converted to feet to make the comparison.

Finally in the Phase IV, the HKP graph with values from both the methods are compared for its coherence. In this phase, the accuracy of the tool developed is measured by comparing the mean ASE value obtained in relative to the mean ASE value obtained of China RMA method.

3.5.1 China RMA ASE Calculation Process

Figure 3.9 and Table 3.2 below shows the general process and its description of China RMA ASE calculation using ABS-B data.

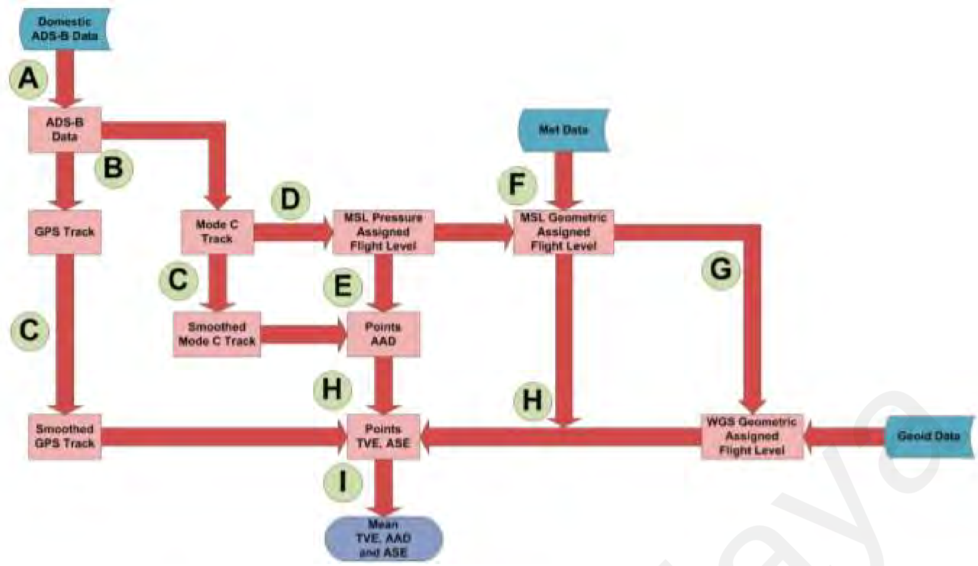

Figure 3. 10: General Process for the China RMA's ASE Calculation (ICAO,2013)

Table 3. 2 China RMA's Altimetry System Error (ASE) Calculation (ICAO,2013)

Step Number	Description of main functions
A	Data required for the ADS-B HKP monitoring.
B	Data pre-processing and Level Straight Segment Extraction
C	Data smooth for the GPS and Mode C Height
D	MSL Pressure Assigned Flight Level Estimation
E	Points AAD Calculation
F	MSL Geometric Assigned Flight Level Converting
G	HAE Geometric Assigned Flight Level Converting
H	Points TVE, ASE Calculation
I	Mean value of the TVE, AAD and ASE Calculation

Step A: Data Requirement for the ADS-B HKP Monitoring

ADS-B Data received from several domestic ADS-B stations are the input to the software and based on the data requirements, the following records were filtered out:

a) Records whose flight levels are not within the 291-411 flight level band.

b) Records whose NUC values are less than 5.

Table 3.3 presents the data items requirements. All of these seven items in the table are mandatory.

Table 3. 3: Data Items Requirement for China RMA's ASE Calculation

	Item	**Unit**
1	UTC Time	millisecond (millisecond from the midnight
2	Mode S Address	hexadecimal
3	Latitude	degree
4	Longitude	degree
5	NUC	integer
6	Geometric Height	feet
7	Mode C Height	feet

Step B: Data Pre-Processing and Level Straight Segment Extraction

Data pre-processing should be conducted to split the whole ADS-B data file into the records of different aircraft. This process will be skipped for the developed tool as the files has been already split.

The Level Straight Segment Extraction includes two separate sub-steps, the first sub-step: level segment extraction and the second sub-step: straight segment extraction. In the level segment extraction, the aircraft movement of climb or descent is used to determine the ending time for the level segment.

The second sub-step: straight segment extraction. For the straight segment extraction, the Pearson Correlation Coefficient of the longitude and latitude was used to determine the turn of the track. If the absolute value of the correlation coefficient is equal or greater than 0.95, the program will consider it as a straight level segment.

Step C: Data Smooth for the GPS and Mode C Height

After obtaining the straight level segment, the next step is to smooth the GPS and Mode C height data. Smoothing is used to reduce random noise in time series of aircraft geometric and pressure height observations and to generate a final height trace that more clearly depicts aircraft height trends.

However, because the ADS-B data is nonparametric, the nonparametric regression method is required. The Kernel Regression Smoothing method is used in RMA's software to smooth both GPS and Mode C data. Kernel regression is a nonparametric technique for estimating a random variable's conditional expectation. The Gaussian Kernel is used in China RMA's ASE software. In the Kernel Smoothing, the bandwidth has a significant impact on the result's accuracy. In China, the RMA's ASE process software employs Bowman, and Azzalini's (1997) recommended optimal bandwidth.

Step D&E: MSL Pressure Assigned Flight Level Estimation and Points AAD Calculation

MSL Pressure Assigned Flight Level Estimation; and Points AAD Calculation are the steps required to calculate ASE. The nearest standard flight level is estimated in China RMA's software based on the Chinese RVSM airspace. The MSL Pressure Assigned Flight Level will be defined as the nearest standard flight level.

The AAD points will be determined by subtracting the Assigned Flight Level from the smoothed Mode C height. Furthermore, for each point AAD on a track (level straight segment), the point's ASE value will be calculated.

Step F: MSL Geometric Assigned Flight Level Converting

Due to the inaccessibility of meteorological data, Step F of the China RMA, MSL Geometric Assigned Flight Level Conversion will be skipped. The data is assumed to be identical to the value for Mode C in Step D.

Step G: HAE Geometric Assigned Flight Level Converting

HAE Geometric Assigned Flight Level Conversion is performed in step G. Geoid values derived from an online calculator (NGA) provided by The National Geospatial-Intelligence Agency (NGA) according EGM 96 model will be used for this purpose in-lieu of FAA's ASE software tool used in China RMA.

Step H&I: TVE Points Calculation, ASE Calculation, and TVE, AAD, and ASE Mean Value Calculation.

These two steps complete the ASE calculation. First, subtract the HAE Geometric Assigned Flight Level from the smoothed GPS height to obtain the points TVE. Second, points TVE will subtract the smoothed points AAD in order to obtain the HAE points ASE.

The step number from A to I can be found in Figure 3.10. The validation will be based on HAE geometric height (Step G) without considering the MSL geometric height (Step F) due to meteorological data's unavailability. The geometric height for this step will be assumed to be the same as the altimeter reading.

The validation will be based on HAE geometric height (Step G) without considering the MSL geometric height (Step F) due to meteorological data's unavailability. The geometric height for this step will be assumed to be the same as the altimeter reading.

China RMA method is used to validate the MatLab algorithm developed in this paper. China RMA is chosen since its method is currently in implementation, developed recently, and the method adopted and the availability of journals and references. Additionally, China RMA validated their findings against AAMA and MAAR, demonstrating the efficacy of the outcome. The ASE results from China RMA were consistent with those from the FAA's code ASE. Due to the unavailability of FAA's code results, China RMA is the available alternative for comparing the algorithm results' accuracy. The result validation enables the MatLab tool developed to demonstrate its accuracy and reliability.

CHAPTER 4: RESULTS AND DISCUSSION

4.1 Introduction

This chapter contains the observation, results, and findings on the outputs from the tool developed. The algorithm and tool output were tested using inputs from ADS-B data obtained from London Terminal Area provided by the airspace operators (NATS) based in the United Kingdom. The ASE value accuracy of the developed tool is then validated against the ASE value obtained using the China RMA system for the same dataset.

4.2 ASE Calculation Process Using the ADS-B Data

The Altimetry System Error algorithm and tool is a comprehensive design which can be easily adapt and used by all the user with simple understanding of the ASE concept and values. The tool is not requiring any special expertise to be onboard to operate and not require any special equipment to operate the tools. Since, nowadays most of the aircraft equipped with the ADS-B. Hence, ADS-B data can be easily accessed to process the ASE values. However, to validate and understand the ASE values aircraft the aircraft maintenance team should acquire the ASE concept and values. Figure 4.1, illustrates processing of the ASE algorithm.

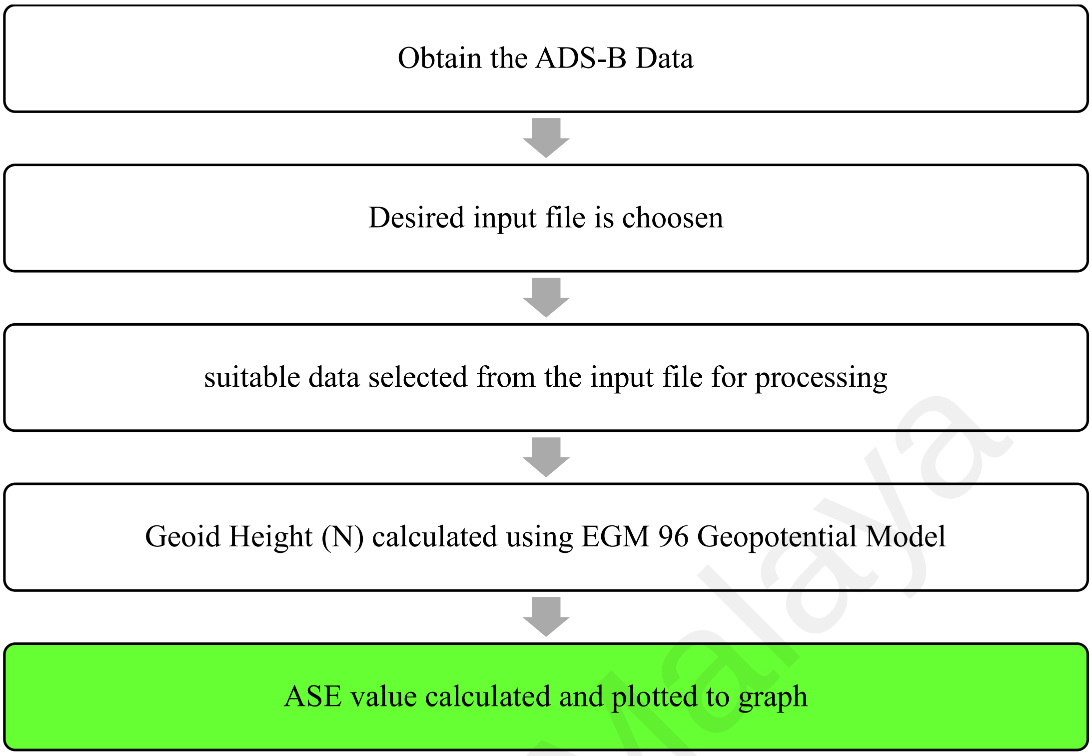

Figure 4. 1: ASE calculation process using the ADS-B Data

With the existing ASE monitoring system, there is a known limitation where the ASE value only will be able to generate when the aircraft fly over the ground station. However, with this algorithm the flight entire data used to process. Hence, it can be easily identified if in any point of time out the ASE values are out of range.

4.3 Altimetry System Error (ASE) Tool inputs and outputs

Few datasets were created from the ADS-B data collected and processed using the ASE tool developed. Figure 4.2 shows home screen of the tool. The ASE calculator button needs to clicks in order move to the next processing screen.

Figure 4. 2: Home screen of ASE Tool

Figure 4.3 below illustrates, input screen. The respective input file needs to be chosen in order the algorithm processed the data.

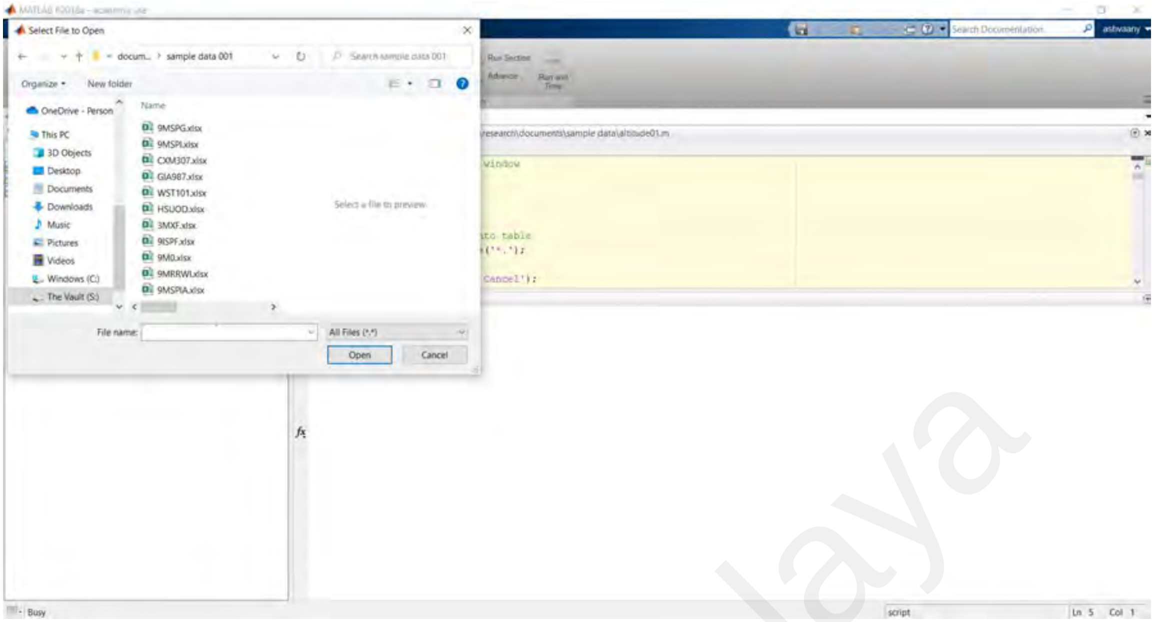

Figure 4. 3: File Input Screen

Figure 4.4 illustrates Dialog box screen appeared upon choosing the aircraft processing file, and value 'No' is choose to process the single aircraft ASE values.

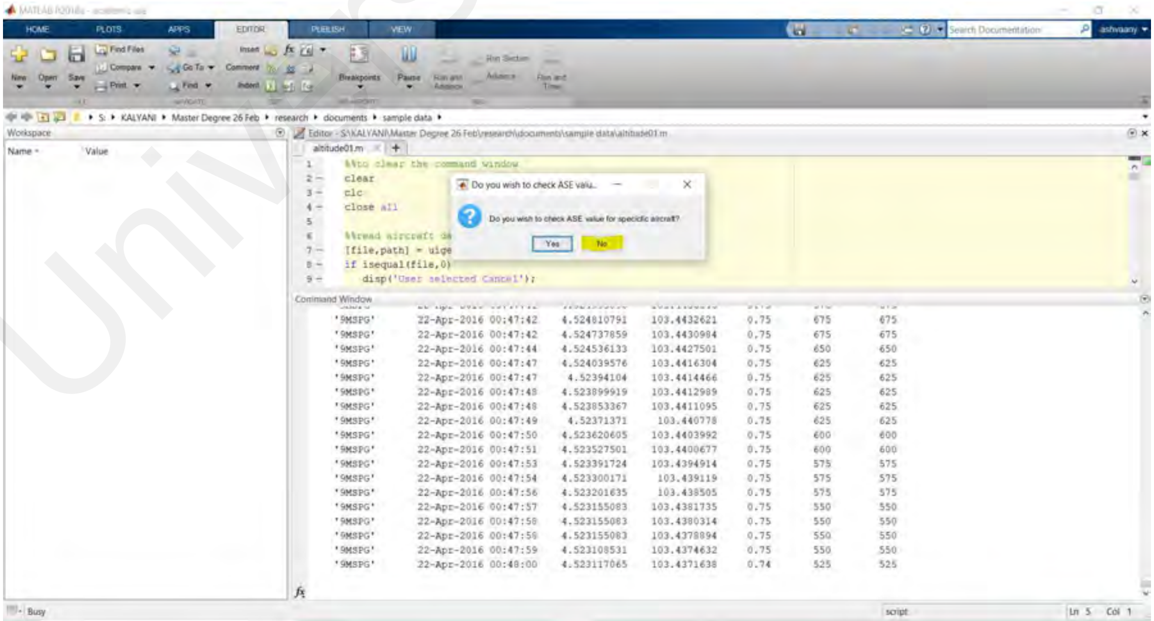

Figure 4. 4: Dialog Box Screen

Figure 4.5 illustrates upon the file gets processed; the aircraft related information such as aircraft name, datetime, latitude, longitude, N, GPS Level and flight level which are extracted from the file get displays in the output panel.

Aircraft	DateTime	Latitude	Longitude	N	GPSLevel	Level
'9MSPG'	22-Apr-2016 00:00:00	5.227157593	104.2946095	0.5249343832021	975	975
'9MSPG'	22-Apr-2016 00:00:01	5.227615356	104.2951215	0.492125984251968	975	975
'9MSPG'	22-Apr-2016 00:00:01	5.227816307	104.2953912	0.492125984251968	975	975
'9MSPG'	22-Apr-2016 00:00:02	5.228027344	104.2956336	0.492125984251968	975	975
'9MSPG'	22-Apr-2016 00:00:03	5.228374934	104.2960068	0.492125984251968	975	975
'9MSPG'	22-Apr-2016 00:00:03	5.22857666	104.2962388	0.492125984251968	950	950
'9MSPG'	22-Apr-2016 00:00:04	5.228793904	104.2964804	0.492125984251968	950	950
'9MSPG'	22-Apr-2016 00:00:05	5.229309082	104.2970767	0.492125984251968	950	950
'9MSPG'	22-Apr-2016 00:00:05	5.22953874	104.2973328	0.492125984251968	950	950
'9MSPG'	22-Apr-2016 00:00:06	5.229771501	104.2976169	0.492125984251968	950	950
'9MSPG'	22-Apr-2016 00:00:06	5.230050814	104.297901	0.492125984251968	950	950
'9MSPG'	22-Apr-2016 00:00:07	5.230270386	104.2981474	0.492125984251968	925	925
'9MSPG'	22-Apr-2016 00:00:08	5.230545044	104.2984733	0.492125984251968	925	925
'9MSPG'	22-Apr-2016 00:00:08	5.230728149	104.2986595	0.492125984251968	925	925
'9MSPG'	22-Apr-2016 00:00:09	5.231277466	104.2992647	0.492125984251968	925	925
'9MSPG'	22-Apr-2016 00:00:10	5.231493934	104.2995111	0.492125984251968	925	925
'9MSPG'	22-Apr-2016 00:00:10	5.231735229	104.2997768	0.492125984251968	925	925
'9MSPG'	22-Apr-2016 00:00:12	5.232421875	104.3005681	0.492125984251968	900	900
'9MSPG'	22-Apr-2016 00:00:12	5.232750844	104.3009317	0.492125984251968	900	900
'9MSPG'	22-Apr-2016 00:00:13	5.233154297	104.3014061	0.492125984251968	900	900
'9MSPG'	22-Apr-2016 00:00:15	5.233635337	104.3019735	0.492125984251968	875	875
'9MSPG'	22-Apr-2016 00:00:16	5.234161377	104.3025233	0.459317585301837	875	875

Figure 4. 5: Aircraft related processed data

Figures 4.6 to 4.9 show the final output from the tool showing ASE results plotted against time and the flight level. Blue dots represent the ASE value of aircraft, and an orange triangle is used to plot flight levels. For an example, Figure 4.6 to Figure 4.9 below shows the outputs for flight 9MSPG, 9MSPI, CXM307 and WST101respectively.

Figure 4.6 below illustrates the ASE patterns of aircraft 9MSPG in relation to flight level. Blue dots represent the ASE values and the majority of the points between 0 and 500 as recommended by ICAO levels.

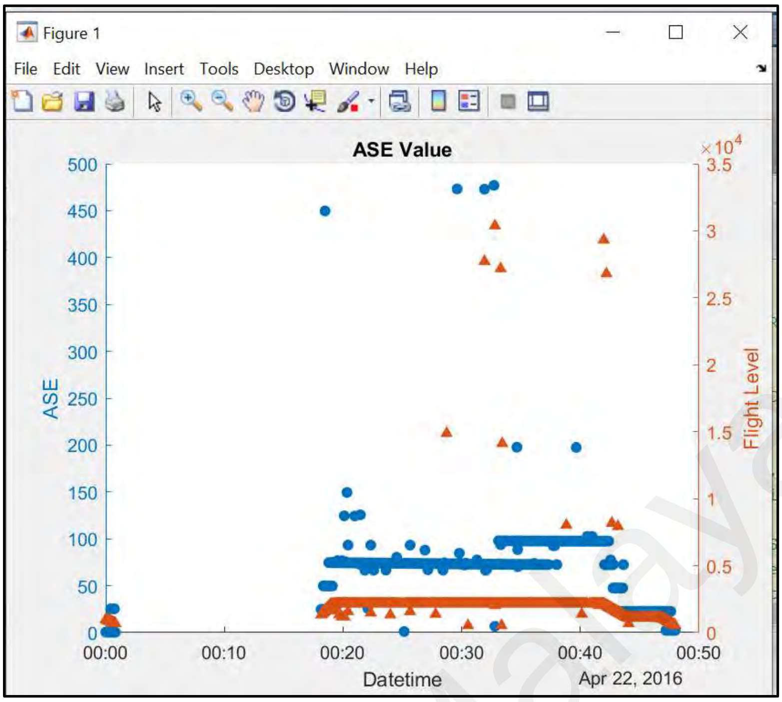

Figure 4. 6: ASE values of aircraft 9MSPG

Figure 4.7 below illustrates the ASE patterns of aircraft 9MSPI in relation to flight level. Blue dots represent the ASE values and the majority of the points between 0 and 600.

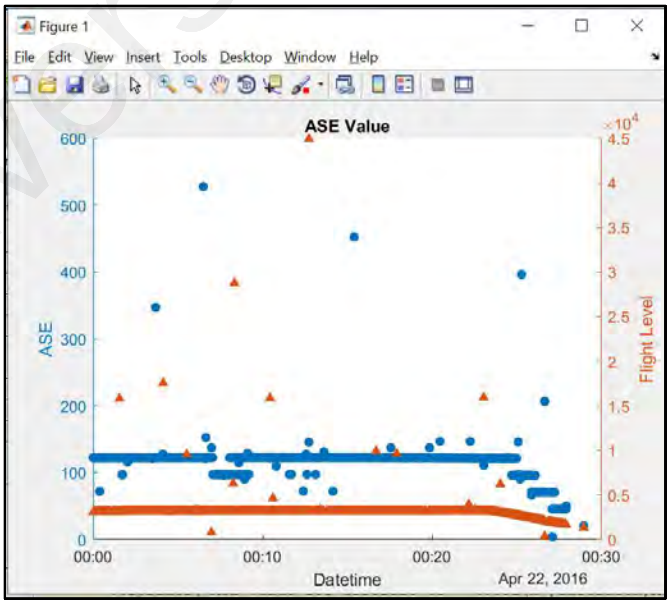

Figure 4. 7: ASE values of aircraft 9MSPI

Figure 4.8 below illustrates ASE patterns of aircraft CXM307 in relation to flight level. Blue dots are presenting the ASE values within the range of 0 to 180.

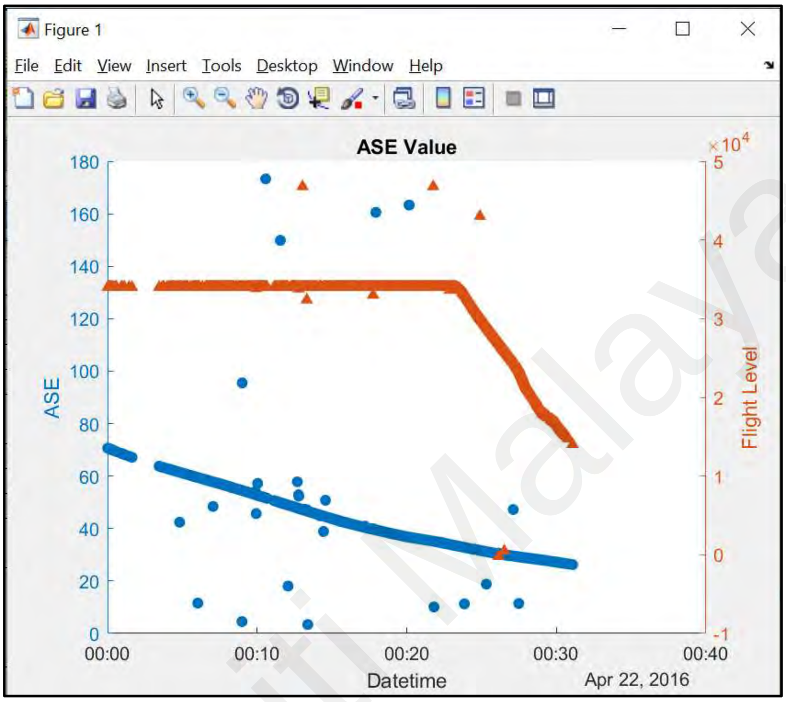

Figure 4. 8: ASE values of aircraft CXM307

Figure 4.9 below illustrates the ASE patterns of the aircraft WST101 in relation to flight level. Blue dots represent the ASE values between 0 and 500.

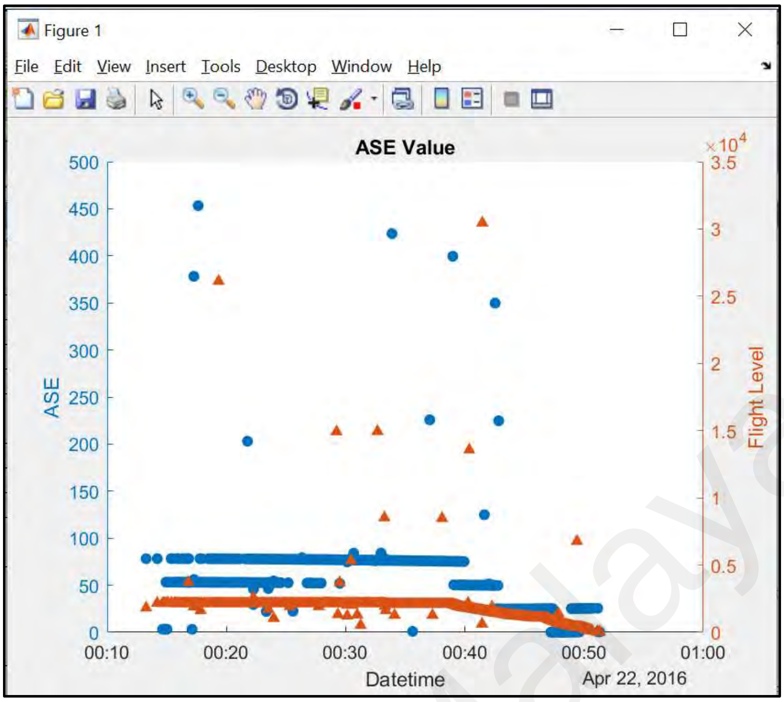

Figure 4. 9: ASE values of aircraft WST101

In general, the results of the developed tool ASE on the sample dataset demonstrated that coherent results are obtained, as the majority of results indicate that ASE values are consistent and within the ICAO recommended range. As part of the research objective, a simple tool for calculating ASE values has been developed. As a result, this tool can be used to monitor Height in Malaysia.

4.4 Altimetry System Error (ASE) Results Validation

<u>Phase I: Flight Dataset for Comparison</u>

Flight 9MSPG is chosen based on the criteria that one segment of the flight ascended to a flight level of 2000 feet. Although the RVSM required to be filtered out in the region of

FL290 (29000 feet) to FL 410 (41000 feet), FL 20 (2000 feet) is chosen to base on the minimum FL allocated in China RVSM FLAS table as shown in Figure 4.6. ADS-B data of Flight 9MSPG will be utilized to generate the data requirement according to Step A of China RMA (table 4.1). The table below shows the data required and its units for China RMA ASE calculations.

Table 4. 1: Complete Dataset of Flight 9MSPG

i	icao24bit	id	seconds since midnight (sec)	latitude (°)	longitude (°)	nuc	Mode C Level (feet)	GPS Level (feet)
1	1.11E+22	47911068	0	5.2272	104.2946	7	975	975
2	1.11E+22	47911069	1	5.2276	104.2951	7	975	975
3	1.11E+22	47911173	1	5.2278	104.2954	7	975	975
4	1.11E+22	47911254	2	5.2280	104.2956	7	975	975
5	1.11E+22	47911345	3	5.2284	104.2960	7	975	975

--- (rows break) ---

3186	1.11E+22	48204586	2877	4.5232	103.4382	7	550	550
3187	1.11E+22	48204587	2878	4.5232	103.4380	7	550	550
3188	1.11E+22	48204588	2878	4.5232	103.4379	7	550	550
3189	1.11E+22	48204589	2879	4.5231	103.4375	7	550	550
3190	1.11E+22	48204647	2880	4.5231	103.4372	7	525	525

The following graph can be plotted using the data in Table 4.1. The following figures illustrated both with and without random noise. To ensure the validity of the results, out-of-range data has been removed, and only data without random noise has been considered for comparison. It can be observed and marked from Figure 4.10 that the flight path has five segments of flight ascend, descend and constant flight level.

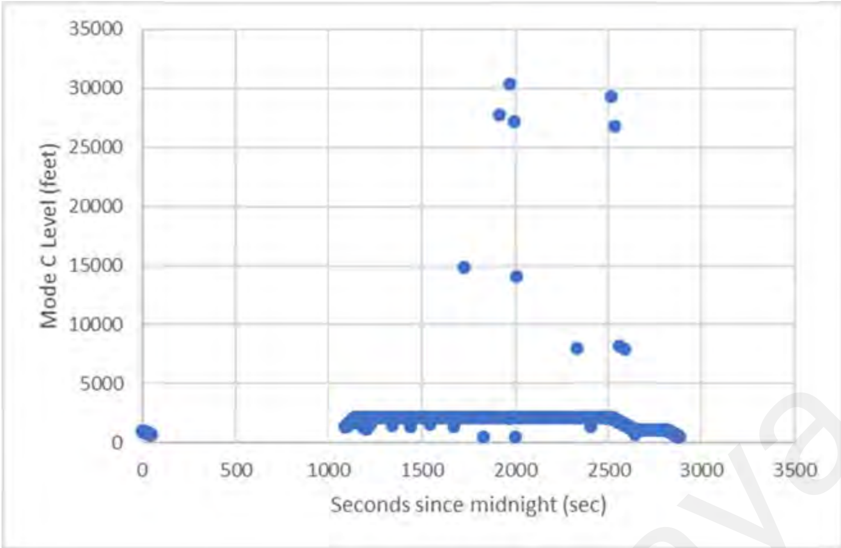

Figure 4. 10: Flight 9MSPG path (with random noise)

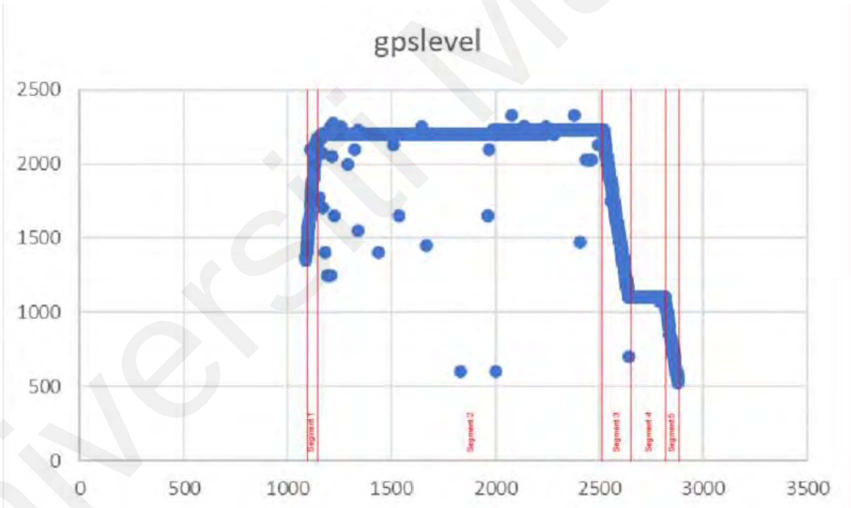

Figure 4. 11: Flight 9MSPG path (without random noise)

According to China RMA Step B: Data Pre-Processing and Level Straight Segment Extraction, the chosen data range is Segment 1 of Figure 4.11; the aircraft ascent from initial 1325 feet to 2125 feet, starting at 1089 seconds and ends at 1164 second, as shown in Figure 4.12 below. Table 4.2 below shows the dataset of the level segment extraction.

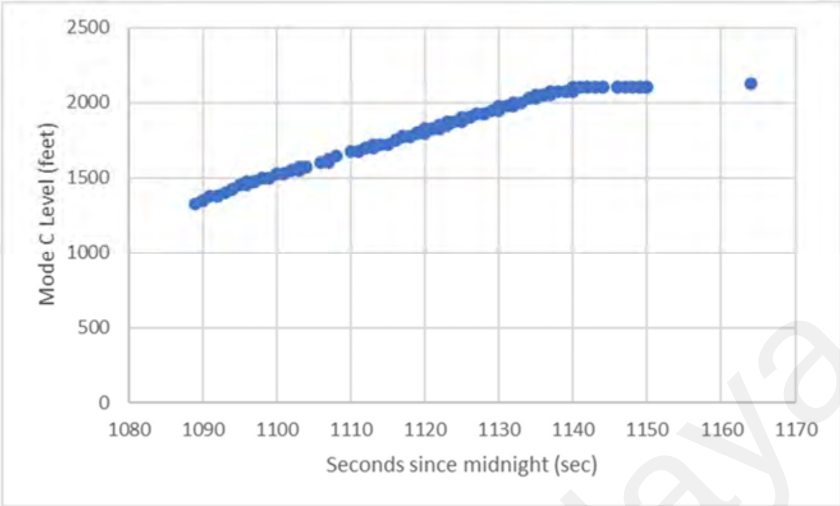

Figure 4. 12: Level segment extraction; Flight Ascent from 1325 feet to 2125

Table 4. 2: Level Segment Extraction Dataset of Flight 9MSPG

N			$\sum x_i$				$\sum y_{i\text{-ModeC}}$	$\sum x_i^2$	$\sum x_i y_{i\text{-ModeC}}$	$\sum y_{i\text{-ModeC}}^2$
103			115381				185025	129284971	207725675	338638125
i			x_i	latitude	longitude		$y_{i\text{-ModeC}}$			
i	icao24bit	id	seconds since midnight (sec)	latitude (°)	longitude (°)	nuc	Mode C Level (feet)	x_i^2	$x_i y_{i\text{-ModeC}}$	$y_{i\text{-ModeC}}^2$
1	1.11E+22	47917843	1089	5.2944	104.3750	7	1325	1185921	1442925	1755625
2	1.11E+22	48065653	1090	5.2941	104.3747	7	1350	1188100	1471500	1822500
3	1.11E+22	48065797	1090	5.2939	104.3745	7	1350	1188100	1471500	1822500
4	1.11E+22	48065798	1091	5.2938	104.3744	7	1375	1190281	1500125	1890625
5	1.11E+22	48065881	1092	5.2937	104.3743	7	1375	1192464	1501500	1890625

--- (rows break) ---

99	1.11E+22	48071065	1149	5.2734	104.3530	7	2100	1320201	2412900	4410000
100	1.11E+22	48071066	1149	5.2733	104.3528	7	2100	1320201	2412900	4410000
101	1.11E+22	48071126	1150	5.2731	104.3526	7	2100	1322500	2415000	4410000
102	1.11E+22	48071127	1150	5.2728	104.3523	7	2100	1322500	2415000	4410000
103	1.11E+22	48072060	1164	5.2667	104.3456	7	2125	1354896	2473500	4515625

The second sub-step of the China RMA Step B:. The Pearson Correlation Coefficient of the longitude and latitude was used to determine the turn of the track.

$$r = \frac{N\sum xy \_ (\sum x)(\sum y)}{\sqrt{[Nx^2 - (\sum x)^2][N\sum y^2 - (\sum y)^2]}}$$ (3) *Pearson correlation coefficient formula*

Where:

N = the number of pairs of scores

$\sum xy$ = the sum of the products of paired scores

$\sum x$ = the sum of x scores

$\sum y$ = the sum of y scores

$\sum y^2$ = the sum of squared y scores

Table 4.3 below shows the values obtained from table 4.2 to calculate the Pearson Correlation Coefficient. The value of the Pearson Correlation Coefficient for this data set is equal to 0.986. Since this value I more than 0.95~~,~~ it is a straight-level segment.

Table 4. 3: Computation of Pearson Correlation Coefficient

	Mode C Level (feet)
N	103
$\sum xy$	207725675
$\sum x$	115381
$\sum y$	185025
$\sum x^2$	129284971
$\sum y^2$	338638125
r	0.9856

Phase II Computing the ASE value based on China RMA procedure.

The Kernel Regression Smoothing method is used in RMA's software to smooth both GPS and Mode C data. The Nadaraya-Watson Kernel Estimation (1964) is as follows:

$$m_{n(x)} = \frac{\sum_{i=1}^{n} \mathrm{K}\left(\frac{x-X_i}{h_n}\right).Y_i}{\sum_{i=1}^{n} K\left(\frac{x-X_i}{h_n}\right)} \qquad \text{(4) Nadaraya-Watson Kernel Estimation (1964)}$$

The Gaussian Kernel is used in China RMA's ASE software because it removes more high-frequency 'noise' from the data.

$$\mathrm{K(u)} = \frac{1}{\sqrt{2\pi}} e^{\frac{-u^2}{2}} \qquad \text{(5) Gaussian Kernel}$$

In China, the RMA's ASE process software employs Bowman, and Azzalini's (1997) recommended optimal bandwidth:

$$h_{x} = \frac{median|x_{i-median(x_i)}}{0.6745} \cdot \left(\frac{4}{3}n\right)^{1/5}$$

$$h_{y} = \frac{median|y_{i-median(y_i)}}{0.6745} \cdot \left(\frac{4}{3}n\right)^{1/5}$$

$$h = \sqrt{h_x}.h_y \qquad \text{(6) Bowman, and Azzalini's (1997)}$$

Table 4.4 and 4.5 below show the calculation of each value required for the Kernel Regression Smoothing for Mode C Level and GPS level, respectively. It is to be noted that value x_j is a linearly spaces series of data points which include observed data points where K values need to be estimated. Table 4.6 shows the computation of bandwidth h value and data smoothed value for the GPS and Mode C Height dataset.

Table 4. 4: Calculation of values required for Kernel Regression Smoothing for Mode C Level

N		$\sum x_i$	$\sum x_j$	$\sum y_{i\text{-ModeC}}$	$\sum y_{i\text{-GPS}}$				$\sum K(u_{ModeC})$	$\sum K(u)*y_{i\text{-ModeC}}$
103		115381	115360	185025	189775				41.05	73737.98
i		x_i	x_j	$y_{i\text{-ModeC}}$	$y_{i\text{-GPS}}$					
i	id	seconds since midnight (sec)		Mode C Level (feet)	GPS Level (feet)	$\lvert x_i$ - median $(x_i)\rvert$	$\lvert y_{i\text{-ModeC}}$ - median $(y_{i\text{-ModeC}})\rvert$	$u = (x_j-x_i)/h_{ModeC}$	$K(u_{i\text{-ModeC}})$	$K(u_i)*y_{i\text{-ModeC}}$
1	47917843	1089	1069	1325	1350	32.00	500	-0.08	0.40	526.92
2	48065653	1090	1070	1350	1375	31.00	475	-0.08	0.40	536.86
3	48065797	1090	1071	1350	1375	31.00	475	-0.08	0.40	537.03
4	48065798	1091	1072	1375	1400	30.00	450	-0.08	0.40	546.98
5	48065881	1092	1073	1375	1400	29.00	450	-0.08	0.40	546.98

--- (rows break) ---

99	48071065	1149	1167	2100	2175	28.00	275	0.07	0.40	835.63
100	48071066	1149	1168	2100	2175	28.00	275	0.08	0.40	835.38
101	48071126	1150	1169	2100	2175	29.00	275	0.08	0.40	835.38
102	48071127	1150	1170	2100	2175	29.00	275	0.08	0.40	835.12
103	48072060	1164	1171	2125	2200	43.00	300	0.03	0.40	847.42

Table 4. 5: Calculation of values required for Kernel Regression Smoothing for GPS Level

N		$\sum x_i$	$\sum x_j$	$\sum y_{i\text{-ModeC}}$	$\sum y_{i\text{-GPS}}$				$\sum K(u_{GPS})$	$\sum K(u)*y_{i\text{-GPS}}$
103		115381	115360	185025	189775				41.05	75631.04
i		x_i	x_j	$y_{i\text{-ModeC}}$	$y_{i\text{-GPS}}$					
i	id	seconds since midnight (sec)		Mode C Level (feet)	GPS Level (feet)	$\lvert x_i$ - median $(x_i)\rvert$	$\lvert y_{i\text{-GPS}}$ - median $(y_{i\text{-GPS}})\rvert$	$u = (x_j-x_i)/h_{GPS}$	$K(u_{i\text{-GPS}})$	$K(u_i)*y_{i\text{-GPS}}$
1	47917843	1089	1069	1325	1350	32.00	525	-0.08	0.40	536.86
2	48065653	1090	1070	1350	1375	31.00	500	-0.08	0.40	546.81
3	48065797	1090	1071	1350	1375	31.00	500	-0.08	0.40	546.98
4	48065798	1091	1072	1375	1400	30.00	475	-0.08	0.40	556.92
5	48065881	1092	1073	1375	1400	29.00	475	-0.08	0.40	556.92

--- (rows break) ---

99	48071065	1149	1167	2100	2175	28.00	300	0.07	0.40	865.47
100	48071066	1149	1168	2100	2175	28.00	300	0.08	0.40	865.22
101	48071126	1150	1169	2100	2175	29.00	300	0.08	0.40	865.22
102	48071127	1150	1170	2100	2175	29.00	300	0.08	0.40	864.95
103	48072060	1164	1171	2125	2200	43.00	325	0.03	0.40	877.33

Table 4. 6: Computation of bandwidth (h) and Kernel Regression Smoothing value $m_n(x)$ for the Mode C and GPS Height

	Mode C Level (feet)	GPS Level (feet)
n	103	103
Median $\lvert x_i$ - median $(x_i)\rvert$	16	16
Median $\lvert y_i$ - median $(y_i)\rvert$	250	250
h_x	63.49	63.49
h_y	992.00	992.00
h (bandwidth)	250.96	250.96
$A=1/\sqrt{(2\pi)}$	0.40	0.40
$\sum K(u)$	41.05	41.05
$\sum K(u)*yi$	73737.98	75631.04
$m_n(x)$	1796.39	1842.51

Figure 4.13 and 4.14 below represent the smooth value $m_n(x)$ against the dataset for Mode C and GPS Height.

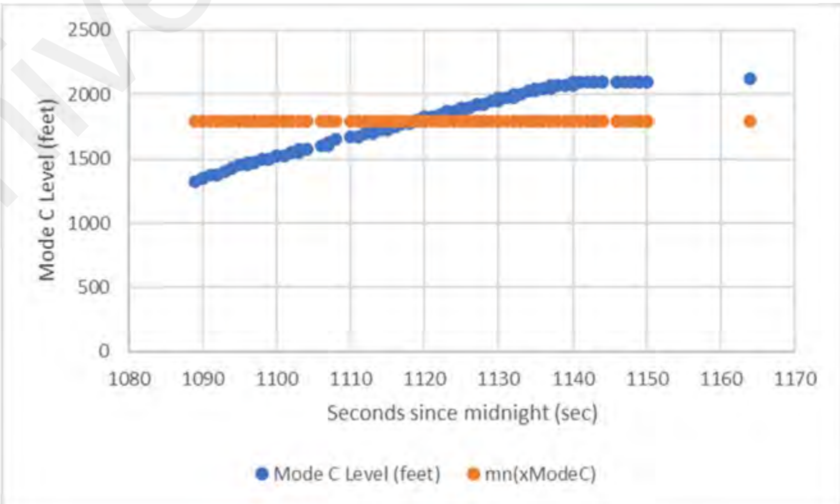

Figure 4. 13: Data Smooth for the Mode C Height

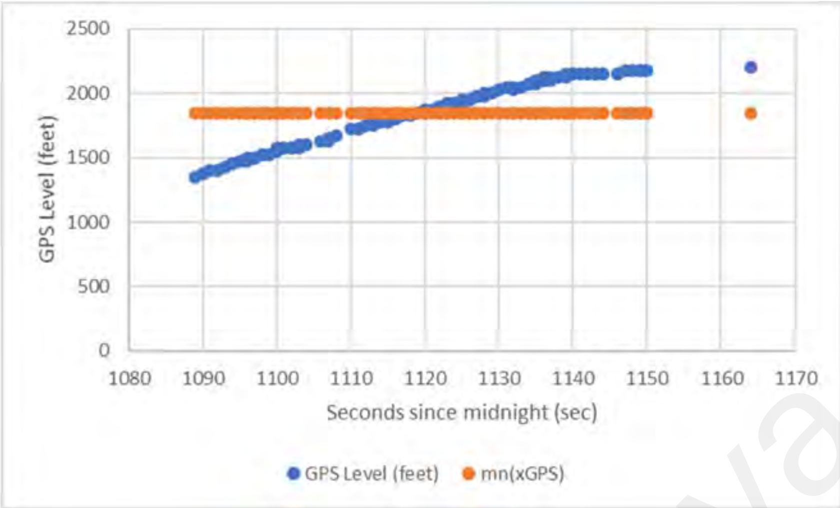

Figure 4. 14: Data Smooth for the GPS Height

Step D&E; MSL Pressure Assigned Flight Level Estimation; and Points AAD Calculation are the steps required to calculate ASE. The nearest standard flight level is estimated in China RMA's software based on the Chinese RVSM airspace. Furthermore, for each point AAD on a track (level straight segment), the point's ASE value will be calculated.

Based on Figure 2.4, the nearest assigned standard flight level to $m_n(x_{ModeC})$ (1796.39) is 2000 feet. Table 4.7 below represents the points AAD calculations, and the values are represented in Figure 4.15.

Table 4. 7: Points AAD calculations

i	id	seconds since midnight (sec)		Mode C Level (feet)	$m_n(x_{ModeC})$	Points AAD
1	47917843	1089	1069	1325	1796.39	-675
2	48065653	1090	1070	1350	1796.39	-650
3	48065797	1090	1071	1350	1796.39	-650
4	48065798	1091	1072	1375	1796.39	-625
5	48065881	1092	1073	1375	1796.39	-625
--- (rows break) ---						
99	48071065	1149	1167	2100	1796.39	100
100	48071066	1149	1168	2100	1796.39	100
101	48071126	1150	1169	2100	1796.39	100
102	48071127	1150	1170	2100	1796.39	100
103	48072060	1164	1171	2125	1796.39	125

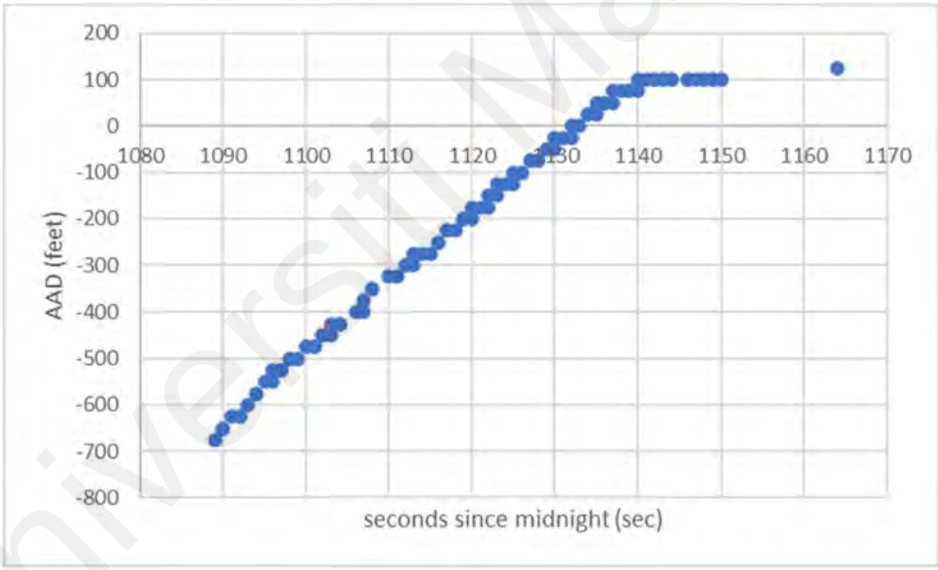

Figure 4. 15: Points AAD vs seconds since midnight (sec)

Step F of MSL Geometric Assigned Flight Level Conversion will be skipped due to the inaccessibility of meteorological data. The data is assumed to be identical to the value for Mode C in Step D. The data is assumed to be identical to the value for Mode C in Step D.

HAE Geometric Assigned Flight Level Conversion is performed in step G of the China RMA by subtracting the geoid from the MSL geometric Assigned Flight Level (2000ft). The outcome is depicted in Table 4.8 and figure 4.16 below;

Table 4. 8: Conversion to HAE Geometric Assigned Flight Level

						Converted to degree, Minute, Second	Converted to degree, Minute, Second	NGA EGM96 GEOID CALCULATOR	
i		x_i	latitude	longitude	$y_{i\text{-}ModeC}$	latitude	longitude	$y_{i\text{-}NGA}$	$y_{i\text{-}HAE\text{-}NGA}$
i	id	seconds since midnight (sec)	latitude (°)	longitude (°)	Mode C Level (feet)	latitude	longitude	$Geoid_{NGA}$ ft	HAE geometric Assigned Flight Level (feet)
1	47917843	1089	5.2944	104.3750	1325	5° 17' 40"	104° 22' 30"	0.22	1999.78
2	48065653	1090	5.2941	104.3747	1350	5° 17' 39"	104° 22' 29"	0.22	1999.78
3	48065797	1090	5.2939	104.3745	1350	5° 17' 38"	104° 22' 28"	0.22	1999.78
4	48065798	1091	5.2938	104.3744	1375	5° 17' 38"	104° 22' 28"	0.22	1999.78
5	48065881	1092	5.2937	104.3743	1375	5° 17' 37"	104° 22' 27"	0.23	1999.77

--- (rows break) ---

99	48071065	1149	5.2734	104.3530	2100	5° 16' 24"	104° 21' 11"	0.33	1999.67
100	48071066	1149	5.2733	104.3528	2100	5° 16' 24"	104° 21' 10"	0.33	1999.67
101	48071126	1150	5.2731	104.3526	2100	5° 16' 23"	104° 21' 9"	0.33	1999.67
102	48071127	1150	5.2728	104.3523	2100	5° 16' 22"	104° 21' 8"	0.33	1999.67
103	48072060	1164	5.2667	104.3456	2125	5° 15' 60"	104° 20' 44"	0.36	1999.64

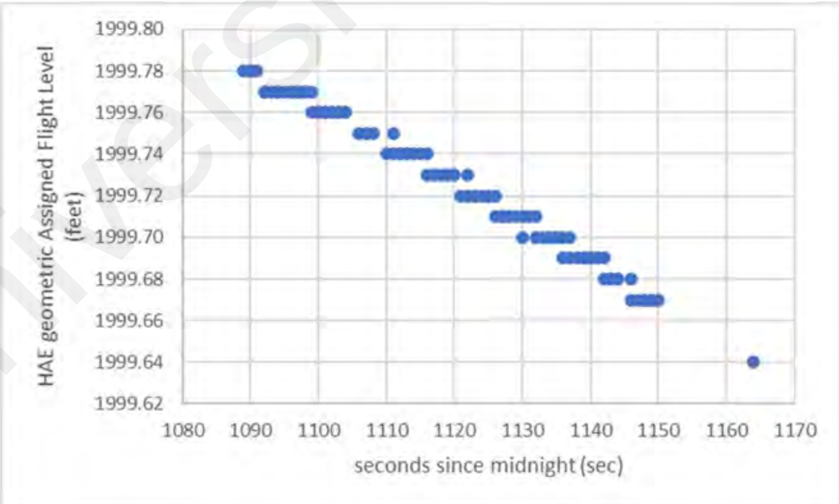

Figure 4. 16: Data for the HAE geometric Assigned Flight Level (Step G Table 2.1)

The final steps of the China RMA method in this phase are Step H&I: TVE Points Calculation, ASE Calculation, and TVE, AAD, and ASE Mean Value CalculationThe outcome is represented in table 4.9 and figure 4.17 below;

Table 4. 9: Calculation of points AAD, TVE, ASE & Mean ASE

N		∑ x_i			∑ $y_{i\text{-ModeC}}$	∑ $y_{i\text{-AAD}}$	∑ $y_{i\text{-HAE-NGA}}$	Average	Mean ASE (feet)
103		115381			185025	-20975	205971.70	-157.25	46.39
i		x_i	latitude	longitude	$y_{i\text{-ModeC}}$	$y_{i\text{-AAD}}$	$y_{i\text{-HAE-NGA}}$		
i	id	seconds since midnight (sec)	latitude (°)	longitude (°)	Mode C Level (feet)	Points AAD	HAE geometric Assigned Flight Level (feet)	Points TVE (feet)	Points ASE (feet)
1	47917843	1089	5.2944	104.3750	1325	-675	1999.78	-649.78	25.22
2	48065653	1090	5.2941	104.3747	1350	-650	1999.78	-624.78	25.22
3	48065797	1090	5.2939	104.3745	1350	-650	1999.78	-624.78	25.22
4	48065798	1091	5.2938	104.3744	1375	-625	1999.78	-599.78	25.22
5	48065881	1092	5.2937	104.3743	1375	-625	1999.77	-599.77	25.23
--- (rows break) ---									
99	48071065	1149	5.2734	104.3530	2100	100	1999.67	175.33	75.33
100	48071066	1149	5.2733	104.3528	2100	100	1999.67	175.33	75.33
101	48071126	1150	5.2731	104.3526	2100	100	1999.67	175.33	75.33
102	48071127	1150	5.2728	104.3523	2100	100	1999.67	175.33	75.33
103	48072060	1164	5.2667	104.3456	2125	125	1999.64	200.36	75.36

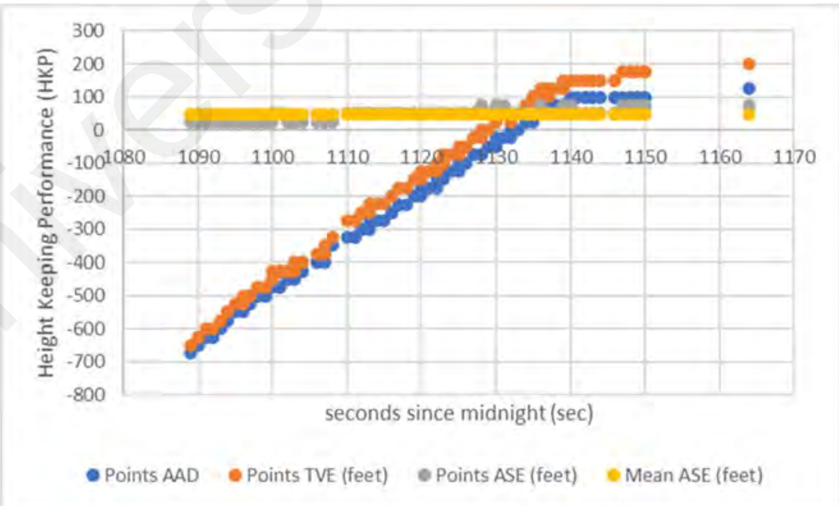

Figure 4. 17: Height Keeping Performance based on China RMA (AAD, TVE, ASE & Mean ASE)

Phase III Computing the ASE value based on an algorithm of this research.

Table 4.10 and Figure 4.18 below represent the points ASE Values obtained from the algorithm and tool developed in this paper and its mean ASE value.

Table 4. 10: Calculation of points ASE Value & Mean ASE using the tool developed

N		$\sum x_i$			$\sum y_{i\text{-ModeC}}$	$\sum y_{i\text{-GPS}}$		$\sum y_{i\text{-Algo}}$		Mean ASE - Algo (feet)
103		115381			185025	189775	om Matlab Algorith	26.97		45.85
							M (Geoid N) based on EGM96	M convert to Ft		
i		x_i	latitude	longitude	$y_{i\text{-ModeC}}$	$y_{i\text{-GPS}}$		$y_{i\text{-Algo}}$	Algorithm	
i	id	seconds since midnight (sec)	latitude (°)	longitude (°)	Mode C Level (feet)	GPS Level (feet)	$Geoid_{Algo}$ N (meter)	$Geoid_{Algo}$ N (feet)	True Height (feet)	Points ASE (feet)
1	47917843	1089	5.2944	104.3750	1325	1350	0.06	0.20	1349.80	24.80
2	48065653	1090	5.2941	104.3747	1350	1375	0.06	0.20	1374.80	24.80
3	48065797	1090	5.2939	104.3745	1350	1375	0.06	0.20	1374.80	24.80
4	48065798	1091	5.2938	104.3744	1375	1400	0.06	0.20	1399.80	24.80
5	48065881	1092	5.2937	104.3743	1375	1400	0.06	0.20	1399.80	24.80

--- (rows break) ---

99	48071065	1149	5.2734	104.3530	2100	2175	0.10	0.33	2174.67	74.67
100	48071066	1149	5.2733	104.3528	2100	2175	0.10	0.33	2174.67	74.67
101	48071126	1150	5.2731	104.3526	2100	2175	0.10	0.33	2174.67	74.67
102	48071127	1150	5.2728	104.3523	2100	2175	0.10	0.33	2174.67	74.67
103	48072060	1164	5.2667	104.3456	2125	2200	0.11	0.36	2199.64	74.64

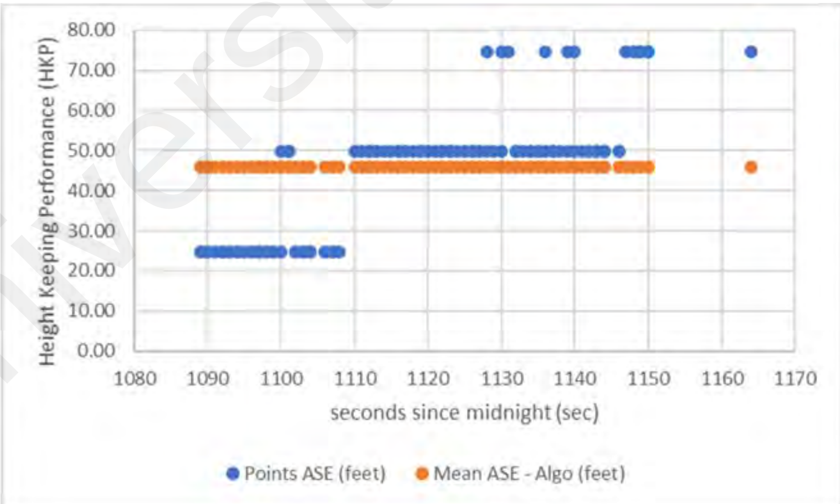

Figure 4. 18: Height Keeping Performance based on a tool developed (ASE & Mean ASE)

Phase IV Compare the pattern and accuracy of the values.

Table 4.11 and Figure 4.19 below represent the Height Keeping Performance (HKP) measurement of points ASE and means ASE values using both methods for comparison.

Table 4. 11: Height Keeping Performance value (ASE & Mean ASE) comparison based on China RMA and the MatLab tool

N		$\sum x_i$			$\sum y_{i\text{-ModeC}}$	$\sum y_{i\text{-GPS}}$	Mean ASE	Mean ASE
103		115381			185025	189775	46.39	45.85
i		x_i	latitude	longitude	$y_{i\text{-ModeC}}$	$y_{i\text{-GPS}}$	China RMA	Matlab Algorithm
i	id	seconds since midnight (sec)	latitude (°)	longitude (°)	Mode C Level (feet)	GPS Level (feet)	Points ASE (feet)	Points ASE (feet)
1	47917843	1089	5.2944	104.3750	1325	1350	25.22	24.80
2	48065653	1090	5.2941	104.3747	1350	1375	25.22	24.80
3	48065797	1090	5.2939	104.3745	1350	1375	25.22	24.80
4	48065798	1091	5.2938	104.3744	1375	1400	25.22	24.80
5	48065881	1092	5.2937	104.3743	1375	1400	25.23	24.80
--- (rows break) ---								
99	48071065	1149	5.2734	104.3530	2100	2175	75.33	74.67
100	48071066	1149	5.2733	104.3528	2100	2175	75.33	74.67
101	48071126	1150	5.2731	104.3526	2100	2175	75.33	74.67
102	48071127	1150	5.2728	104.3523	2100	2175	75.33	74.67
103	48072060	1164	5.2667	104.3456	2125	2200	75.36	74.64

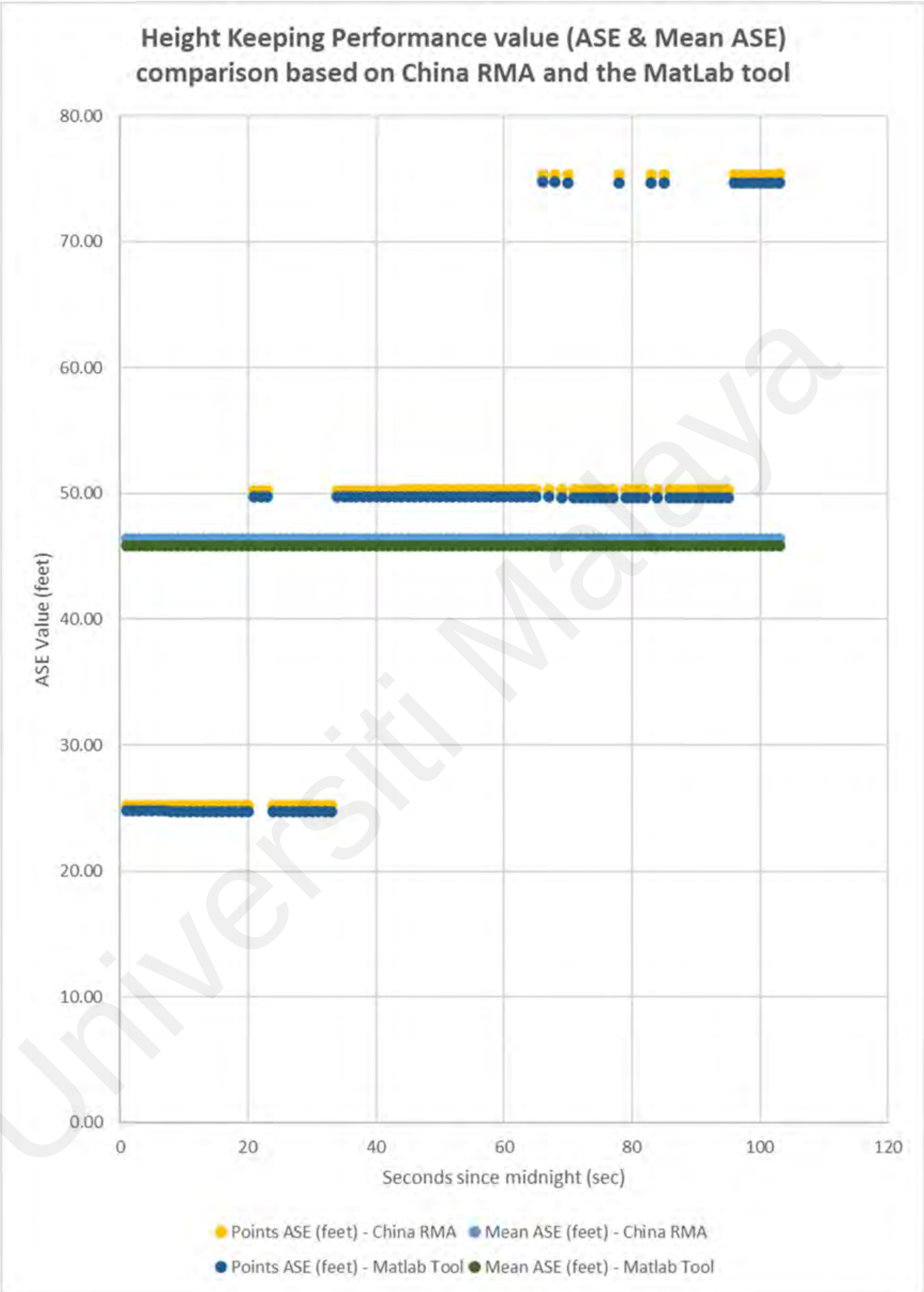

Figure 4. 19: Height Keeping Performance value (ASE & Mean ASE) comparison based on China RMA and the MatLab tool

Mean ASE value obtained from China RMA procedure = 46.39 feet

Mean ASE value obtained from an algorithm developed in this research = 45.85 feet

Accuracy of mean ASE value obtained from MatLab tool compared to the value obtained from China RMA method

= (8) / (7) x 100%

= 45.85 feet / 46.39 feet x 100%

= 98.84 %

The complete spreadsheet for complete spreadsheet of ASE results comparison between the developed algorithm and China RMA method can be found at Appendix B: It can be observed from Figure 4.13 above that the values obtained from both methods are in coherent. Thus, it reaffirms that the MatLab tool developed can measure HKP of aircraft and can be utilized by the Civil Aviation Authority of Malaysia through further development and enhancement.

The accuracy of 98.84% is deemed acceptable. It can be observed that the minor deviation between both values is due to the slight differences between geoid values obtained from each method. However, both are based on EGM 96, an online calculator provided by The National Geospatial-Intelligence Agency (NGA) and MatLab Algorithm developed in this research.

Furthermore, the China RMA method is developed in collaboration with The Federal Aviation Administration (FAA) and with a benchmark against the Australian Airspace Monitoring Agency (AAMA) and Monitoring Agency for Asia Region (MAAR) using the domestic ADS-B data. To measure the actual performance and reliability of the MatLab algorithm and tool developed, discussions and technical assistance is required from FAA, ICAO and other RMAs in the region.

CHAPTER 5: CONCLUSION

5.1 Summary of the work

As part of this research paper, the existing method and system to measure ASE has been reviewed and analyzed. The limitations of each method are evaluated to identifies the gap in existing methods or systems. A simpler process in calculating ASE is identified as part of this research. An algorithm is developed to calculates the ASE value. The pattern of Figure 4.21 and Figure 4.22 in the result section show that both graphs behave in the same way. The accuracy of each measurement is 98.84%. This means the algorithm developed is on par with other RMAs in the region. The principles of algorithm have been used to solved the problem discussed in this interdisciplinary research by having an input and processing it through the 6 elements of the algorithm to achieve the desired output.

5.2 Fulfilment of Research Aims and Objectives

The overall aim of this research to develop an algorithm that can calculate the ASE using ADS-B data. To achieve the overall research, aim the objectives are break down to the following:

5.2.1. Fulfilling Objective 1

The first objective is to identify a process involve in measuring ASE values using the ADS-B Dataset. This objective is achieved where a simpler process identified in processing the ADS-B data and calculate the ASE values. In an existing method, there is a various limitation where an expert must be onboard, aircraft must be equipped with special equipment and the aircraft must flyover the ground station. However, with this simplify process there is no need of any expert to be onboard and the ASE can be determined during the aircraft maintenance activity with the availability of the ADS-B Data.

5.2.2. Fulfilling Objective 2

The second objective is to develop an algorithm to calculate the Aircraft Altimetry System Error. An algorithm developed to achieved objective 2. The algorithm designed is a simple and independent tool and produced an accurate result. The algorithm also developed only require minimal software knowledge to use the tool and easily used by all.

5.2.3. Fulfilling Objective 3

The third objective is to evaluate or validate the performance of the developed ASE tool in terms of accuracy by benchmarking against existing methods. This objective is achieved by measuring the mean ASE values of the same flight by comparing the ASE value derived from the China RMA method and the algorithm built as part of this research paper. Overall, 98.84 % of accuracy is achieved when compare algorithm results against the China RMA method. The limitations are the unavailability of the existing software to measure the ASE using ADS-B data as it has been developed in house by the China RMA team for their application.

5.3 Limitations of this research

As of now, there is no specific RMA body in Malaysia to monitor the HKP. Hence, there is no access to the Malaysia meteorological data. The meteorological data are requiring to converting the pressure altitude to the geometric height. Meteorological data is needed to determine the assigned flight level's geometric height. However, in this research, we cannot perform a comparison against meteorological data due to the data unavailability.

5.4 Implications of the research work and recommendations

This research work will incentivize the Malaysian aviation industry to develop and use the ADS-B data for ASE calculations. The ASE tool can be used as part of aircraft maintenance and inspection checks by the aircraft maintenance engineers as the tool does not require any device or machine to be installed to validate the aircraft the ASE. The tool will help capture the ASE value in the spots where the existing systems failed to capture the flight ASE value. For instance, the existing AGHME requires the aircraft to passing through the AGHME coverage volume to capture the ASE values. The ASE patterns of each aircraft will be analyzed, and the respective team will be educated and notify if there is any alarming ASE value. Based on the ASE results, necessary actions that need to be taken can improve aircraft performance and safety. The algorithm can be further developed to include TVE and AAD calculations. Meteorological data needs to include the data into the algorithm to increase the HKP measurement accuracy. Cooperation with DCA of Malaysia, meteorological department of Malaysia, international Aviation bodies to develop a fully functional application that can be utilized to measure HKP of flights utilizing Malaysian in particular and the region in general.

5.5 Future work

This research work contributes to the Malaysia ATC to monitor and evaluate the aircraft ASE's. At present, the input data has been channeled through CSV or Excel files. However, further research work needs to study whether the algorithm can be enhanced to read the real-time data directly from the ADS-B data device. The algorithms can also be improved by incorporating some smoothing technique to remove noise data in the time series of aircraft geometric and pressure height to increase the accuracy of the ASE calculation accuracy (ICAO,2013). The algorithm has been built based on the EGM96 model, and further studies are proposed to explore implications using the latest EGM2008 model. Further studies require incorporating the algorithm into the real-time Air Traffic Controller System and can be further improved with the Big Data Analytics approach in the future when it comes to processing more volume and variety of data.

APPENDICES

Appendix A: MATLAB Algorithm for Calculation of ASE

Editor - S:\KALYANI\Master Degree 26 Feb\research\documents\sample data\ASE_calculator_tool.m

ASE_calculator_tool.m

```
function varargout = ASE_calculator_tool(varargin)
% ASE_CALCULATOR_TOOL MATLAB code for ASE_calculator_tool.fig
%      ASE_CALCULATOR_TOOL, by itself, creates a new ASE_CALCULATOR_TOOL or raises the existing
%      singleton*.
%
%      H = ASE_CALCULATOR_TOOL returns the handle to a new ASE_CALCULATOR_TOOL or the handle to
%      the existing singleton*.
%
%      ASE_CALCULATOR_TOOL('CALLBACK',hObject,eventData,handles,...) calls the local
%      function named CALLBACK in ASE_CALCULATOR_TOOL.M with the given input arguments.
%
%      ASE_CALCULATOR_TOOL('Property','Value',...) creates a new ASE_CALCULATOR_TOOL or raises the
%      existing singleton*.  Starting from the left, property value pairs are
%      applied to the GUI before ASE_calculator_tool_OpeningFcn gets called.  An
%      unrecognized property name or invalid value makes property application
%      stop.  All inputs are passed to ASE_calculator_tool_OpeningFcn via varargin.
%
%      *See GUI Options on GUIDE's Tools menu.  Choose "GUI allows only one
%      instance to run (singleton)".
%
% See also: GUIDE, GUIDATA, GUIHANDLES

% Edit the above text to modify the response to help ASE_calculator_tool

% Last Modified by GUIDE v2.5 17-Oct-2020 23:33:07

% Begin initialization code - DO NOT EDIT
```

```
gui_Singleton = 1;
gui_State = struct('gui_Name',       mfilename, ...
                   'gui_Singleton',  gui_Singleton, ...
                   'gui_OpeningFcn', @ASE_calculator_tool_OpeningFcn, ...
                   'gui_OutputFcn',  @ASE_calculator_tool_OutputFcn, ...
                   'gui_LayoutFcn',  [] , ...
                   'gui_Callback',   []);
if nargin && ischar(varargin{1})
    gui_State.gui_Callback = str2func(varargin{1});
end

if nargout
    [varargout{1:nargout}] = gui_mainfcn(gui_State, varargin{:});
else
    gui_mainfcn(gui_State, varargin{:});
end
% End initialization code - DO NOT EDIT




% --- Executes just before ASE_calculator_tool is made visible.
function ASE_calculator_tool_OpeningFcn(hObject, ~, handles, varargin)
% This function has no output args, see OutputFcn.
% hObject    handle to figure
% eventdata  reserved - to be defined in a future version of MATLAB
```

Appendix A: MATLAB Algorithm for Calculation of ASE (Continued)

```
% handles    structure with handles and user data (see GUIDATA)
% varargin   command line arguments to ASE_calculator_tool (see VARARGIN)

% Choose default command line output for ASE_calculator_tool
handles.output = hObject;
% create an axes that spans the whole gui

ah = axes('unit', 'normalized', 'position', [0 0 1 1]);

% import the background image and show it on the axes

bg = imread('your_image.jpg'); imagesc(bg);

% prevent plotting over the background and turn the axis off

set(ah,'handlevisibility','off','visible','off')

% making sure the background is behind all the other uicontrols
uistack(ah, 'bottom');
% Update handles structure
guidata(hObject, handles);

% UIWAIT makes ASE_calculator_tool wait for user response (see UIRESUME)
% uiwait(handles.figure1);

```

```
% --- Outputs from this function are returned to the command line.
function varargout = ASE_calculator_tool_OutputFcn(~, ~, handles)
% varargout  cell array for returning output args (see VARARGOUT);
% hObject    handle to figure
% eventdata  reserved - to be defined in a future version of MATLAB
% handles    structure with handles and user data (see GUIDATA)

% Get default command line output from handles structure
varargout{1} = handles.output;


% --- Executes on button press in pushbutton1.
function pushbutton1_Callback(~, ~,~)
% hObject    handle to pushbutton1 (see GCBO)
% eventdata  reserved - to be defined in a future version of MATLAB
% handles    structure with handles and user data (see GUIDATA)
%%to clear the command window
clear
clc
close all

%%read aircraft data into table
[file,path] = uigetfile('*.');
if isequal(file,0)
   disp('User selected Cancel');
else
```

```
else
   disp(['User selected ', fullfile(path,file)]);
end
%%aircraftfile = 'S:\KALYANI\Master Degree 26 Feb\research\documents\sample data\2018_ADSBOutput_1.csv';
aircraftfile=fullfile(path,file);
airlinedata = readtable(aircraftfile,'ReadRowNames',true);

rownumber = size(airlinedata,1);

%%create subtable on selected coulmns
aircraftdata=airlinedata(1:rownumber,1:19);
aircraftdata.Properties.Description = 'Aircraft Data';

%%calculates the geoid height using the EGM96 Geopotential Model
N=round((geoidheight(aircraftdata.latitude,aircraftdata.longitude))',3);
N = convlength(N,'m','ft');

aircraftGU = table(aircraftdata.callsign,aircraftdata.datadate,aircraftdata.latitude,aircraftdata.longitude,N,aircraftdata.gpslevel
aircraftGU.Properties.VariableNames = {'Aircraft' 'DateTime' 'Latitude' 'Longitude' 'N' 'GPSLevel' 'Level'};
display(aircraftGU );

row = rownumber;
i=1;
arrayA = nan(row, 1);
arrayB = nan(row, 1);
arrayC = NaT(row, 1);
arrayD = cell(row,1);
```

Appendix A: MATLAB Algorithm for Calculation of ASE (Continued)

```
arrayE = nan(row, 1);
arrayF = nan(row, 1);
arrayG = cell(i, 1);

dlgTitle    = 'User Choice';
dlgQuestion = 'Do you wish to check ASE value for specicfic aircraft?';
option = questdlg(dlgQuestion,dlgQuestion', 'Yes','No','Yes');

switch option
    case 'Yes'
        choice = 0;
    case 'No'
        choice = 1;
end


if choice == 1
 %% Now let's iterate over all columns using column number.
 prev_aircraft = ' ';

for row = 1:size(aircraftGU,1) %columns in table

       aircraftN = string(aircraftGU.Aircraft(row));

       air = aircraftGU.Aircraft(row);

       if string(air) ~= string(prev_aircraft)
```

```
       if string(air) ~= string(prev_aircraft)
          arrayG(i,:) =  air;
          i = i + 1;
       end
       prev_aircraft= air;

       geoidN = aircraftGU.N(row);
       h = aircraftGU.GPSLevel(row);
       FL = aircraftGU.Level(row);
       datetime1 = datetime(aircraftGU.DateTime(row));
       %%calculate true height/orthometric height
       H = h - geoidN;
       %%fprintf('Actual height for aircraft %s = %0.3f\n',aircraftN,H);
       %%calculate Altimetry system error
       %%absolute/modulus ASE
       ASE = abs(FL - H);
       %%fprintf('ASE value for aircraft %s = %0.3f\n',aircraftN,ASE);


arrayA(row,:) = FL;
arrayB(row,:) = ASE;
arrayC(row,:) = datetime1;
arrayD(row,:) = air;
arrayE(row,:) = geoidN;
arrayF(row,:) = H;
end
```

Appendix B: Complete Spreadsheet of ASE Results Comparison between the Developed Algorithm and China RMA Method.

COLUMN / RAW	A	B	C	D	E	F	G	H	I	J	K
1		ADS-B DATA									
2	N				date/time/sec	$\sum x_i$				$\sum y_{i\text{-ModeC}}$	$\sum y_{i\text{-GPS}}$
3	103					115381				185025	189775
4	i					x_i	latitude	longitude		$y_{i\text{-ModeC}}$	$y_{i\text{-GPS}}$
5	i	icao24bit	callsign	id	datadate	seconds since midnight (sec)	latitude (°)	longitude (°)	nuc	Mode C Level (feet)	GPS Level (feet)
6	1	1.11E+22	9MSPG	47917843	4/22/2016 0:18:09	1089	5.2944	104.3750	7	1325	1350
7	2	1.11E+22	9MSPG	48065653	4/22/2016 0:18:10	1090	5.2941	104.3747	7	1350	1375
8	3	1.11E+22	9MSPG	48065797	4/22/2016 0:18:10	1090	5.2939	104.3745	7	1350	1375
9	4	1.11E+22	9MSPG	48065798	4/22/2016 0:18:11	1091	5.2938	104.3744	7	1375	1400
10	5	1.11E+22	9MSPG	48065881	4/22/2016 0:18:12	1092	5.2937	104.3743	7	1375	1400
11	6	1.11E+22	9MSPG	48065942	4/22/2016 0:18:12	1092	5.2935	104.3741	7	1375	1400
12	7	1.11E+22	9MSPG	48065943	4/22/2016 0:18:13	1093	5.2933	104.3738	7	1400	1425
13	8	1.11E+22	9MSPG	48066010	4/22/2016 0:18:14	1094	5.2930	104.3735	7	1425	1450
14	9	1.11E+22	9MSPG	48066082	4/22/2016 0:18:14	1094	5.2928	104.3733	7	1425	1450
15	10	1.11E+22	9MSPG	48066083	4/22/2016 0:18:15	1095	5.2927	104.3731	7	1450	1475
16	11	1.11E+22	9MSPG	48066226	4/22/2016 0:18:16	1096	5.2925	104.3730	7	1450	1475
17	12	1.11E+22	9MSPG	48066227	4/22/2016 0:18:16	1096	5.2923	104.3728	7	1475	1500
18	13	1.11E+22	9MSPG	48066381	4/22/2016 0:18:17	1097	5.2922	104.3727	7	1475	1500
19	14	1.11E+22	9MSPG	48066455	4/22/2016 0:18:17	1097	5.2922	104.3725	7	1475	1500
20	15	1.11E+22	9MSPG	48066528	4/22/2016 0:18:17	1097	5.2920	104.3724	7	1475	1500
21	16	1.11E+22	9MSPG	48066597	4/22/2016 0:18:18	1098	5.2918	104.3723	7	1500	1525
22	17	1.11E+22	9MSPG	48066677	4/22/2016 0:18:18	1098	5.2917	104.3721	7	1500	1525
23	18	1.11E+22	9MSPG	48066745	4/22/2016 0:18:19	1099	5.2916	104.3719	7	1500	1525
24	19	1.11E+22	9MSPG	48066746	4/22/2016 0:18:19	1099	5.2914	104.3717	7	1500	1525
25	20	1.11E+22	9MSPG	48066817	4/22/2016 0:18:20	1100	5.2912	104.3716	7	1525	1550
26	21	1.11E+22	9MSPG	48066818	4/22/2016 0:18:20	1100	5.2911	104.3714	7	1525	1575
27	22	1.11E+22	9MSPG	48066881	4/22/2016 0:18:21	1101	5.2909	104.3713	7	1525	1575
28	23	1.11E+22	9MSPG	48066882	4/22/2016 0:18:21	1101	5.2908	104.3711	7	1525	1575
29	24	1.11E+22	9MSPG	48066944	4/22/2016 0:18:22	1102	5.2906	104.3709	7	1550	1575
30	25	1.11E+22	9MSPG	48066945	4/22/2016 0:18:22	1102	5.2904	104.3707	7	1550	1575
31	26	1.11E+22	9MSPG	48067011	4/22/2016 0:18:23	1103	5.2903	104.3706	7	1550	1575
32	27	1.11E+22	9MSPG	48067012	4/22/2016 0:18:23	1103	5.2901	104.3704	7	1575	1600
33	28	1.11E+22	9MSPG	48067087	4/22/2016 0:18:24	1104	5.2900	104.3703	7	1575	1600
34	29	1.11E+22	9MSPG	48067088	4/22/2016 0:18:24	1104	5.2898	104.3701	7	1575	1600
35	30	1.11E+22	9MSPG	48067155	4/22/2016 0:18:26	1106	5.2893	104.3695	7	1600	1625
36	31	1.11E+22	9MSPG	48067227	4/22/2016 0:18:27	1107	5.2891	104.3694	7	1600	1625
37	32	1.11E+22	9MSPG	48067290	4/22/2016 0:18:27	1107	5.2889	104.3692	7	1625	1650
38	33	1.11E+22	9MSPG	48067359	4/22/2016 0:18:28	1108	5.2884	104.3686	7	1650	1675
39	34	1.11E+22	9MSPG	48067524	4/22/2016 0:18:30	1110	5.2877	104.3679	7	1675	1725
40	35	1.11E+22	9MSPG	48067586	4/22/2016 0:18:31	1111	5.2876	104.3678	7	1675	1725
41	36	1.11E+22	9MSPG	48067587	4/22/2016 0:18:31	1111	5.2874	104.3676	7	1675	1725
42	37	1.11E+22	9MSPG	48067633	4/22/2016 0:18:32	1112	5.2872	104.3675	7	1700	1750
43	38	1.11E+22	9MSPG	48067636	4/22/2016 0:18:32	1112	5.2871	104.3673	7	1700	1750
44	39	1.11E+22	9MSPG	48067709	4/22/2016 0:18:33	1113	5.2869	104.3671	7	1700	1750
45	40	1.11E+22	9MSPG	48067767	4/22/2016 0:18:33	1113	5.2867	104.3669	7	1725	1775
46	41	1.11E+22	9MSPG	48067840	4/22/2016 0:18:34	1114	5.2864	104.3666	7	1725	1775
47	42	1.11E+22	9MSPG	48068060	4/22/2016 0:18:35	1115	5.2861	104.3663	7	1725	1775
48	43	1.11E+22	9MSPG	48068135	4/22/2016 0:18:36	1116	5.2858	104.3659	7	1750	1800
49	44	1.11E+22	9MSPG	48068190	4/22/2016 0:18:36	1116	5.2856	104.3658	7	1750	1800
50	45	1.11E+22	9MSPG	48068410	4/22/2016 0:18:37	1117	5.2855	104.3656	7	1775	1825
51	46	1.11E+22	9MSPG	48068473	4/22/2016 0:18:37	1117	5.2852	104.3654	7	1775	1825
52	47	1.11E+22	9MSPG	48068474	4/22/2016 0:18:38	1118	5.2851	104.3652	7	1775	1825
53	48	1.11E+22	9MSPG	48068699	4/22/2016 0:18:39	1119	5.2847	104.3649	7	1800	1850
54	49	1.11E+22	9MSPG	48068747	4/22/2016 0:18:39	1119	5.2845	104.3647	7	1800	1850
55	50	1.11E+22	9MSPG	48068825	4/22/2016 0:18:40	1120	5.2844	104.3645	7	1800	1850
56	51	1.11E+22	9MSPG	48068866	4/22/2016 0:18:40	1120	5.2842	104.3643	7	1825	1875
57	52	1.11E+22	9MSPG	48068867	4/22/2016 0:18:41	1121	5.2840	104.3642	7	1825	1875
58	53	1.11E+22	9MSPG	48068971	4/22/2016 0:18:42	1122	5.2838	104.3639	7	1825	1875
59	54	1.11E+22	9MSPG	48069024	4/22/2016 0:18:42	1122	5.2836	104.3637	7	1850	1900
60	55	1.11E+22	9MSPG	48069025	4/22/2016 0:18:43	1123	5.2834	104.3635	7	1850	1900

Appendix B: Complete Spreadsheet of ASE Results Comparison between the Developed Algorithm and China RMA Method. (Continued)

COLUMN / RAW	A	B	C	D	E	F	G	H	I	J	K
1		ADS-B DATA									
2	N				date/time/sec	$\sum x_i$				$\sum y_{i\text{-ModeC}}$	$\sum y_{i\text{-GPS}}$
3	103					115381				185025	189775
4	i					x_i	latitude	longitude		$y_{i\text{-ModeC}}$	$y_{i\text{-GPS}}$
5	i	icao24bit	callsign	id	datadate	seconds since midnight (sec)	latitude (°)	longitude (°)	nuc	Mode C Level (feet)	GPS Level (feet)
61	56	1.11E+22	9MSPG	48069114	4/22/2016 0:18:43	1123	5.2833	104.3634	7	1850	1900
62	57	1.11E+22	9MSPG	48069199	4/22/2016 0:18:43	1123	5.2831	104.3631	7	1875	1925
63	58	1.11E+22	9MSPG	48069202	4/22/2016 0:18:44	1124	5.2827	104.3628	7	1875	1925
64	59	1.11E+22	9MSPG	48069335	4/22/2016 0:18:45	1125	5.2825	104.3626	7	1875	1925
65	60	1.11E+22	9MSPG	48069478	4/22/2016 0:18:45	1125	5.2824	104.3624	7	1900	1950
66	61	1.11E+22	9MSPG	48069479	4/22/2016 0:18:46	1126	5.2822	104.3622	7	1900	1950
67	62	1.11E+22	9MSPG	48069531	4/22/2016 0:18:46	1126	5.2820	104.3621	7	1900	1950
68	63	1.11E+22	9MSPG	48069591	4/22/2016 0:18:47	1127	5.2818	104.3619	7	1925	1975
69	64	1.11E+22	9MSPG	48069659	4/22/2016 0:18:47	1127	5.2816	104.3617	7	1925	1975
70	65	1.11E+22	9MSPG	48069660	4/22/2016 0:18:48	1128	5.2814	104.3615	7	1925	1975
71	66	1.11E+22	9MSPG	48069736	4/22/2016 0:18:48	1128	5.2813	104.3614	7	1925	2000
72	67	1.11E+22	9MSPG	48069834	4/22/2016 0:18:49	1129	5.2810	104.3611	7	1950	2000
73	68	1.11E+22	9MSPG	48069835	4/22/2016 0:18:50	1130	5.2809	104.3609	7	1950	2025
74	69	1.11E+22	9MSPG	48069906	4/22/2016 0:18:50	1130	5.2807	104.3607	7	1975	2025
75	70	1.11E+22	9MSPG	48069908	4/22/2016 0:18:51	1131	5.2805	104.3605	7	1975	2050
76	71	1.11E+22	9MSPG	48069971	4/22/2016 0:18:52	1132	5.2801	104.3601	7	1975	2025
77	72	1.11E+22	9MSPG	48069972	4/22/2016 0:18:52	1132	5.2800	104.3600	7	2000	2050
78	73	1.11E+22	9MSPG	48070052	4/22/2016 0:18:53	1133	5.2796	104.3595	7	2000	2050
79	74	1.11E+22	9MSPG	48070053	4/22/2016 0:18:54	1134	5.2794	104.3593	7	2025	2075
80	75	1.11E+22	9MSPG	48070110	4/22/2016 0:18:54	1134	5.2792	104.3591	7	2025	2075
81	76	1.11E+22	9MSPG	48070111	4/22/2016 0:18:55	1135	5.2790	104.3589	7	2025	2075
82	77	1.11E+22	9MSPG	48070199	4/22/2016 0:18:55	1135	5.2788	104.3587	7	2050	2100
83	78	1.11E+22	9MSPG	48070274	4/22/2016 0:18:56	1136	5.2787	104.3586	7	2050	2125
84	79	1.11E+22	9MSPG	48070345	4/22/2016 0:18:56	1136	5.2785	104.3584	7	2050	2100
85	80	1.11E+22	9MSPG	48070346	4/22/2016 0:18:57	1137	5.2783	104.3582	7	2050	2100
86	81	1.11E+22	9MSPG	48070400	4/22/2016 0:18:57	1137	5.2781	104.3579	7	2075	2125
87	82	1.11E+22	9MSPG	48070476	4/22/2016 0:18:58	1138	5.2777	104.3576	7	2075	2125
88	83	1.11E+22	9MSPG	48070477	4/22/2016 0:18:59	1139	5.2775	104.3574	7	2075	2150
89	84	1.11E+22	9MSPG	48070606	4/22/2016 0:18:59	1139	5.2773	104.3571	7	2075	2125
90	85	1.11E+22	9MSPG	48070665	4/22/2016 0:19:00	1140	5.2771	104.3569	7	2075	2150
91	86	1.11E+22	9MSPG	48070667	4/22/2016 0:19:00	1140	5.2770	104.3567	7	2100	2150
92	87	1.11E+22	9MSPG	48070668	4/22/2016 0:19:01	1141	5.2767	104.3565	7	2100	2150
93	88	1.11E+22	9MSPG	48070715	4/22/2016 0:19:02	1142	5.2763	104.3561	7	2100	2150
94	89	1.11E+22	9MSPG	48070716	4/22/2016 0:19:02	1142	5.2761	104.3559	7	2100	2150
95	90	1.11E+22	9MSPG	48070717	4/22/2016 0:19:03	1143	5.2760	104.3556	7	2100	2150
96	91	1.11E+22	9MSPG	48070787	4/22/2016 0:19:03	1143	5.2757	104.3554	7	2100	2150
97	92	1.11E+22	9MSPG	48070788	4/22/2016 0:19:04	1144	5.2755	104.3552	7	2100	2150
98	93	1.11E+22	9MSPG	48070790	4/22/2016 0:19:04	1144	5.2753	104.3550	7	2100	2150
99	94	1.11E+22	9MSPG	48070863	4/22/2016 0:19:06	1146	5.2747	104.3543	7	2100	2150
100	95	1.11E+22	9MSPG	48070864	4/22/2016 0:19:06	1146	5.2746	104.3542	7	2100	2150
101	96	1.11E+22	9MSPG	48070940	4/22/2016 0:19:07	1147	5.2743	104.3539	7	2100	2175
102	97	1.11E+22	9MSPG	48070941	4/22/2016 0:19:08	1148	5.2739	104.3535	7	2100	2175
103	98	1.11E+22	9MSPG	48070992	4/22/2016 0:19:08	1148	5.2737	104.3532	7	2100	2175
104	99	1.11E+22	9MSPG	48071065	4/22/2016 0:19:09	1149	5.2734	104.3530	7	2100	2175
105	100	1.11E+22	9MSPG	48071066	4/22/2016 0:19:09	1149	5.2733	104.3528	7	2100	2175
106	101	1.11E+22	9MSPG	48071126	4/22/2016 0:19:10	1150	5.2731	104.3526	7	2100	2175
107	102	1.11E+22	9MSPG	48071127	4/22/2016 0:19:10	1150	5.2728	104.3523	7	2100	2175
108	103	1.11E+22	9MSPG	48072060	4/22/2016 0:19:24	1164	5.2667	104.3456	7	2125	2200

Appendix B: Complete Spreadsheet of ASE Results Comparison between the Developed Algorithm and China RMA Method. (Continued)

COLUMN / RAW	A	L	M	N	O
1		ADS-B DATA PROCESSING			
2	N	$\sum y_{i-AAD}$	$\sum x_j$	$\sum x_i^2$	
3	103	-20975	115360	129284971	
4	i	y_{i-AAD}			
5	i	Points AAD	x_j	x_i^2	$\lvert x_i - \text{median}(x_i) \rvert$
6	1	-675	1069	1185921	32.00
7	2	-650	1070	1188100	31.00
8	3	-650	1071	1188100	31.00
9	4	-625	1072	1190281	30.00
10	5	-625	1073	1192464	29.00
11	6	-625	1074	1192464	29.00
12	7	-600	1075	1194649	28.00
13	8	-575	1076	1196836	27.00
14	9	-575	1077	1196836	27.00
15	10	-550	1078	1199025	26.00
16	11	-550	1079	1201216	25.00
17	12	-525	1080	1201216	25.00
18	13	-525	1081	1203409	24.00
19	14	-525	1082	1203409	24.00
20	15	-525	1083	1203409	24.00
21	16	-500	1084	1205604	23.00
22	17	-500	1085	1205604	23.00
23	18	-500	1086	1207801	22.00
24	19	-500	1087	1207801	22.00
25	20	-475	1088	1210000	21.00
26	21	-475	1089	1210000	21.00
27	22	-475	1090	1212201	20.00
28	23	-475	1091	1212201	20.00
29	24	-450	1092	1214404	19.00
30	25	-450	1093	1214404	19.00
31	26	-450	1094	1216609	18.00
32	27	-425	1095	1216609	18.00
33	28	-425	1096	1218816	17.00
34	29	-425	1097	1218816	17.00
35	30	-400	1098	1223236	15.00
36	31	-400	1099	1225449	14.00
37	32	-375	1100	1225449	14.00
38	33	-350	1101	1227664	13.00
39	34	-325	1102	1232100	11.00
40	35	-325	1103	1234321	10.00
41	36	-325	1104	1234321	10.00
42	37	-300	1105	1236544	9.00
43	38	-300	1106	1236544	9.00
44	39	-300	1107	1238769	8.00
45	40	-275	1108	1238769	8.00
46	41	-275	1109	1240996	7.00
47	42	-275	1110	1243225	6.00
48	43	-250	1111	1245456	5.00
49	44	-250	1112	1245456	5.00
50	45	-225	1113	1247689	4.00
51	46	-225	1114	1247689	4.00
52	47	-225	1115	1249924	3.00
53	48	-200	1116	1252161	2.00
54	49	-200	1117	1252161	2.00
55	50	-200	1118	1254400	1.00
56	51	-175	1119	1254400	1.00
57	52	-175	1120	1256641	0.00
58	53	-175	1121	1258884	1.00
59	54	-150	1122	1258884	1.00
60	55	-150	1123	1261129	2.00

Appendix B: Complete Spreadsheet of ASE Results Comparison between the Developed Algorithm and China RMA Method. (Continued)

COLUMN / RAW	A	L	M	N	O
1		ADS-B DATA PROCESSING			
2	N	$\sum y_{i\text{-AAD}}$	$\sum x_j$	$\sum x_i^2$	
3	103	-20975	115360	129284971	
4	i	$y_{i\text{-AAD}}$			
5	i	Points AAD	x_j	x_i^2	$\lvert x_i - \text{median}(x_i)\rvert$
61	56	-150	1124	1261129	2.00
62	57	-125	1125	1261129	2.00
63	58	-125	1126	1263376	3.00
64	59	-125	1127	1265625	4.00
65	60	-100	1128	1265625	4.00
66	61	-100	1129	1267876	5.00
67	62	-100	1130	1267876	5.00
68	63	-75	1131	1270129	6.00
69	64	-75	1132	1270129	6.00
70	65	-75	1133	1272384	7.00
71	66	-75	1134	1272384	7.00
72	67	-50	1135	1274641	8.00
73	68	-50	1136	1276900	9.00
74	69	-25	1137	1276900	9.00
75	70	-25	1138	1279161	10.00
76	71	-25	1139	1281424	11.00
77	72	0	1140	1281424	11.00
78	73	0	1141	1283689	12.00
79	74	25	1142	1285956	13.00
80	75	25	1143	1285956	13.00
81	76	25	1144	1288225	14.00
82	77	50	1145	1288225	14.00
83	78	50	1146	1290496	15.00
84	79	50	1147	1290496	15.00
85	80	50	1148	1292769	16.00
86	81	75	1149	1292769	16.00
87	82	75	1150	1295044	17.00
88	83	75	1151	1297321	18.00
89	84	75	1152	1297321	18.00
90	85	75	1153	1299600	19.00
91	86	100	1154	1299600	19.00
92	87	100	1155	1301881	20.00
93	88	100	1156	1304164	21.00
94	89	100	1157	1304164	21.00
95	90	100	1158	1306449	22.00
96	91	100	1159	1306449	22.00
97	92	100	1160	1308736	23.00
98	93	100	1161	1308736	23.00
99	94	100	1162	1313316	25.00
100	95	100	1163	1313316	25.00
101	96	100	1164	1315609	26.00
102	97	100	1165	1317904	27.00
103	98	100	1166	1317904	27.00
104	99	100	1167	1320201	28.00
105	100	100	1168	1320201	28.00
106	101	100	1169	1322500	29.00
107	102	100	1170	1322500	29.00
108	103	125	1171	1354896	43.00

Appendix B: Complete Spreadsheet of ASE Results Comparison between the Developed Algorithm and China RMA Method. (Continued)

COLUMN / RAW	A	P	Q	R	S	T	U	V
1		ADS-B MODE C DATA PROCESSING						
2	N	$\sum x_i y_{i\text{-ModeC}}$	$\sum y_{i\text{-ModeC}}^2$			$\sum K(u_{ModeC})$	$\sum K(u)^* y_{i\text{-ModeC}}$	
3	103	207725675	338638125			41.05	73737.98	
4	i							
5	i	$x_i y_{i\text{-ModeC}}$	$y_{i\text{-ModeC}}^2$	$\lvert y_{i\text{-ModeC}}$ - median $(y_{i\text{-ModeC}})\rvert$	$u = (x_j - x_i)/h_{ModeC}$	$K(u_{i\text{-ModeC}})$	$K(u_i)^* y_{i\text{-ModeC}}$	$m_n(x_{ModeC})$
6	1	1442925	1755625	500	-0.08	0.40	526.92	1796.39
7	2	1471500	1822500	475	-0.08	0.40	536.86	1796.39
8	3	1471500	1822500	475	-0.08	0.40	537.03	1796.39
9	4	1500125	1890625	450	-0.08	0.40	546.98	1796.39
10	5	1501500	1890625	450	-0.08	0.40	546.98	1796.39
11	6	1501500	1890625	450	-0.07	0.40	547.14	1796.39
12	7	1530200	1960000	425	-0.07	0.40	557.08	1796.39
13	8	1558950	2030625	400	-0.07	0.40	567.03	1796.39
14	9	1558950	2030625	400	-0.07	0.40	567.19	1796.39
15	10	1587750	2102500	375	-0.07	0.40	577.14	1796.39
16	11	1589200	2102500	375	-0.07	0.40	577.14	1796.39
17	12	1616600	2175625	350	-0.06	0.40	587.25	1796.39
18	13	1618075	2175625	350	-0.06	0.40	587.25	1796.39
19	14	1618075	2175625	350	-0.06	0.40	587.39	1796.39
20	15	1618075	2175625	350	-0.06	0.40	587.52	1796.39
21	16	1647000	2250000	325	-0.06	0.40	597.48	1796.39
22	17	1647000	2250000	325	-0.05	0.40	597.61	1796.39
23	18	1648500	2250000	325	-0.05	0.40	597.61	1796.39
24	19	1648500	2250000	325	-0.05	0.40	597.73	1796.39
25	20	1677500	2325625	300	-0.05	0.40	607.69	1796.39
26	21	1677500	2325625	300	-0.04	0.40	607.80	1796.39
27	22	1679025	2325625	300	-0.04	0.40	607.80	1796.39
28	23	1679025	2325625	300	-0.04	0.40	607.90	1796.39
29	24	1708100	2402500	275	-0.04	0.40	617.87	1796.39
30	25	1708100	2402500	275	-0.04	0.40	617.96	1796.39
31	26	1709650	2402500	275	-0.04	0.40	617.96	1796.39
32	27	1737225	2480625	250	-0.03	0.40	628.01	1796.39
33	28	1738800	2480625	250	-0.03	0.40	628.01	1796.39
34	29	1738800	2480625	250	-0.03	0.40	628.09	1796.39
35	30	1769600	2560000	225	-0.03	0.40	637.98	1796.39
36	31	1771200	2560000	225	-0.03	0.40	637.98	1796.39
37	32	1798875	2640625	200	-0.03	0.40	648.03	1796.39
38	33	1828200	2722500	175	-0.03	0.40	658.00	1796.39
39	34	1859250	2805625	150	-0.03	0.40	667.89	1796.39
40	35	1860925	2805625	150	-0.03	0.40	667.89	1796.39
41	36	1860925	2805625	150	-0.03	0.40	667.97	1796.39
42	37	1890400.001	2890000	125	-0.03	0.40	677.94	1796.39
43	38	1890400.001	2890000	125	-0.02	0.40	678.01	1796.39
44	39	1892100	2890000	125	-0.02	0.40	678.01	1796.39
45	40	1919925	2975625	100	-0.02	0.40	688.04	1796.39
46	41	1921650	2975625	100	-0.02	0.40	688.04	1796.39
47	42	1923375	2975625	100	-0.02	0.40	688.04	1796.39
48	43	1953000	3062500	75	-0.02	0.40	698.01	1796.39
49	44	1953000	3062500	75	-0.02	0.40	698.06	1796.39
50	45	1982675	3150625	50	-0.02	0.40	708.03	1796.39
51	46	1982675	3150625	50	-0.01	0.40	708.07	1796.39
52	47	1984450	3150625	50	-0.01	0.40	708.07	1796.39
53	48	2014200	3240000	25	-0.01	0.40	718.04	1796.39
54	49	2014200	3240000	25	-0.01	0.40	718.07	1796.39
55	50	2016000.001	3240000	25	-0.01	0.40	718.07	1796.39
56	51	2044000.001	3330625	0	0.00	0.40	728.06	1796.39
57	52	2045825	3330625	0	0.00	0.40	728.06	1796.39
58	53	2047650	3330625	0	0.00	0.40	728.06	1796.39
59	54	2075700	3422500	25	0.00	0.40	738.04	1796.39
60	55	2077550	3422500	25	0.00	0.40	738.04	1796.39

Appendix B: Complete Spreadsheet of ASE Results Comparison between the Developed Algorithm and China RMA Method. (Continued)

COLUMN / RAW	A	P	Q	R	S	T	U	V
1		ADS-B MODE C DATA PROCESSING						
2	N	$\sum x_i y_{i\text{-ModeC}}$	$\sum y_{i\text{-ModeC}}^2$			$\sum K(u_{ModeC})$	$\sum K(u)*y_{i\text{-ModeC}}$	
3	103	207725675	338638125			41.05	73737.98	
4	i							
5	i	$x_i y_{i\text{-ModeC}}$	$y_{i\text{-ModeC}}^2$	$\lvert y_{i\text{-ModeC}} - \text{median}(y_{i\text{-ModeC}})\rvert$	$u = (x_j - x_i)/h_{ModeC}$	$K(u_{i\text{-ModeC}})$	$K(u_i)*y_{i\text{-ModeC}}$	$m_n(x_{ModeC})$
61	56	2077550	3422500	25	0.00	0.40	738.04	1796.39
62	57	2105625	3515625	50	0.01	0.40	747.99	1796.39
63	58	2107500	3515625	50	0.01	0.40	747.99	1796.39
64	59	2109375	3515625	50	0.01	0.40	747.99	1796.39
65	60	2137500	3610000	75	0.01	0.40	757.94	1796.39
66	61	2139400	3610000	75	0.01	0.40	757.94	1796.39
67	62	2139400	3610000	75	0.02	0.40	757.89	1796.39
68	63	2169475	3705625	100	0.02	0.40	767.87	1796.39
69	64	2169475	3705625	100	0.02	0.40	767.81	1796.39
70	65	2171400.001	3705625	100	0.02	0.40	767.81	1796.39
71	66	2171400.001	3705625	100	0.02	0.40	767.74	1796.39
72	67	2201550	3802500	125	0.02	0.40	777.72	1796.39
73	68	2203500	3802500	125	0.02	0.40	777.72	1796.39
74	69	2231750	3900625	150	0.03	0.40	787.60	1796.39
75	70	2233724.999	3900625	150	0.03	0.40	787.60	1796.39
76	71	2235700	3900625	150	0.03	0.40	787.60	1796.39
77	72	2264000	4000000	175	0.03	0.40	797.48	1796.39
78	73	2266000	4000000	175	0.03	0.40	797.48	1796.39
79	74	2296350	4100625	200	0.03	0.40	807.45	1796.39
80	75	2296350	4100625	200	0.04	0.40	807.34	1796.39
81	76	2298375	4100625	200	0.04	0.40	807.34	1796.39
82	77	2326750	4202500	225	0.04	0.40	817.18	1796.39
83	78	2328800.001	4202500	225	0.04	0.40	817.18	1796.39
84	79	2328800.001	4202500	225	0.04	0.40	817.05	1796.39
85	80	2330850	4202500	225	0.04	0.40	817.05	1796.39
86	81	2359275	4305625	250	0.05	0.40	826.86	1796.39
87	82	2361350	4305625	250	0.05	0.40	826.86	1796.39
88	83	2363424.999	4305625	250	0.05	0.40	826.86	1796.39
89	84	2363424.999	4305625	250	0.05	0.40	826.70	1796.39
90	85	2365500	4305625	250	0.05	0.40	826.70	1796.39
91	86	2394000	4410000	275	0.06	0.40	836.48	1796.39
92	87	2396100	4410000	275	0.06	0.40	836.48	1796.39
93	88	2398200	4410000	275	0.06	0.40	836.48	1796.39
94	89	2398200	4410000	275	0.06	0.40	836.28	1796.39
95	90	2400300	4410000	275	0.06	0.40	836.28	1796.39
96	91	2400300	4410000	275	0.06	0.40	836.08	1796.39
97	92	2402400.001	4410000	275	0.06	0.40	836.08	1796.39
98	93	2402400.001	4410000	275	0.07	0.40	835.86	1796.39
99	94	2406600	4410000	275	0.06	0.40	836.08	1796.39
100	95	2406600	4410000	275	0.07	0.40	835.86	1796.39
101	96	2408699.999	4410000	275	0.07	0.40	835.86	1796.39
102	97	2410800	4410000	275	0.07	0.40	835.86	1796.39
103	98	2410800	4410000	275	0.07	0.40	835.63	1796.39
104	99	2412900	4410000	275	0.07	0.40	835.63	1796.39
105	100	2412900	4410000	275	0.08	0.40	835.38	1796.39
106	101	2415000	4410000	275	0.08	0.40	835.38	1796.39
107	102	2415000	4410000	275	0.08	0.40	835.12	1796.39
108	103	2473500	4515625	300	0.03	0.40	847.42	1796.39

Appendix B: Complete Spreadsheet of ASE Results Comparison between the Developed Algorithm and China RMA Method. (Continued)

COLUMN / RAW	A	W	X	Y	Z	AA	AB	AC
1	ADS-B GPS DATA PROCESSING							
2	N	$\sum x_i y_{i\text{-}GPS}$	$\sum y_{i\text{-}GPS}^2$			$\sum K(u_{GPS})$	$\sum K(u)*y_{i\text{-}GPS}$	
3	103	213071375	356600625			41.05	75631.04	
4	i							
5	i	$x_i y_{i\text{-}GPS}$	$y_{i\text{-}GPS}^2$	$\lvert y_{i\text{-}GPS} - \text{median}(y_{i\text{-}GPS})\rvert$	$u = (x_j - x_i)/h_{GPS}$	$K(u_{i\text{-}GPS})$	$K(u_i)*y_{i\text{-}GPS}$	$m_n(x_{GPS})$
6	1	1470150	1822500	525	-0.08	0.40	536.86	1842.51
7	2	1498750	1890625	500	-0.08	0.40	546.81	1842.51
8	3	1498750	1890625	500	-0.08	0.40	546.98	1842.51
9	4	1527400	1960000	475	-0.08	0.40	556.92	1842.51
10	5	1528800	1960000	475	-0.08	0.40	556.92	1842.51
11	6	1528800	1960000	475	-0.07	0.40	557.08	1842.51
12	7	1557525	2030625	450	-0.07	0.40	567.03	1842.51
13	8	1586300	2102500	425	-0.07	0.40	576.98	1842.51
14	9	1586300	2102500	425	-0.07	0.40	577.14	1842.51
15	10	1615125	2175625	400	-0.07	0.40	587.09	1842.51
16	11	1616600	2175625	400	-0.07	0.40	587.09	1842.51
17	12	1644000	2250000	375	-0.06	0.40	597.20	1842.51
18	13	1645500	2250000	375	-0.06	0.40	597.20	1842.51
19	14	1645500	2250000	375	-0.06	0.40	597.35	1842.51
20	15	1645500	2250000	375	-0.06	0.40	597.48	1842.51
21	16	1674450	2325625	350	-0.06	0.40	607.44	1842.51
22	17	1674450	2325625	350	-0.05	0.40	607.57	1842.51
23	18	1675975	2325625	350	-0.05	0.40	607.57	1842.51
24	19	1675975	2325625	350	-0.05	0.40	607.69	1842.51
25	20	1705000	2402500	325	-0.05	0.40	617.65	1842.51
26	21	1732500	2480625	300	-0.04	0.40	627.73	1842.51
27	22	1734075	2480625	300	-0.04	0.40	627.73	1842.51
28	23	1734075	2480625	300	-0.04	0.40	627.84	1842.51
29	24	1735650	2480625	300	-0.04	0.40	627.84	1842.51
30	25	1735650	2480625	300	-0.04	0.40	627.93	1842.51
31	26	1737225	2480625	300	-0.04	0.40	627.93	1842.51
32	27	1764800	2560000	275	-0.03	0.40	637.98	1842.51
33	28	1766400	2560000	275	-0.03	0.40	637.98	1842.51
34	29	1766400	2560000	275	-0.03	0.40	638.06	1842.51
35	30	1797250	2640625	250	-0.03	0.40	647.95	1842.51
36	31	1798875	2640625	250	-0.03	0.40	647.95	1842.51
37	32	1826550	2722500	225	-0.03	0.40	658.00	1842.51
38	33	1855900	2805625	200	-0.03	0.40	667.97	1842.51
39	34	1914750	2975625	150	-0.03	0.40	687.83	1842.51
40	35	1916475	2975625	150	-0.03	0.40	687.83	1842.51
41	36	1916475	2975625	150	-0.03	0.40	687.91	1842.51
42	37	1946000.001	3062500	125	-0.03	0.40	697.88	1842.51
43	38	1946000.001	3062500	125	-0.02	0.40	697.95	1842.51
44	39	1947750	3062500	125	-0.02	0.40	697.95	1842.51
45	40	1975575	3150625	100	-0.02	0.40	707.98	1842.51
46	41	1977350	3150625	100	-0.02	0.40	707.98	1842.51
47	42	1979125	3150625	100	-0.02	0.40	707.98	1842.51
48	43	2008800	3240000	75	-0.02	0.40	717.95	1842.51
49	44	2008800	3240000	75	-0.02	0.40	718.00	1842.51
50	45	2038525	3330625	50	-0.02	0.40	727.98	1842.51
51	46	2038525	3330625	50	-0.01	0.40	728.02	1842.51
52	47	2040350	3330625	50	-0.01	0.40	728.02	1842.51
53	48	2070150	3422500	25	-0.01	0.40	737.99	1842.51
54	49	2070150	3422500	25	-0.01	0.40	738.02	1842.51
55	50	2072000.001	3422500	25	-0.01	0.40	738.02	1842.51
56	51	2100000.001	3515625	0	0.00	0.40	748.01	1842.51
57	52	2101875	3515625	0	0.00	0.40	748.01	1842.51
58	53	2103750	3515625	0	0.00	0.40	748.01	1842.51
59	54	2131800	3610000	25	0.00	0.40	757.99	1842.51
60	55	2133700	3610000	25	0.00	0.40	757.99	1842.51

Appendix B: Complete Spreadsheet of ASE Results Comparison between the Developed Algorithm and China RMA Method. (Continued)

COLUMN / RAW	A	W	X	Y	Z	AA	AB	AC
1		ADS-B GPS DATA PROCESSING						
2	N	$\sum x_i y_{i\text{-}GPS}$	$\sum y_{i\text{-}GPS}^2$			$\sum K(u_{GPS})$	$\sum K(u)*y_{i\text{-}GPS}$	
3	103	213071375	356600625			41.05	75631.04	
4	i							
5	i	$x_i y_{i\text{-}GPS}$	$y_{i\text{-}GPS}^2$	$\lvert y_{i\text{-}GPS}$ - median $(y_{i\text{-}GPS})\rvert$	$u = (x_j - x_i)/h_{GPS}$	$K(u_{i\text{-}GPS})$	$K(u_i)*y_{i\text{-}GPS}$	$m_n(x_{GPS})$
61	56	2133700	3610000	25	0.00	0.40	757.98	1842.51
62	57	2161775	3705625	50	0.01	0.40	767.94	1842.51
63	58	2163700	3705625	50	0.01	0.40	767.94	1842.51
64	59	2165625	3705625	50	0.01	0.40	767.94	1842.51
65	60	2193750	3802500	75	0.01	0.40	777.88	1842.51
66	61	2195700	3802500	75	0.01	0.40	777.88	1842.51
67	62	2195700	3802500	75	0.02	0.40	777.84	1842.51
68	63	2225825	3900625	100	0.02	0.40	787.81	1842.51
69	64	2225825	3900625	100	0.02	0.40	787.75	1842.51
70	65	2227800.001	3900625	100	0.02	0.40	787.75	1842.51
71	66	2256000.001	4000000	125	0.02	0.40	797.66	1842.51
72	67	2258000	4000000	125	0.02	0.40	797.66	1842.51
73	68	2288250	4100625	150	0.02	0.40	807.63	1842.51
74	69	2288250	4100625	150	0.03	0.40	807.54	1842.51
75	70	2318549.999	4202500	175	0.03	0.40	817.51	1842.51
76	71	2292300	4100625	150	0.03	0.40	807.54	1842.51
77	72	2320600	4202500	175	0.03	0.40	817.42	1842.51
78	73	2322650	4202500	175	0.03	0.40	817.42	1842.51
79	74	2353050	4305625	200	0.03	0.40	827.38	1842.51
80	75	2353050	4305625	200	0.04	0.40	827.27	1842.51
81	76	2355125	4305625	200	0.04	0.40	827.27	1842.51
82	77	2383500	4410000	225	0.04	0.40	837.11	1842.51
83	78	2414000.001	4515625	250	0.04	0.40	847.08	1842.51
84	79	2385600.001	4410000	225	0.04	0.40	836.97	1842.51
85	80	2387700	4410000	225	0.04	0.40	836.97	1842.51
86	81	2416125	4515625	250	0.05	0.40	846.78	1842.51
87	82	2418250	4515625	250	0.05	0.40	846.78	1842.51
88	83	2448849.999	4622500	275	0.05	0.40	856.75	1842.51
89	84	2420374.999	4515625	250	0.05	0.40	846.62	1842.51
90	85	2451000	4622500	275	0.05	0.40	856.58	1842.51
91	86	2451000	4622500	275	0.06	0.40	856.39	1842.51
92	87	2453150	4622500	275	0.06	0.40	856.39	1842.51
93	88	2455300	4622500	275	0.06	0.40	856.39	1842.51
94	89	2455300	4622500	275	0.06	0.40	856.20	1842.51
95	90	2457450	4622500	275	0.06	0.40	856.20	1842.51
96	91	2457450	4622500	275	0.06	0.40	855.98	1842.51
97	92	2459600.001	4622500	275	0.06	0.40	855.98	1842.51
98	93	2459600.001	4622500	275	0.07	0.40	855.76	1842.51
99	94	2463900	4622500	275	0.06	0.40	855.98	1842.51
100	95	2463900	4622500	275	0.07	0.40	855.76	1842.51
101	96	2494724.999	4730625	300	0.07	0.40	865.71	1842.51
102	97	2496900	4730625	300	0.07	0.40	865.71	1842.51
103	98	2496900	4730625	300	0.07	0.40	865.47	1842.51
104	99	2499075	4730625	300	0.07	0.40	865.47	1842.51
105	100	2499075	4730625	300	0.08	0.40	865.22	1842.51
106	101	2501249.999	4730625	300	0.08	0.40	865.22	1842.51
107	102	2501249.999	4730625	300	0.08	0.40	864.95	1842.51
108	103	2560800	4840000	325	0.03	0.40	877.33	1842.51

Appendix B: Complete Spreadsheet of ASE Results Comparison between the Developed Algorithm and China RMA Method. (Continued)

COLUMN / RAW	A	AD	AE	AF	AG	AH	AI	AJ
1		NGA EGM96 GEOID CALCULATOR & CHINA RMA METHOD						
2	N			$\sum y_{i\text{-}NGA}$	$\sum y_{i\text{-}HAE\text{-}NGA}$	Average	Average	
3	103			28.30	205971.70	-157.25	46.39	
4	i	latitude	longitude	$y_{i\text{-}NGA}$	$y_{i\text{-}HAE\text{-}NGA}$			
5	i	latitude	longitude	$Geoid_{NGA}$ ft	HAE geometric Assigned Flight Level (feet)	Points TVE (feet)	Points ASE (feet) - China RMA	Mean ASE (feet) - China RMA
6	1	5° 17' 40''	104° 22' 30''	0.22	1999.78	-649.78	25.22	46.39
7	2	5° 17' 39''	104° 22' 29''	0.22	1999.78	-624.78	25.22	46.39
8	3	5° 17' 38''	104° 22' 28''	0.22	1999.78	-624.78	25.22	46.39
9	4	5° 17' 38''	104° 22' 28''	0.22	1999.78	-599.78	25.22	46.39
10	5	5° 17' 37''	104° 22' 27''	0.23	1999.77	-599.77	25.23	46.39
11	6	5° 17' 37''	104° 22' 27''	0.23	1999.77	-599.77	25.23	46.39
12	7	5° 17' 36''	104° 22' 26''	0.23	1999.77	-574.77	25.23	46.39
13	8	5° 17' 35''	104° 22' 24''	0.23	1999.77	-549.77	25.23	46.39
14	9	5° 17' 34''	104° 22' 24''	0.23	1999.77	-549.77	25.23	46.39
15	10	5° 17' 34''	104° 22' 23''	0.23	1999.77	-524.77	25.23	46.39
16	11	5° 17' 33''	104° 22' 23''	0.23	1999.77	-524.77	25.23	46.39
17	12	5° 17' 32''	104° 22' 22''	0.23	1999.77	-499.77	25.23	46.39
18	13	5° 17' 32''	104° 22' 22''	0.23	1999.77	-499.77	25.23	46.39
19	14	5° 17' 32''	104° 22' 21''	0.23	1999.77	-499.77	25.23	46.39
20	15	5° 17' 31''	104° 22' 20''	0.23	1999.77	-499.77	25.23	46.39
21	16	5° 17' 31''	104° 22' 20''	0.23	1999.77	-474.77	25.23	46.39
22	17	5° 17' 30''	104° 22' 19''	0.23	1999.77	-474.77	25.23	46.39
23	18	5° 17' 30''	104° 22' 19''	0.23	1999.77	-474.77	25.23	46.39
24	19	5° 17' 29''	104° 22' 18''	0.24	1999.76	-474.76	25.24	46.39
25	20	5° 17' 28''	104° 22' 18''	0.24	1999.76	-449.76	25.24	46.39
26	21	5° 17' 28''	104° 22' 17''	0.24	1999.76	-424.76	50.24	46.39
27	22	5° 17' 27''	104° 22' 17''	0.24	1999.76	-424.76	50.24	46.39
28	23	5° 17' 27''	104° 22' 16''	0.24	1999.76	-424.76	50.24	46.39
29	24	5° 17' 26''	104° 22' 15''	0.24	1999.76	-424.76	25.24	46.39
30	25	5° 17' 26''	104° 22' 15''	0.24	1999.76	-424.76	25.24	46.39
31	26	5° 17' 25''	104° 22' 14''	0.24	1999.76	-424.76	25.24	46.39
32	27	5° 17' 24''	104° 22' 13''	0.24	1999.76	-399.76	25.24	46.39
33	28	5° 17' 24''	104° 22' 13''	0.24	1999.76	-399.76	25.24	46.39
34	29	5° 17' 23''	104° 22' 12''	0.24	1999.76	-399.76	25.24	46.39
35	30	5° 17' 21''	104° 22' 10''	0.25	1999.75	-374.75	25.25	46.39
36	31	5° 17' 21''	104° 22' 10''	0.25	1999.75	-374.75	25.25	46.39
37	32	5° 17' 20''	104° 22' 9''	0.25	1999.75	-349.75	25.25	46.39
38	33	5° 17' 18''	104° 22' 7''	0.25	1999.75	-324.75	25.25	46.39
39	34	5° 17' 16''	104° 22' 5''	0.26	1999.74	-274.74	50.26	46.39
40	35	5° 17' 15''	104° 22' 4''	0.26	1999.74	-274.74	50.26	46.39
41	36	5° 17' 15''	104° 22' 3''	0.25	1999.75	-274.75	50.25	46.39
42	37	5° 17' 14''	104° 22' 3''	0.26	1999.74	-249.74	50.26	46.39
43	38	5° 17' 13''	104° 22' 2''	0.26	1999.74	-249.74	50.26	46.39
44	39	5° 17' 13''	104° 22' 2''	0.26	1999.74	-249.74	50.26	46.39
45	40	5° 17' 12''	104° 22' 1''	0.26	1999.74	-224.74	50.26	46.39
46	41	5° 17' 11''	104° 21' 60''	0.26	1999.74	-224.74	50.26	46.39
47	42	5° 17' 10''	104° 21' 59''	0.26	1999.74	-224.74	50.26	46.39
48	43	5° 17' 9''	104° 21' 57''	0.26	1999.74	-199.74	50.26	46.39
49	44	5° 17' 8''	104° 21' 57''	0.27	1999.73	-199.73	50.27	46.39
50	45	5° 17' 8''	104° 21' 56''	0.27	1999.73	-174.73	50.27	46.39
51	46	5° 17' 7''	104° 21' 55''	0.27	1999.73	-174.73	50.27	46.39
52	47	5° 17' 6''	104° 21' 55''	0.27	1999.73	-174.73	50.27	46.39
53	48	5° 17' 5''	104° 21' 54''	0.27	1999.73	-149.73	50.27	46.39
54	49	5° 17' 4''	104° 21' 53''	0.27	1999.73	-149.73	50.27	46.39
55	50	5° 17' 4''	104° 21' 52''	0.27	1999.73	-149.73	50.27	46.39
56	51	5° 17' 3''	104° 21' 51''	0.27	1999.73	-124.73	50.27	46.39
57	52	5° 17' 2''	104° 21' 51''	0.28	1999.72	-124.72	50.28	46.39
58	53	5° 17' 2''	104° 21' 50''	0.27	1999.73	-124.73	50.27	46.39
59	54	5° 17' 1''	104° 21' 49''	0.28	1999.72	-99.72	50.28	46.39
60	55	5° 17' 0''	104° 21' 49''	0.28	1999.72	-99.72	50.28	46.39

Appendix B: Complete Spreadsheet of ASE Results Comparison between the Developed Algorithm and China RMA Method. (Continued)

COLUMN / RAW	A	AD	AE	AF	AG	AH	AI	AJ
1		NGA EGM96 GEOID CALCULATOR & CHINA RMA METHOD						
2	N			$\sum y_{i\text{-NGA}}$	$\sum y_{i\text{-HAE-NGA}}$	Average	Average	
3	103			28.30	205971.70	-157.25	46.39	
4	i	latitude	longitude	$y_{i\text{-NGA}}$	$y_{i\text{-HAE-NGA}}$			
5	i	latitude	longitude	Geoid $_{NGA}$ ft	HAE geometric Assigned Flight Level (feet)	Points TVE (feet)	Points ASE (feet) - China RMA	Mean ASE (feet) - China RMA
61	56	5° 16' 60''	104° 21' 48''	0.28	1999.72	-99.72	50.28	46.39
62	57	5° 16' 59''	104° 21' 47''	0.28	1999.72	-74.72	50.28	46.39
63	58	5° 16' 58''	104° 21' 46''	0.28	1999.72	-74.72	50.28	46.39
64	59	5° 16' 57''	104° 21' 45''	0.28	1999.72	-74.72	50.28	46.39
65	60	5° 16' 57''	104° 21' 45''	0.28	1999.72	-49.72	50.28	46.39
66	61	5° 16' 56''	104° 21' 44''	0.28	1999.72	-49.72	50.28	46.39
67	62	5° 16' 55''	104° 21' 43''	0.29	1999.71	-49.71	50.29	46.39
68	63	5° 16' 55''	104° 21' 43''	0.29	1999.71	-24.71	50.29	46.39
69	64	5° 16' 54''	104° 21' 42''	0.29	1999.71	-24.71	50.29	46.39
70	65	5° 16' 53''	104° 21' 41''	0.29	1999.71	-24.71	50.29	46.39
71	66	5° 16' 53''	104° 21' 41''	0.29	1999.71	0.29	75.29	46.39
72	67	5° 16' 52''	104° 21' 40''	0.29	1999.71	0.29	50.29	46.39
73	68	5° 16' 51''	104° 21' 39''	0.29	1999.71	25.29	75.29	46.39
74	69	5° 16' 50''	104° 21' 39''	0.30	1999.70	25.30	50.30	46.39
75	70	5° 16' 50''	104° 21' 38''	0.29	1999.71	50.29	75.29	46.39
76	71	5° 16' 49''	104° 21' 36''	0.29	1999.71	25.29	50.29	46.39
77	72	5° 16' 48''	104° 21' 36''	0.30	1999.70	50.30	50.30	46.39
78	73	5° 16' 46''	104° 21' 34''	0.30	1999.70	50.30	50.30	46.39
79	74	5° 16' 46''	104° 21' 34''	0.30	1999.70	75.30	50.30	46.39
80	75	5° 16' 45''	104° 21' 33''	0.30	1999.70	75.30	50.30	46.39
81	76	5° 16' 44''	104° 21' 32''	0.30	1999.70	75.30	50.30	46.39
82	77	5° 16' 44''	104° 21' 31''	0.30	1999.70	100.30	50.30	46.39
83	78	5° 16' 43''	104° 21' 31''	0.30	1999.70	125.30	75.30	46.39
84	79	5° 16' 42''	104° 21' 30''	0.31	1999.69	100.31	50.31	46.39
85	80	5° 16' 42''	104° 21' 29''	0.30	1999.70	100.30	50.30	46.39
86	81	5° 16' 41''	104° 21' 29''	0.31	1999.69	125.31	50.31	46.39
87	82	5° 16' 40''	104° 21' 27''	0.31	1999.69	125.31	50.31	46.39
88	83	5° 16' 39''	104° 21' 27''	0.31	1999.69	150.31	75.31	46.39
89	84	5° 16' 38''	104° 21' 26''	0.31	1999.69	125.31	50.31	46.39
90	85	5° 16' 38''	104° 21' 25''	0.31	1999.69	150.31	75.31	46.39
91	86	5° 16' 37''	104° 21' 24''	0.31	1999.69	150.31	50.31	46.39
92	87	5° 16' 36''	104° 21' 23''	0.31	1999.69	150.31	50.31	46.39
93	88	5° 16' 35''	104° 21' 22''	0.31	1999.69	150.31	50.31	46.39
94	89	5° 16' 34''	104° 21' 21''	0.32	1999.68	150.32	50.32	46.39
95	90	5° 16' 33''	104° 21' 20''	0.32	1999.68	150.32	50.32	46.39
96	91	5° 16' 32''	104° 21' 19''	0.32	1999.68	150.32	50.32	46.39
97	92	5° 16' 32''	104° 21' 19''	0.32	1999.68	150.32	50.32	46.39
98	93	5° 16' 31''	104° 21' 18''	0.32	1999.68	150.32	50.32	46.39
99	94	5° 16' 29''	104° 21' 16''	0.32	1999.68	150.32	50.32	46.39
100	95	5° 16' 28''	104° 21' 15''	0.33	1999.67	150.33	50.33	46.39
101	96	5° 16' 27''	104° 21' 14''	0.33	1999.67	175.33	75.33	46.39
102	97	5° 16' 26''	104° 21' 13''	0.33	1999.67	175.33	75.33	46.39
103	98	5° 16' 25''	104° 21' 12''	0.33	1999.67	175.33	75.33	46.39
104	99	5° 16' 24''	104° 21' 11''	0.33	1999.67	175.33	75.33	46.39
105	100	5° 16' 24''	104° 21' 10''	0.33	1999.67	175.33	75.33	46.39
106	101	5° 16' 23''	104° 21' 9''	0.33	1999.67	175.33	75.33	46.39
107	102	5° 16' 22''	104° 21' 8''	0.33	1999.67	175.33	75.33	46.39
108	103	5° 15' 60''	104° 20' 44''	0.36	1999.64	200.36	75.36	46.39

Appendix B: Complete Spreadsheet of ASE Results Comparison between the Developed Algorithm and China RMA Method. (Continued)

COLUMN / RAW	A	AJ	AK	AL	AM	AN
1		MATLAB ALGORITHM OF THIS RESEARCH				
2	N		$\sum y_{i\text{-}Algo}$		Mean Value	Accuracy
3	103		26.97		45.85	98.84%
4	i		$y_{i\text{-}Algo}$	Algorithm		
5	i	$Geoid_{Algo}$ N (meter)	$Geoid_{Algo}$ N (feet)	True Height (feet)	Points ASE (feet) - Matlab Tool	Mean ASE (feet) - Matlab Tool
6	1	0.06	0.20	1349.80	24.80	45.85
7	2	0.06	0.20	1374.80	24.80	45.85
8	3	0.06	0.20	1374.80	24.80	45.85
9	4	0.06	0.20	1399.80	24.80	45.85
10	5	0.06	0.20	1399.80	24.80	45.85
11	6	0.06	0.20	1399.80	24.80	45.85
12	7	0.06	0.20	1424.80	24.80	45.85
13	8	0.07	0.23	1449.77	24.77	45.85
14	9	0.07	0.23	1449.77	24.77	45.85
15	10	0.07	0.23	1474.77	24.77	45.85
16	11	0.07	0.23	1474.77	24.77	45.85
17	12	0.07	0.23	1499.77	24.77	45.85
18	13	0.07	0.23	1499.77	24.77	45.85
19	14	0.07	0.23	1499.77	24.77	45.85
20	15	0.07	0.23	1499.77	24.77	45.85
21	16	0.07	0.23	1524.77	24.77	45.85
22	17	0.07	0.23	1524.77	24.77	45.85
23	18	0.07	0.23	1524.77	24.77	45.85
24	19	0.07	0.23	1524.77	24.77	45.85
25	20	0.07	0.23	1549.77	24.77	45.85
26	21	0.07	0.23	1574.77	49.77	45.85
27	22	0.07	0.23	1574.77	49.77	45.85
28	23	0.07	0.23	1574.77	49.77	45.85
29	24	0.07	0.23	1574.77	24.77	45.85
30	25	0.07	0.23	1574.77	24.77	45.85
31	26	0.07	0.23	1574.77	24.77	45.85
32	27	0.07	0.23	1599.77	24.77	45.85
33	28	0.07	0.23	1599.77	24.77	45.85
34	29	0.07	0.23	1599.77	24.77	45.85
35	30	0.07	0.23	1624.77	24.77	45.85
36	31	0.07	0.23	1624.77	24.77	45.85
37	32	0.07	0.23	1649.77	24.77	45.85
38	33	0.07	0.23	1674.77	24.77	45.85
39	34	0.07	0.23	1724.77	49.77	45.85
40	35	0.07	0.23	1724.77	49.77	45.85
41	36	0.07	0.23	1724.77	49.77	45.85
42	37	0.07	0.23	1749.77	49.77	45.85
43	38	0.07	0.23	1749.77	49.77	45.85
44	39	0.07	0.23	1749.77	49.77	45.85
45	40	0.08	0.26	1774.74	49.74	45.85
46	41	0.08	0.26	1774.74	49.74	45.85
47	42	0.08	0.26	1774.74	49.74	45.85
48	43	0.08	0.26	1799.74	49.74	45.85
49	44	0.08	0.26	1799.74	49.74	45.85
50	45	0.08	0.26	1824.74	49.74	45.85
51	46	0.08	0.26	1824.74	49.74	45.85
52	47	0.08	0.26	1824.74	49.74	45.85
53	48	0.08	0.26	1849.74	49.74	45.85
54	49	0.08	0.26	1849.74	49.74	45.85
55	50	0.08	0.26	1849.74	49.74	45.85
56	51	0.08	0.26	1874.74	49.74	45.85
57	52	0.08	0.26	1874.74	49.74	45.85
58	53	0.08	0.26	1874.74	49.74	45.85
59	54	0.08	0.26	1899.74	49.74	45.85
60	55	0.08	0.26	1899.74	49.74	45.85

Appendix B: Complete Spreadsheet of ASE Results Comparison between the Developed Algorithm and China RMA Method. (Continued)

COLUMN / RAW	A	AJ	AK	AL	AM	AN
1		MATLAB ALGORITHM OF THIS RESEARCH				
2	N		$\sum y_{i\text{-}Algo}$		Mean Value	Accuracy
3	103		26.97		45.85	98.84%
4	i		$y_{i\text{-}Algo}$	Algorithm		
5	i	$Geoid_{Algo}$ N (meter)	$Geoid_{Algo}$ N (feet)	True Height (feet)	Points ASE (feet) - Matlab Tool	Mean ASE (feet) - Matlab Tool
61	56	0.08	0.26	1899.74	49.74	45.85
62	57	0.08	0.26	1924.74	49.74	45.85
63	58	0.08	0.26	1924.74	49.74	45.85
64	59	0.08	0.26	1924.74	49.74	45.85
65	60	0.08	0.26	1949.74	49.74	45.85
66	61	0.08	0.26	1949.74	49.74	45.85
67	62	0.08	0.26	1949.74	49.74	45.85
68	63	0.08	0.26	1974.74	49.74	45.85
69	64	0.08	0.26	1974.74	49.74	45.85
70	65	0.08	0.26	1974.74	49.74	45.85
71	66	0.08	0.26	1999.74	74.74	45.85
72	67	0.08	0.26	1999.74	49.74	45.85
73	68	0.08	0.26	2024.74	74.74	45.85
74	69	0.09	0.30	2024.70	49.70	45.85
75	70	0.09	0.30	2049.70	74.70	45.85
76	71	0.09	0.30	2024.70	49.70	45.85
77	72	0.09	0.30	2049.70	49.70	45.85
78	73	0.09	0.30	2049.70	49.70	45.85
79	74	0.09	0.30	2074.70	49.70	45.85
80	75	0.09	0.30	2074.70	49.70	45.85
81	76	0.09	0.30	2074.70	49.70	45.85
82	77	0.09	0.30	2099.70	49.70	45.85
83	78	0.09	0.30	2124.70	74.70	45.85
84	79	0.09	0.30	2099.70	49.70	45.85
85	80	0.09	0.30	2099.70	49.70	45.85
86	81	0.09	0.30	2124.70	49.70	45.85
87	82	0.09	0.30	2124.70	49.70	45.85
88	83	0.09	0.30	2149.70	74.70	45.85
89	84	0.09	0.30	2124.70	49.70	45.85
90	85	0.09	0.30	2149.70	74.70	45.85
91	86	0.09	0.30	2149.70	49.70	45.85
92	87	0.09	0.30	2149.70	49.70	45.85
93	88	0.09	0.30	2149.70	49.70	45.85
94	89	0.09	0.30	2149.70	49.70	45.85
95	90	0.09	0.30	2149.70	49.70	45.85
96	91	0.09	0.30	2149.70	49.70	45.85
97	92	0.09	0.30	2149.70	49.70	45.85
98	93	0.09	0.30	2149.70	49.70	45.85
99	94	0.09	0.30	2149.70	49.70	45.85
100	95	0.09	0.30	2149.70	49.70	45.85
101	96	0.10	0.33	2174.67	74.67	45.85
102	97	0.10	0.33	2174.67	74.67	45.85
103	98	0.10	0.33	2174.67	74.67	45.85
104	99	0.10	0.33	2174.67	74.67	45.85
105	100	0.10	0.33	2174.67	74.67	45.85
106	101	0.10	0.33	2174.67	74.67	45.85
107	102	0.10	0.33	2174.67	74.67	45.85
108	103	0.11	0.36	2199.64	74.64	45.85

REFERENCE

Abdullah, K. A. (1995). Height Determination using GPS Data, Local Geoid and Global Geopotential Model.

Administration, F. A. (2014). *RVSM Height Monitoring Guide for U.S. Operators*.

AIS. (2008). AIP Italia.

Ali, B. S., Schuster, W., Ochieng, W., & Majumdar, A. (2015). Analysis of anomalies in ADSB and its GPS data.

Ali, N. A. A. T. B. S. (2016). An Analysis of Geometric Altitude Data in ADS-B Messages. doi:10.33012/2016.13392

AlliedSignal. (1999). *Description of Geometric Altitude for the EGPWS*.

Australia. (2011). *Implementation of Monitoring Aircraft Altimetry System Error Using Automatic Dependent Surveillance-Broadcast Data*.

Authority, C. A. (2002). EUR RVSM Post-Implementation Height Monitoring Requirements.

Barhydt, R., & Warren, A. W. (2002). *Newly Enacted Intent Changes to ADS-B MASPS:Emphasis on Operations,Compatibility and Integrity*. *AIAA*.

Barry, D. S., Aldis, D. G., & Jason-Jones, A. (2013). *Further Corrections to ADS-B ASE Results*.

Bhardwaj, A. (2020). Evaluating terrain type using geoid heights obtained from different geoids in varied topographic regions with different complexity. *Evaluating terrain type using geoid heights obtained from different geoids in varied topographic regions with different complexity*, 5.

ERROR Paper presented at the The Twenty-First Meeting of the APANPIRG ATM/AIS/SAR Sub-Group(ATM/AIS/SAR/SG/21) Bangkok, Thailand.

McFadyen, A., & Martin, T. (2018). Understanding Vertical Collision Risk and. *Understanding Vertical Collision Risk and*, 10.

Schultz, M., Olive, X., Rosenow, J., Fricke, H., & Alam, S. (2020). Analysis of airport ground operations based on ADS-B data. *Analysis of airport ground operations based on ADS-B data*, 9.

Taib, B. S. (2019). A Study on Geometric and Barometric. *A Study on Geometric and Barometric*, 19.

CAA. (2012). *ADS-B*. In.

CAA. (2014). *Advisory Circular: Reduced Vertical Separation Minimum (RVSM)*. Retrieved from

CFR. (2014). *Appendix G to Part 91-Operations in Reduced Vertical Separation Minimum (RVSM) Airspace. United States.*

China. (2012). *Use of Barometric Altitude and Geometric Altitude Information in ADS-B Message for ATC Applications*. Paper presented at the The Eight Meeting Of The Southeast Asia and Bay of Bengal Sub-Regional ADS-B Implementation Working Group (SEA/BOB ADS-B WG/8) Provisional Agenda, Yangon, Myanmar.

Controlled Flight Into Terrain (1999). *Flight Safety Australia*.

ENRI. (2014, 22-25 April 2014). *"RESEARCH PLAN FOR AIRCRAFT HEIGHT-KEEPING PERFORMANCE MONITORING WITH ADS-B DATA IN JAPAN". Paper presented at the Automatic Dependent Surveillance Broadcast Seminar and Thirteenth Meeting of Automatic Dependent Surveillance Broadcast Study and Implementation Task Force (ADS-B SITF 13), Hong Kong,China.*

FAA. (2009). *Authorization of Aircraft and Operators for Flight in Reduced Vertical Separation Minimum Airspace*. Federal Aviation Administration.

FAA. (2011a). Automatic Dependent Surveillance - Broadcast (ADS-B) In-Trail Procedures (ITP) Operational Flight Trial Project Overview.

FAA. (2011b). *Progress on the Research Conducted to Determine the Use of Automatic Dependent Surveillance-Broadcast Data for Monitoring Aircraft Altimetry System Error*.

FAA. (2014). *Job Aid - Altimetry System Error-Report (ASE-R) (F. A. Administration, Trans.). FAA, & Australia, A. (2011, 27/6–01/7/2011). ENDORSEMENT OF AUTOMATIC DEPENDENT SURVEILLANCE-BROADCAST DATA FOR MONITORING RVSM AIRCRAFT ALTIMETRY SYSTEM*.

Falk, C., Aldis, D. G., & Butcher, R. (2010). Progress on the Research Conducted to Determine the Use of Automatic Dependent Surveillance-Broadcast Data for Monitoring Aircraft Altimetry System Error.

Falk, C., Gonzalez, J., & Perez, J. (2010). *Using Automatic Dependent Surveillance-Broadcast Data for Monitoring Aircraft Altimetry System Error*

Fisher, A. B. (2014). *The Case for Geometric Altimetry*

Garrigues, M. Y. (2002). Installation and Flight Inspection of Height Monitoring Stations (HMU) in Europe.

Higgins, M. B. (2000). *HEIGHTING WITH GPS: POSSIBILITIES AND LIMITATIONS. 14(2).*

http://aviation-safety.net/database/record.php?id=20090225-0.

https://flightsafety.org/asw-article/faulty-altimeter-spurs-near-collision/.

https://news.aviation-safety.net/2013/01/24/altimeter-problems-caused-fatal-antonov-72-cfit-accident-in-kazakhstan/.

https://sma.nasa.gov/docs/default-source/safety-messages/safetymessage-2009-01-01-usafb2mishap.pdf?sfvrsn=d3a91ef8_4.

https://www.eurocontrol.int/service/european-regional-monitoring-agency.

https://www.faa.gov/air_traffic/separation_standards/rvsm/documents/ASE/1.3_RMA_Roles_and_NAARMO_Overview.pdf.

https://www.flightglobal.com/news/articles/mid-air-collision-jet-had-near-identical-earlier-inc-440477/.

Iatrou, K. (2014). 100 Years of Commercial Aviation.

ICAO. (2002). *Manual on Implementation of a 300 m (1 000 ft) Vertical Separation Minimum Between FL 290 and FL 410 Inclusive*. ICAO.

IVAO. (2015a). *Altimetry for air traffic controller*.

IVAO. (2015b). *Height Altitude Flight Level*.

Jan, S.-S., Gebre-Egziabher, D., Walter, T., & Enge, P. (2002). *Worst-Case Analysis of a 3-Frequency Receiver to Land a General Aviation Airplane*. Paper presented at the ION ITM 2002.

Jong, J. L. d. (2010). *Reading Flight Levels from QNH-altimeters*. In E. U. o. Technology (Ed.).

Kexi, Z., Jun, Z., & Xuejun, Z. (2010). *Research on ADS-B Geometric Height Information for Height Keeping Performance Surveillance*.

Kunzi, F., & Hansman, R. J. (2011). *ADS-B Benefits to General Aviation and Barriers in Implementation*.

Lehtinen, O. (2013). *Barometric Assistance Service for Assisted GNSS Receiver.* Tampere University of Technology,

Li, X., & Gotzez, H.-J. . (2001). *Ellipsoid, geoid, gravity, geodesy, and geophysics Geophysics (Vol. 66, pp. 1660-1668). Houston, Texas*.

MAAR. (2015). *Utilization of India ADS-B Data for Height-Keeping Performance Monitoring*.

MAAR, A. (2012, 28-31/8/2012). *PROGRESS ON THE USE OF ADS-B DATA TO MONITOR ASE. Paper presented at the The 17th Meeting of the Regional Airspace Safety Monitoring Advisory Group (RASMAG/17), Bangkok, Thailand.*

Martin, L., Falk, C., & Perez, J. L. (2008). *Investigation into the use of Automatic Dependent Surveillance-Broadcast Data for Monitoring Aircraft Altimetry System Error*. *AIAA*.

McFadyen, A., & Martin, T. (2018). Understanding Vertical Collision Risk and. *Understanding Vertical Collision Risk and*, 10.

Schultz, M., Olive, X., Rosenow, J., Fricke, H., & Alam, S. (2020). Analysis of airport ground operations based on ADS-B data. *Analysis of airport ground operations based on ADS-B data*, 9.

Taib, B. S. (2019). A Study on Geometric and Barometric. *A Study on Geometric and Barometric*, 19.

Thomas H. Cormen, C. E. (2009). *INTRODUCTION TO ALGORITHM.* London: Cambridge, Massachusetts.

Mosbeh R. Kaloop, A. Z.-A. (2020). Optimizing Local Geoid Undulation Model using. *Optimizing Local Geoid Undulation Model using*, 12.

Nusyirwan, I. F., & Perumah2, K. (2012). RVSM Implementation in Malaysia doi:10.4028/www.scientific.net/AMM.225.522

PARMO. (2014). *Comparisons Of Average ASE For Aircraft Monitoring Groups*. Paper presented at the The Nineteenth Meeting of the Regional Airspace Safety Monitoring Advisory Group

(RASMAG/19), Pattaya, Thailand.

PARMO. (2015a). *Pacific GPS-based Monitoring System (GMS) Monitoring Procedures*.

PARMO. (2015b). PARMO Assesment on Non-RVSM Approved Aircraft.

Pilotext. (2008). Reduced Vertical Separation Minimum.

Portugal, N. (2003). *Reduced Vertical Separation Minimum (RVSM)*.

RAPP, R. H., & WANG, Y. M. . (1993). *GEOID UNDULATION DIFFERENCES BETWEEN GEOPOTENTIAL MODELS. Surveys in Geophysics,*, 373-380.

RMA(CHINA). (2013, 1-4/4/2013). *CHINA RMA'S EVALUATION OF ALTIMETRY SYSTEM ERROR USING ADS-B. Paper presented at the The 18th Meeting of the Regional Airspace Safety Monitoring Advisory Group(RASMAG/18), Bangkok, Thailand*.

RVSM Heightens Need for Precision in Altitude Measurement. (2005). *Avionics News*.

Schultz, M., Olive, X., Rosenow, J., Fricke, H., & Alam, S. (2020). Analysis of airport ground operations based on ADS-B data. Analysis of airport ground operations based on ADS-B data, 9.

McFadyen, A., & Martin, T. (2018). Understanding Vertical Collision Risk and. *Understanding Vertical Collision Risk and*, 10.

Schultz, M., Olive, X., Rosenow, J., Fricke, H., & Alam, S. (2020). Analysis of airport ground operations based on ADS-B data. *Analysis of airport ground operations based on ADS-B data*, 9.

Taib, B. S. (2019). A Study on Geometric and Barometric. *A Study on Geometric and Barometric*, 19.

Veronez, M. R., Thum, A. B., & Souza, G. C. d. (2006). *A new method for obtaining geoidal undulations through Artificial Neural Networks. Paper presented at the 7th International Symposium on Spatial Accuracy Assessment in Natural Resources and Environmental Sciences.*

Wiolland, K. (2007). *Enhanced Ground Proximity Warning Systems Evolve, Provide Greater Safety*. *Avionics News*.